PASSIVE METHODS FOR SUPPRESSING ACOUSTIC RESONANCE EXCITATION IN SHALLOW RECTANGULAR CAVITIES

By

Ahmed Omer

B.Sc. (Mechanical Engineering), University of Khartoum, 2009

A Thesis Submitted in Partial Fulfillment of the Requirements for the Degree of

Master of Applied Science in Mechanical Engineering

Supervisor: Dr. Atef Mohany, P. Eng

Faculty of Engineering and Applied Science

University of Ontario Institute of Technology

August 2014

Abstract

The flow-excited acoustic resonance in shallow rectangular cavities can be a source of severe noise and/or excessive vibration. This phenomenon is excited when one of the acoustic modes in the accommodating enclosure is coupled with the flow instabilities resulting from the shear layer formation at the cavity mouth. In this thesis, two passive methods for suppressing the flow-excited acoustic resonance phenomenon are addressed. The first passive method considers the edge geometry effect on the phenomenon. Several edge geometries including chamfered, round, and different configurations of spoilers are considered. The effect of the spoilers dimensions is investigated to provide criteria that help designing and optimizing spoilers. Some of the spoilers are found to be effective in suppressing the acoustic resonance excitation, while some other edges including chamfered and round edges result in shifting the resonance excitations to higher velocities with amplification in the acoustic pressure. To enrich the understanding of the suppression mechanism introduced by these passive methods, hotwire measurements are performed revealing the existence of orthogonal vortices interacting with the shear layer at the cavity mouth. The second passive method investigated is the effect of placing a high frequency vortex generator (control cylinder) in vicinity of the upstream edge of the cavity on the acoustic resonance excitation. The method is investigated experimentally and numerically. The effectiveness of the control cylinder method is studied by investigating different cylinder diameters and locations on both horizontal and vertical directions. It is found that locating the cylinder at relatively small height from the bottom wall and with a distance of 25.4 mm upstream the leading edge can significantly suppress the resonance excitation. To further understand the interaction between the cylinder vortex shedding and the shear layer at the cavity mouth and the influence on the shear layer thickness, a 2D numerical simulation using K-epsilon and Detached Eddy Simulation (DES) models has been carried out and compared to the experimental results. For both passive methods, the study included two cavities with different aspect ratios (L/D=1.0 and L/D=1.67, L: cavity length, D: cavity depth) to address the effectiveness of the methods with respect to the cavity depth. The methods are investigated in flow with Mach number up to 0.45. All different configurations investigated are compared to the base case which is the bare cavity with sharp edges installed upstream and downstream.

Acknowledgments

Foremost, I would like to express my special appreciation and thanks to my advisor Dr. Atef Mohany for the continuous support, motivation, and enthusiasm. His guidance helped me in all the time of research and writing of this thesis and added considerably to my graduate experience.

My sincere thanks also goes out to Dr. Marwan Hassan from university of Guelph for his enormous support and help. I would also like to thank Dr. Ramani Ramakrishnan, and Mr. Hidayat Shahid, for their help in 3D printing the edge spoilers.

I sincerely thank my fellow in Aeroacoustics and noise control research group, Nadim Arafa, Mahmoud Imam, Omer Sadik, Hakan Ciloglu, Mohamed ALziadah, Mohamed Elkasaby, and Ibrahim Naeem for their priceless Support and help, without them it would have not been possible to write this thesis. Special thanks for Omar Afifi, Richard Hawa, and Nart for building the Hotwire mechanism that enormously enriched this thesis.

Last but not Least, very special thanks to my family for supporting and encouraging me through all this time.

Contents

List of Tables

List of Figures

Nomenclature

L	Length of the cavity
D	Depth of the cavity
H	Height of the test section
N	Number of Shear layer mode
n	Number of acoustic mode
St	Strouhal number
f	Frequency of dominant shear layer oscillations
f_a	Frequency of acoustic resonance mode
U	Mean flow velocity
c	Speed of sound
u	Local velocity
$u`$	Instantaneous velocity
x	Horizontal direction
y	Lateral direction
z	Vertical direction
r	Radius of round edge
l	Length of chamfer
t	Thickness of spoiler
h	Height of spoiler
s	Spacing between spoilers
d	Cylinder diameter
δ	Shear layer thickness
ρ	Fluid density
Re	Reynolds number
M	Mach number
α	Phase lag - empirical constant in Rossiter formula
k	Empirical constant in Rossiter formula
θ	Shear layer momentum thickness

1. Introduction

1.1. Motivation

Flow over cavity is considered one of the complex cases that has been under intensive research for the last six decades, the boundary layer separation at the upstream edge and the formation of a shear layer at the cavity mouth is the reason of the complexity and different phenomena can be excited by this boundary layer separation. One of the phenomena that can be excited when flow passes over a cavity is the flow-excited acoustic resonance. The flow-excited acoustic resonance phenomenon is created when the flow instability oscillations are coupled with one of the acoustic modes in the accommodating enclosure. This phenomenon has been observed in many engineering applications such as; aircraft weapon bays, aircraft landing gear cavity, gate valves in piping systems, and many other applications that involve flow over cavities. In these applications, the excitation of the acoustic resonance can result in a severe noise that can harm the environment around the source and also may lead to structural damage caused by the excessive vibration generated. Moreover, acoustic resonance can significantly increase the aerodynamic drag associated with flow over cavities, this increase can reach up to 250% of the drag of the normal case without resonance (Rowley and Williams, 2006). Over the last few decades, intensive research efforts have been made to mitigate and suppress these undesirable effects. As flows over cavities are essential in many engineering applications, the motivation for this work arises, the main objective is to develop passive methods that can significantly suppress the flow-excited acoustic resonance in shallow rectangular cavities and to help characterize the main parameters that improve the performance of the suppression methods to achieve the most practical and effective way to mitigate the flow-excited acoustic resonance phenomenon. In this study, the effect of two passive methods on suppressing the acoustic resonance excitation in shallow rectangular cavities is experimentally investigated, the first method is modifying the cavity edge geometry by introducing chamfered, rounded edges and different types of spoilers, the second method is placing a high frequency vortex generator in vicinity of the upstream edge, several configurations have been investigated

in flow with Mach number up to 0.45. Furthermore detailed measurements and numerical analysis have been conducted to help understand the reasons behind the suppression mechanism, so the methods can be developed and optimized accordingly.

1.2. Organization of the thesis

In the first chapter of this thesis the characteristics of the flow over cavities is discussed including the shear layer formation, the feedback mechanism in cavities, the vortical structures impingements and the flow-excited acoustic resonance phenomenon which is the subject matter of this study. Chapter two is a literature review for the methods that have been investigated to suppress the oscillations of flow over cavities, and describes the very recent methods developed. In chapter three, the experimental setup used is described in details. In chapter four the results of the experiments are presented and discussed. Chapter five presents and discusses the numerical simulation results. Finally the conclusions of the research are presented in chapter six and further recommendations are addressed.

1.3. Background

1.3.1. Categorization of cavities

Cavities can be categorized upon many parameters. Depending on the geometry, cavities are categorized into shallow and deep cavities where shallow cavity has a length larger than its depth (i.e. $L/D > 1$, where L is the cavity length and D is the cavity depth, see Figure 1-1) and vice versa for the deep cavity. Cavities can also be categorized upon the flow behaviour to open, transitional and closed cavities; in open cavities the flow separates at the upstream edge and the separated flow reattaches with the main flow at the downstream edge without reaching the cavity bottom wall, in closed cavities the flow reattaches to the bottom wall of the cavity, this classification is dependent on the flow characteristics such as the velocity and the incoming boundary layer (Lawson and Barakos, 2011). The pressure behavior in the cavity is highly influenced by the attachment of the flow to the cavity floor. Figure 1-2 shows a schematic of flow in cases of closed, transitional and open cavities, the pressure behaviour is also illustrated in Figure 1-3.

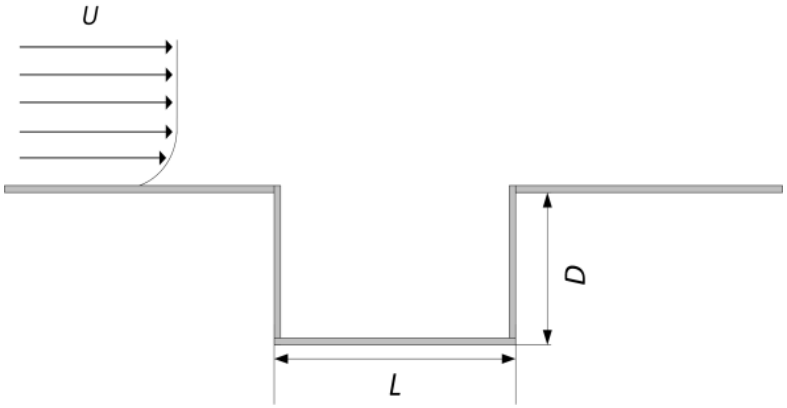

Figure 1-1: schematic drawing of a cavity

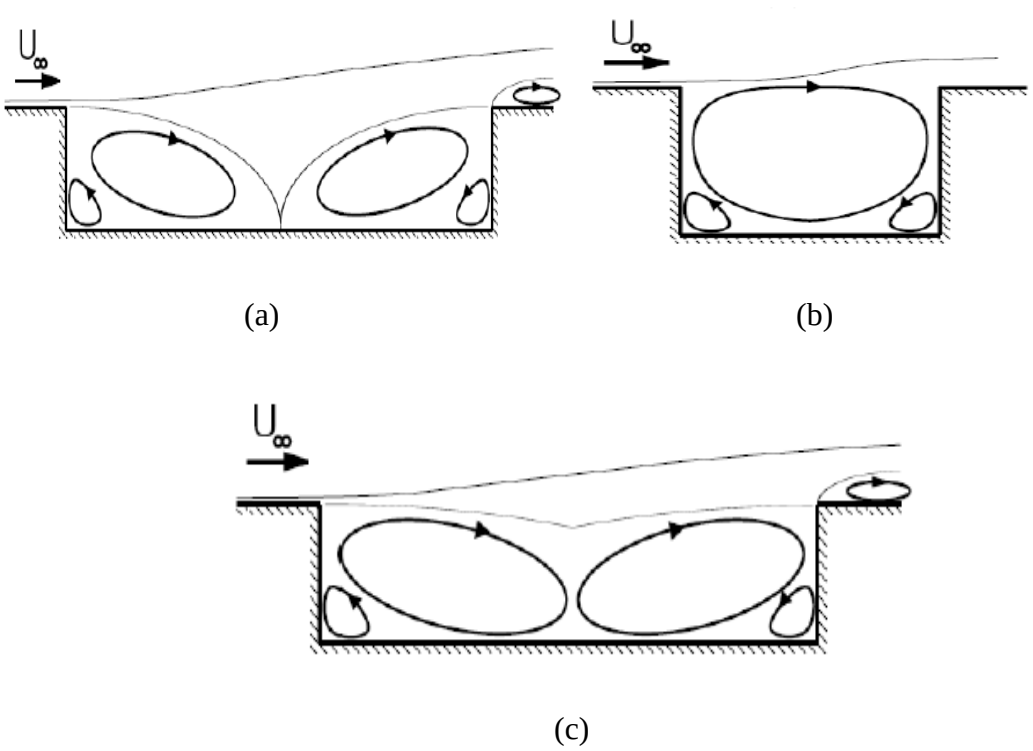

Figure 1-2: schematic of (a) closed cavity (b) open cavity (c) transitional cavity ***(Gloerfelt, 2009)***

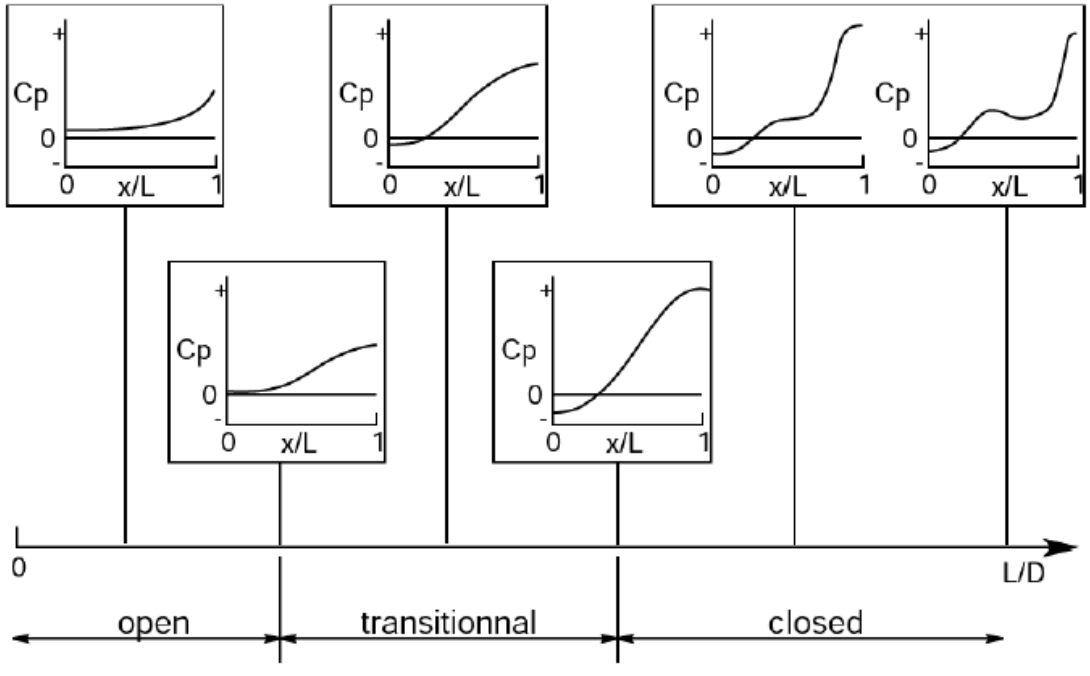

Figure 1-3: cavity floor pressure distribution for open, transitional, and closed cavities ***(Gloerfelt, 2009)***

1.3.2. Applications in industry

Flow over cavities is involved in many engineering applications and the increase of the interest in this field over the last few decades attracted many researchers to further understand the complex flow disturbances around cavities and also to mitigate the undesirable effects excited by this type of flow. One of the well-known applications that involve flow over rectangular cavity is the weapon bays in military aircrafts (Rossiter and Kurn, 1965). Another aerospace application is the open landing gear bay in aircrafts which shapes a cavity at the landing gear deployment, as shown in Figure 1-4. This is known to generate excessive noise that harms the area around the airports.

Flow through gate valves also resembles flow over cavities, as the bottom seat of the gate shapes a cavity. This is known to be a source of excessive noise in steam lines of power plants (Lacombe et al., 2013). Safety relief valves, shown in Figure 1-5, also known to excite acoustic resonance, which may lead to severe failures in steam generation piping systems of power plants. An additional application that resembles flow over deep cavities is the side branches in HVAC and piping systems, this is also known to generate acute noise during operation.

Figure 1-4: weapons bay and landing gear in aircrafts

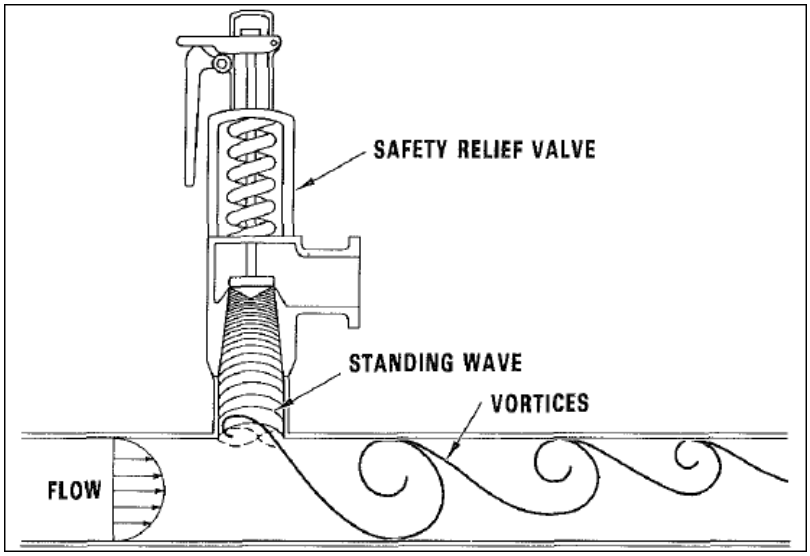

Figure 1-5: schematic of vortices in a safety relief valve ***(Baldwin and Simmons, 1986)***

1.3.3. Self-sustained oscillations in cavities

In this section, the self-sustained oscillation generated when flow passes over a cavity is explained. There are many aspects associated with the self-sustained oscillations in cavities including the feedback mechanism and the disturbances propagations along the impingement length, also these oscillations might be coupled with the acoustic standing waves as will be explained in the flow-excited acoustic resonance section.

The feedback loop in the cavity self-sustained oscillations is the substantial mechanism that magnifies the pressure perturbations in the flow. This mechanism occurs as the flow instability created due to the boundary layer separation results in shear layer formation at the cavity mouth, this shear layer amplify and shed along the impingement length resulting in interaction between the vortical structures in the shear layer with the downstream edge of the cavity. This interaction generates perturbations in form of waves that propagate upstream, these perturbations that propagate upstream organize the instability at the upstream edge of the cavity, and hence, closing a cycle of feedback oscillations. Rockwell and Knisely (1979) described the effect of the downstream edge and the closed cycle on the self-sustained oscillations by measuring the velocity fluctuations at different distances with and without an impinging edge, this is illustrated

in Figure 1-6. The impingement at the downstream edge can be categorized upon the clipping of the vortex at the edge to complete clipping, partial clipping, escape from clipping, and partial escaping as described in Figure 1-7.

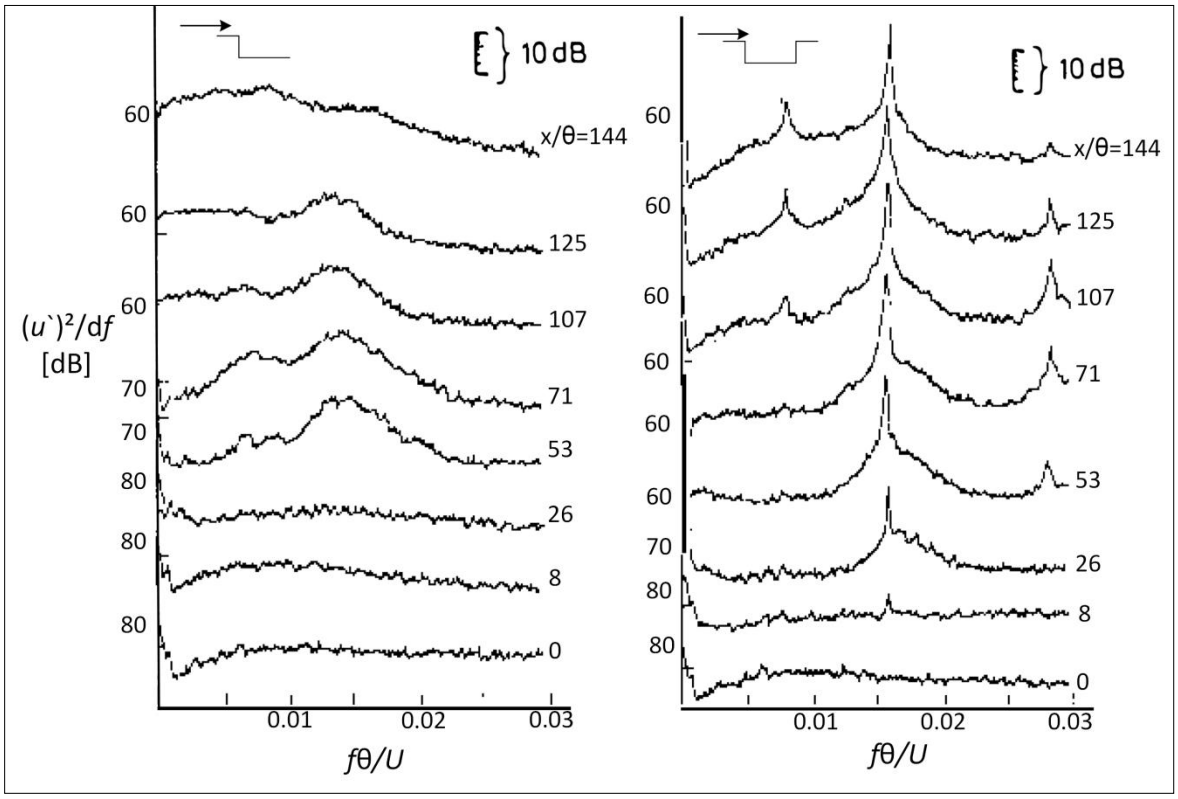

Figure 1-6 : the effect of the downstream impingement in the flow oscillations ***(Rockwell and Knisely, 1979)***

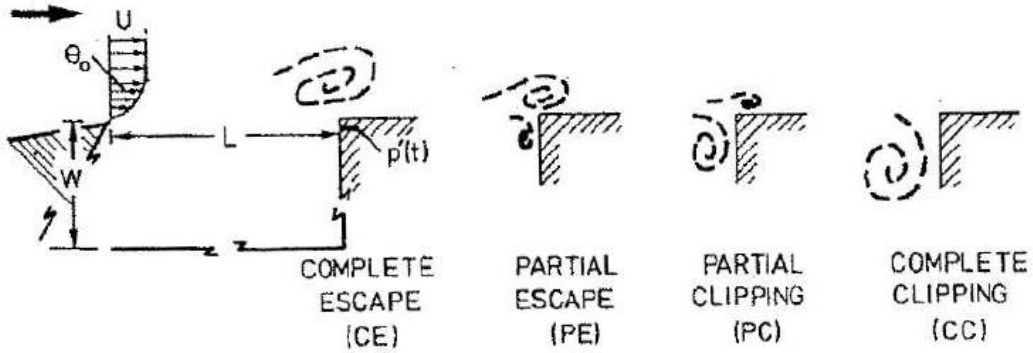

Figure 1-7 : impingement at the downstream edge ***(Gloerfelt, 2009)***

Heller and Bliss (1975) suggested that the pressure wave generated at the downstream edge results from a mass exchange process, this periodic mass addition and removal process generates a pressure wave in the cavity that propagates upstream to reflect at the upstream side of the cavity and propagates downstream. This mass exchange process can be resembled with a piston movement installed at the downstream side of the cavity. The propagation of the pressure wave introduces instability to the shear layer at the cavity mouth which interacts with the downstream edge. Therefore, a feedback loop is closed.

The oscillations generated when flow passes over a cavity were observed to have a specific frequency dependent on the impingement length and the flow velocity. The well known factor that describes the frequency of the oscillations is Strouhal number:

$$S_t = \frac{fL}{U} \qquad (1)$$

where St is Strouhal number, U is the upstream flow velocity, f is the frequency of the dominant oscillations, and L is the characteristic length which is the cavity length in this case.

The values for Strouhal number were observed to follow specific trends as illustrated in Figure 1-8, where each segment has a specific Strouhal number. The same trends in the oscillations frequencies were observed in other impinging configurations including jet edge oscillations and mixing layer edge oscillations which correlate all these types of oscillations and indicate the common driving mechanism. Further visualization studies proved that each stage represents a number of vortices structured along the impingement length, as shown in Figure 1-9, known as shear layer modes (Ziada and Rockwell (1982))

1.3.4. Flow-excited acoustic resonance

The self-sustained oscillations developed when flow passes over a cavity can cause severe noise and/or excessive vibrations that sometimes may lead to structural failures. Naudascher (1967) categorized the self-sustained oscillations into: fluid dynamic, fluid resonant, and fluid elastic types of oscillations as shown in Figure 1-10. Fluid dynamic oscillation is generated by the unsteadiness of the flow generated by the boundary layer separation at the upstream edge of the cavity. The fluid resonant oscillation which is the

subject matter of this work occurs when the flow oscillations are affected by the acoustic waves generated in the flow. The fluid elastic type involves a motion of a boundary of the flow enclosure as illustrated in Figure 1-10.

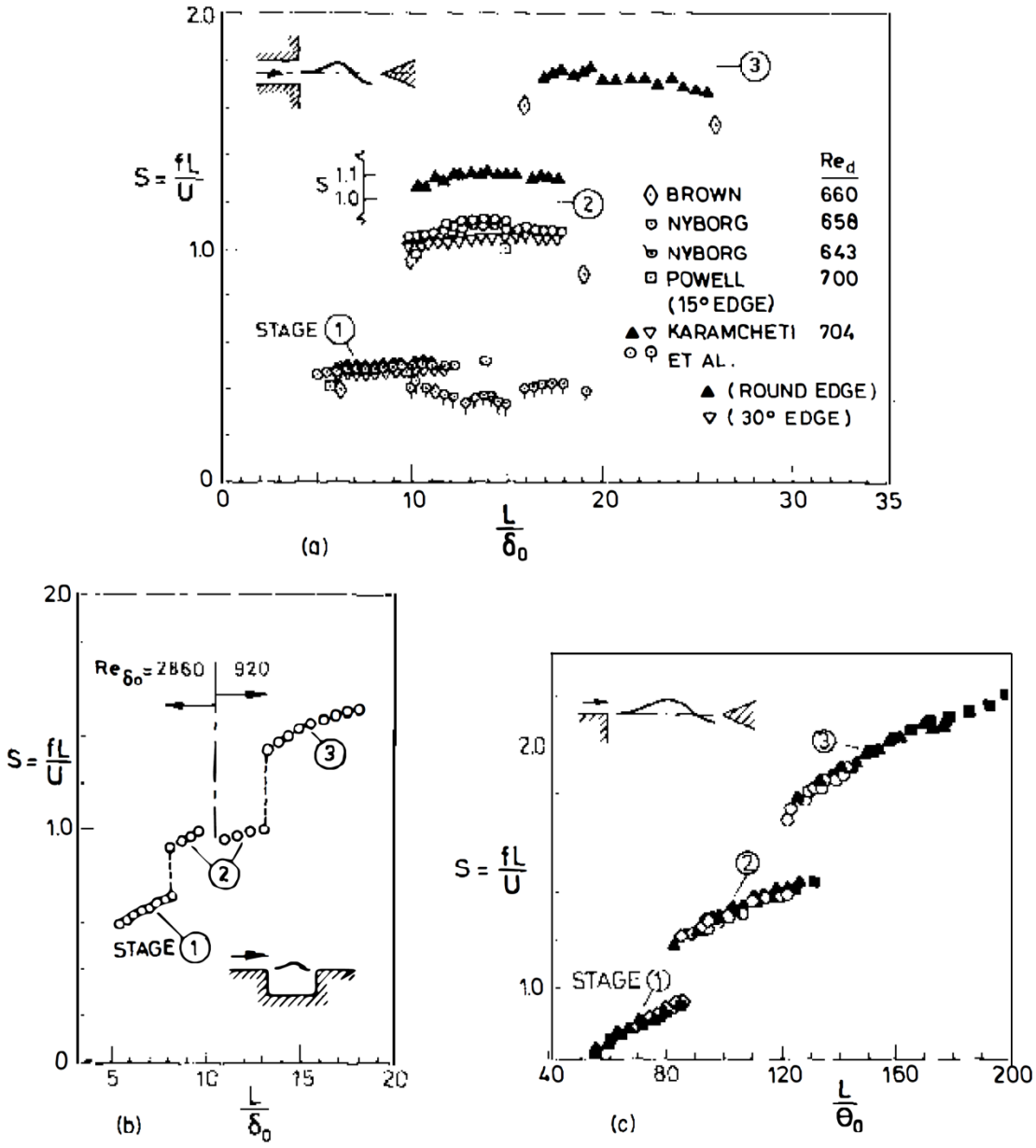

Figure 1-8: relation between Strouhal number and the dimensionless impinging length for (a) jet-edge oscillation (b) cavity oscillations (c) mixing layer edge oscillations ***(Rockwell and Naudascher, 1979)***

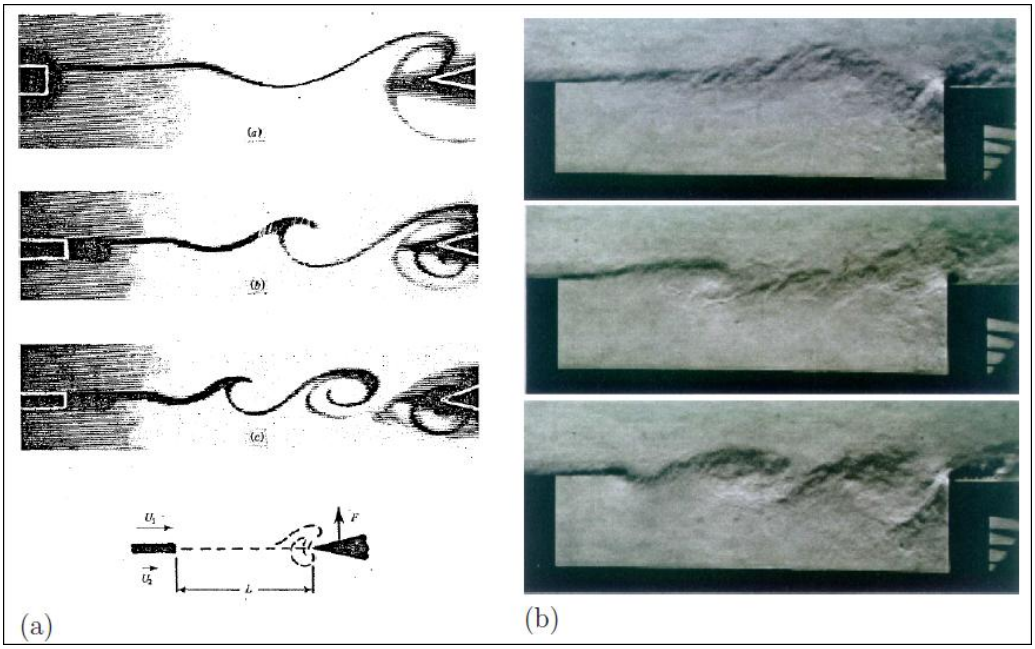

Figure 1-9 : number of vortices in (a) mixing layer edge flow ***(Ziada and Rockwell, 1982)****(b) flow over cavity* ***(Cattafesta et al., 1998)***

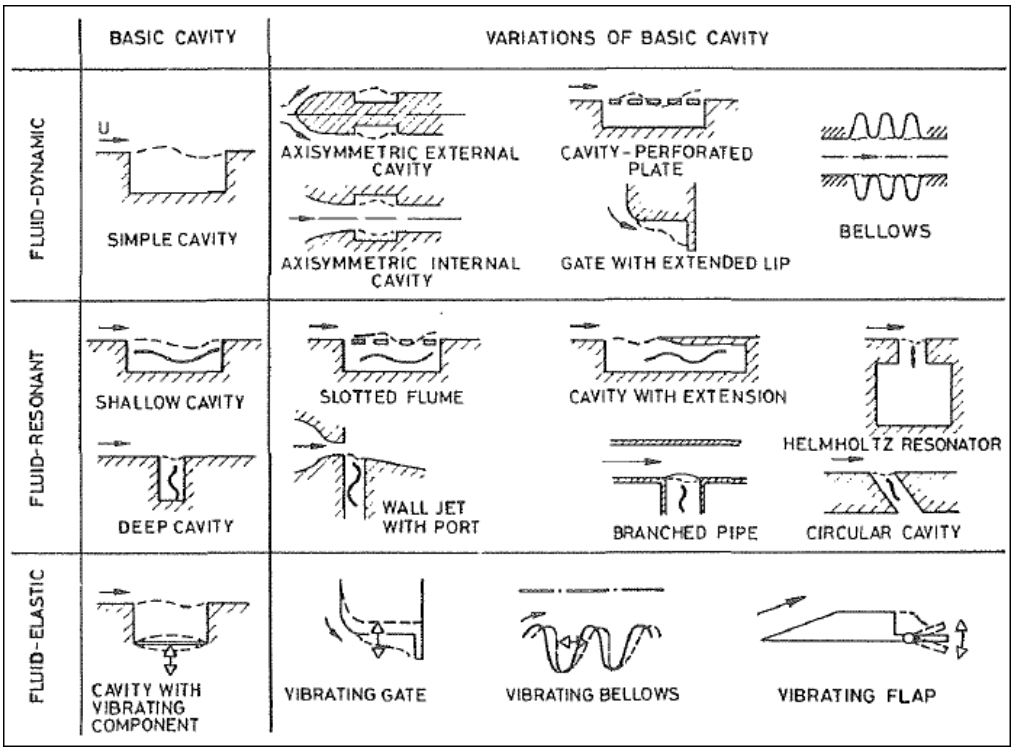

Figure 1-10: Fluid dynamic, fluid resonant, and fluid elastic types of oscillations ***(Rockwell and Naudascher, 1978)***

When flow passes over a cavity, a boundary layer separation occurs at the upstream edge and results in a formation of a shear layer over the cavity mouth, as shown schematically in Figure 1-11. The shear layer formation creates vortices that are carried with the flow to impinge on the downstream edge. The impingement of these vortices on the downstream edge generates pressure perturbations at the downstream edge of the cavity that travel upstream and enhance the shear layer separation at the upstream edge and act as a feedback cycle of oscillations. Moreover, a sound generation occurs at the downstream edge caused by the vortices impingement and creating standing waves known as acoustic modes in the accommodating enclosure for the case of confined cavities. The sound wave coupling with the flow oscillations results in what so called flow-excited acoustic resonance (Mohany and Ziada (2005), Blevins (2001),Rockwell et al. (2003)). When this phenomenon is excited the acoustic pressure amplifies significantly which can be harmful in many ways, also the phenomenon is associated with a significant increase in the flow drag. When the flow-excited acoustic resonance is generated a lock in region is observed, where the shear layer oscillation frequency locks into one of the acoustic resonance frequency of the confined enclosure over a certain range of flow velocity. The geometry of the upstream and downstream edges plays a significant role as the upstream edge controls the boundary layer separation and the vortices formation in the cavity, while the downstream edge controls the vortices impingement, the feedback oscillations, and the sound generation.

The number of vortices developed by the shear layer in the cavity represents the shear layer modes. These shear layer modes may excite the acoustic resonance whenever the flow has enough energy to overcome the acoustic damping of the system and the oscillation frequency coincides with one of the acoustic natural frequencies of the accommodating enclosure, as shown schematically in Figure 1-12. The shear layer modes behavior is governed by the Strouhal relationship.

The standing waves formed in the accommodating enclosure is dependent on the enclosure dimensions and confinement of the cavity. Many acoustic modes can develop in the enclosure including longitudinal, cross sectional and stream wise modes.

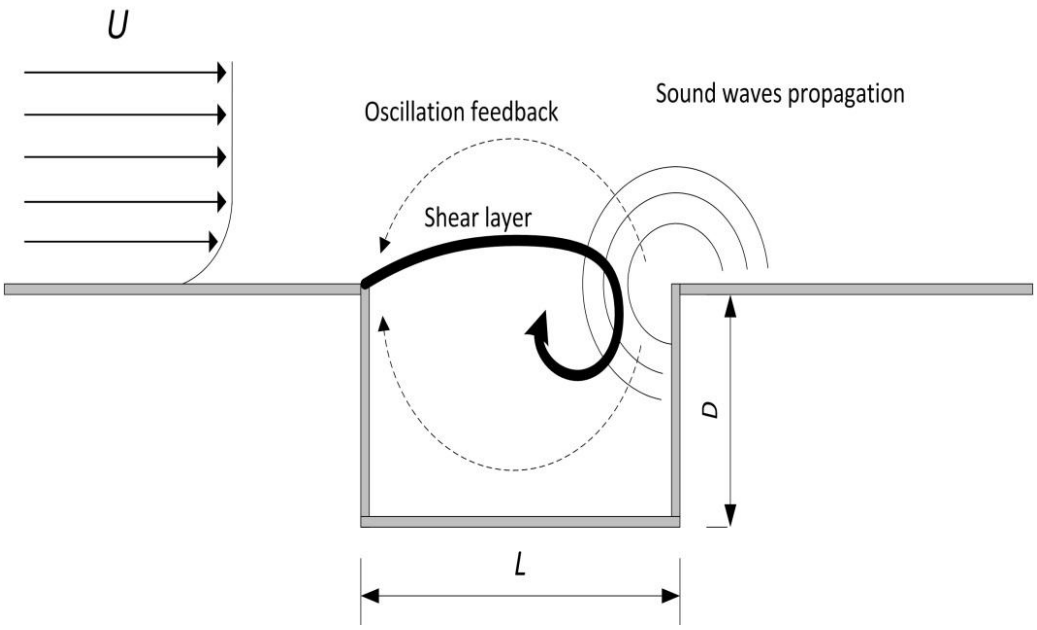

Figure 1-11: schematic of flow over cavity and propagation of sound

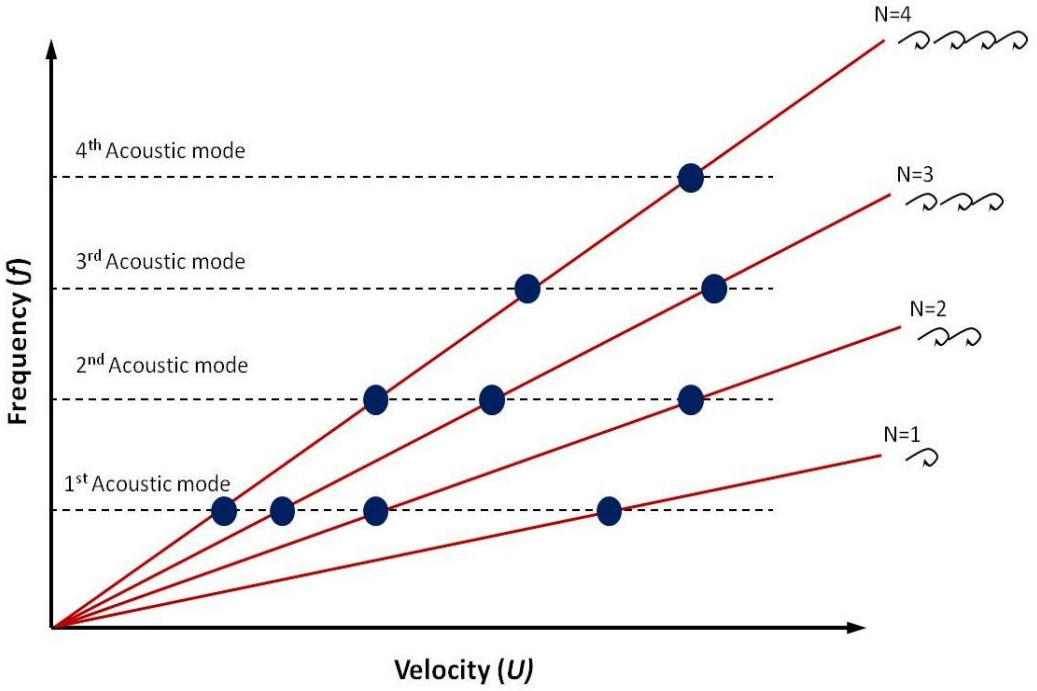

Figure 1-12: schematic of the shear layer modes and the acoustic modes

1.3.5. Rossiter formula

The frequency of the oscillations in the cavity can be predicted by a formula developed by Rossiter (1964). As mentioned earlier the vortices interaction at the downstream edge generates sound that influence the flow instabilities. Rossiter formula postulates that the time required from the vortices to travel downstream to the trailing edge and the opposite travel by the sound to the upstream edge governs the frequency of the oscillations in the cavity. The time required by the vortices to travel along the cavity is *L/U* where *L* is the cavity length and *U* is the main flow velocity that carries the voritces. The time required from the sound to travel upstream to the separation point is *L/c* where *c* is the speed of sound. Hence, the frequency *f* of the oscillations can be obtained from

$$\frac{L}{c} + \frac{L}{U} = \frac{n}{f} \qquad (2)$$

where n is the number of the mode as described earlier. To fit the results obtained from the experiments with the theoretical results, Rossiter postulated a phase lag between the downstream interaction and the sound emission by α. The final formula can be written as (Gloerfelt, 2009);

$$St = \frac{n-\alpha}{\frac{1}{k}+M} \qquad (3)$$

Where n is the number of the mode, α=0.25 and k=0.57 are empirical constants, and M is Mach number. The values of the phase lag needs to be adjusted according to the *L/D* ratio to obtain the most accurate results, these values are summarized in Table 1-1. Rossiter formula was found to have a quite accurate estimation compared to the experimental results, Figure 1-13 shows the agreement between the values from the formula and experimental data obtained by Kegerise (1999).

Table 1-1: phase lag values for different L/D ratios

L/D	α
4	0.25
6	0.38
8	0.54
10	0.58

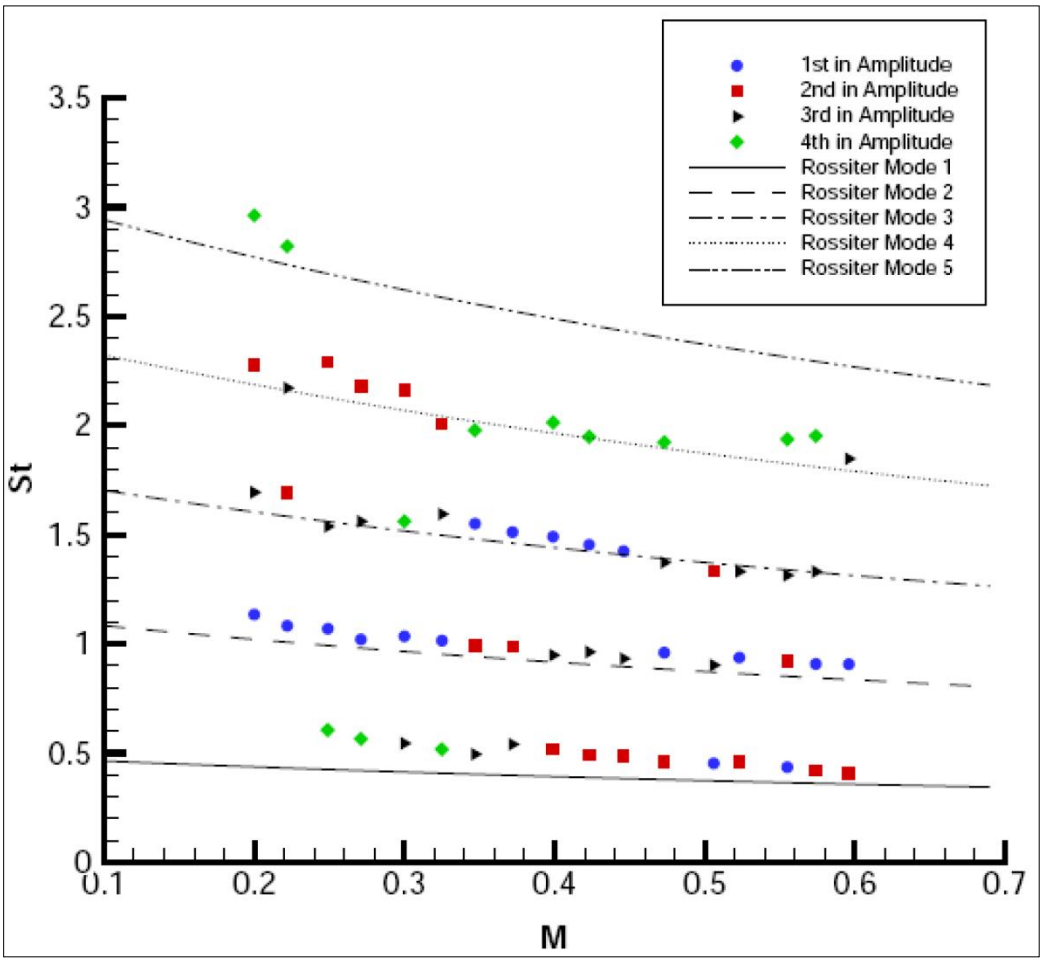

Figure 1-13: shear layer modes frequencies obtained experimentally and theoretically using Rossiter formula ***(Kegerise, 1999)***

The cavity dimensions play a significant role in the pressure behaviour and the flow oscillations in the cavity, and many research efforts were done towards the understanding of the cavity oscillations with different cavity dimensions. The oscillations in the cavity are strongly related with the cavity length, and many studies found that there is a

minimum length for the cavity to sustain the oscillations. Sarohia (1977) related the dimensionless length ($L_m.Re^{1/2}/\delta$), where δ is the shear layer thickness at the separation point, with the occurrence of the oscillations. Sarohia found that the minimum length for the onset of oscillations in the case of cavity with depth more than twice the shear layer thickness seems to be independent of the cavity depth, this is illustrated in Figure 1-14 .

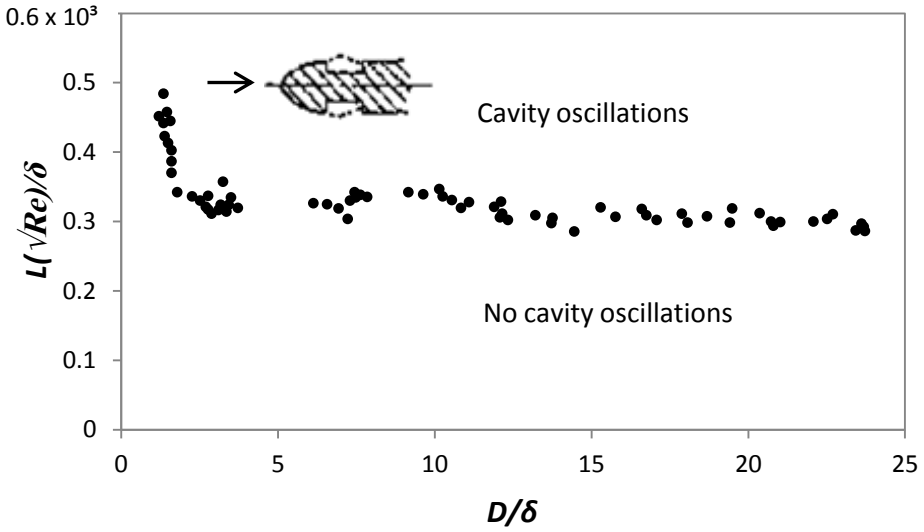

Figure 1-14: minimum cavity length for onset of oscillations with respect to cavity depth and shear layer thickness ratio, regenerated from ***(Sarohia, 1977)***

The depth of the cavity has a major effect on the oscillations generated, where the very deep cavities have more of broadband spectra without distinguished self sustaining oscillations when compared to shallow cavities. Nakiboğlu et al. (2012) presented intensive experimental and numerical studies on the effect of the depth of cavities on the longitudinal modes excited in axisymmetric cavities. The experiments were conducted in two different configurations depending on the cavity location from the test section inlet. Several cavities with different aspect ratios (*L/D*) ranging from 0.85 to 5 were tested. Nakiboglu et al. (2012) found that for the cavities with aspect ratios ranging from 2 to 5, increasing the depth of the cavity results in shifting the Strouhal number of the modes to higher values, and the dimensionless pressure fluctuations $|u`|/U$ increase as well. For the aspect ratios from 0.85 to 1.48 the pressure fluctuations are not significantly affected by the cavity depth, this is illustrated in Figure 1-15. When comparing the dimensionless acoustic source power for the different aspect ratios, Nakiboglu et al. (2012) found that

the peaks are shifted to higher Strouhal numbers within the first range and have no significant change within the second range as observed with the pressure fluctuations.

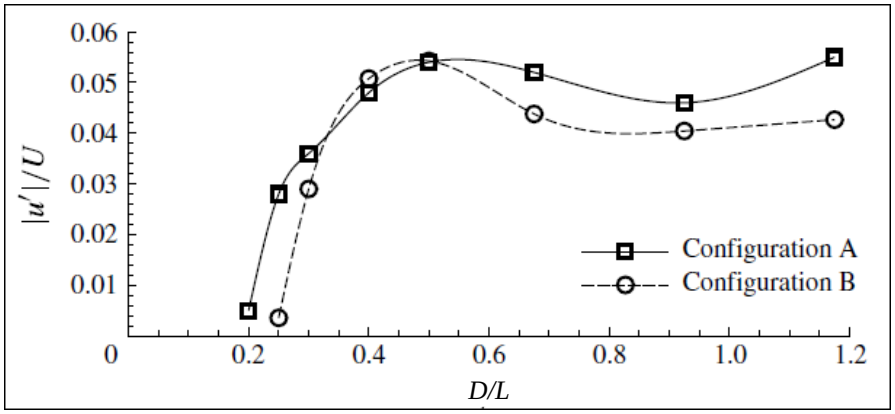

Figure 1-15: pressure fluctuations for several depth to length cavity ratios (A) the cavity installed at the end of the test section (B)the cavity installed at the beginning of the test section ***(Nakiboğlu et al., 2012)***

2. Literature review

The study of flow past cavities has driven numerous research efforts since the early 1950's by Krishnamurty (1955) and Roshko (1955) because of its relevant importance in many engineering applications such as aircraft weapon bays [e.g.Rossiter and Kurn, (1965), Lawson and Barakos (2011)], side branches in piping systems and HVAC [e.g. Bruggeman et al. (1991), Knotts and Selamet (2003)], and valves [e.g. Baldwin and Simmons (1986), Lacombe et al. (2013)]. As the significance of this topic is interestingly increasing, several review articles about the flow over cavities have been published [e.g. Rockwell and Naudascher (1978), Lawson and Barakos (2011), Ziada and Lafon (2013), Gloerfelt (2009)]. Several techniques have been developed to suppress the undesirable effects associated with the flow-excited acoustic resonance and they can be categorized into active and passive techniques as shown in Figure 2-1. The active techniques involve control loops that apply external energy to the system [e.g. Cattafesta and Williams (2003), Ziada et al. (2003), McGarth and Shaw (1996), Sarno and Franke (1994), Rowley and Williams (2006)], while the passive techniques are achieved by modifying the geometries in a way that changes the flow characteristics. The passive techniques used in attenuating the flow oscillations and the resonance effect have been the subject of many studies including modifying the geometry of the upstream and downstream edges.

Rossiter (1964) work contributed considerably to the understanding of the pressure behaviour for flow over cavities. The study included shallow and deep cavities and the pressure measurements were taken at nine different locations along the cavity. Rossiter (1964) noticed that the pressure fluctuations are generally periodic and a distinguishable peak in the pressure spectrum appears at specific frequency. Moreover, Rossiter (1964) found that decreasing the cavity depth results in random pressure spectrum and for a very shallow cavity the pressure spectrum turn into smooth broad band spectrum. Rossiter suggested that the periodic pressure fluctuations are produced because of acoustic resonance in the cavity. To suppress these pressure fluctuations Rossiter (1964) investigated different spoilers placed near the upstream edge of the cavity; it was found that these spoilers can significantly mitigate the pressure fluctuations. Since the work of Rossiter (1964), many research efforts have been dedicated to develop suppression

methods for flows over cavities. Many methods have been investigated including modifying the cavity geometry by chamfering or rounding the cavity edges, introducing spoilers and vortex generators, and using high frequency vortex generator (control cylinder). However, the physics of the suppression effect of these techniques on the acoustic resonance excitation is not clearly understood, and the spoilers dimensions and configurations are not fully addressed. In the following sections the history of these methods is discussed.

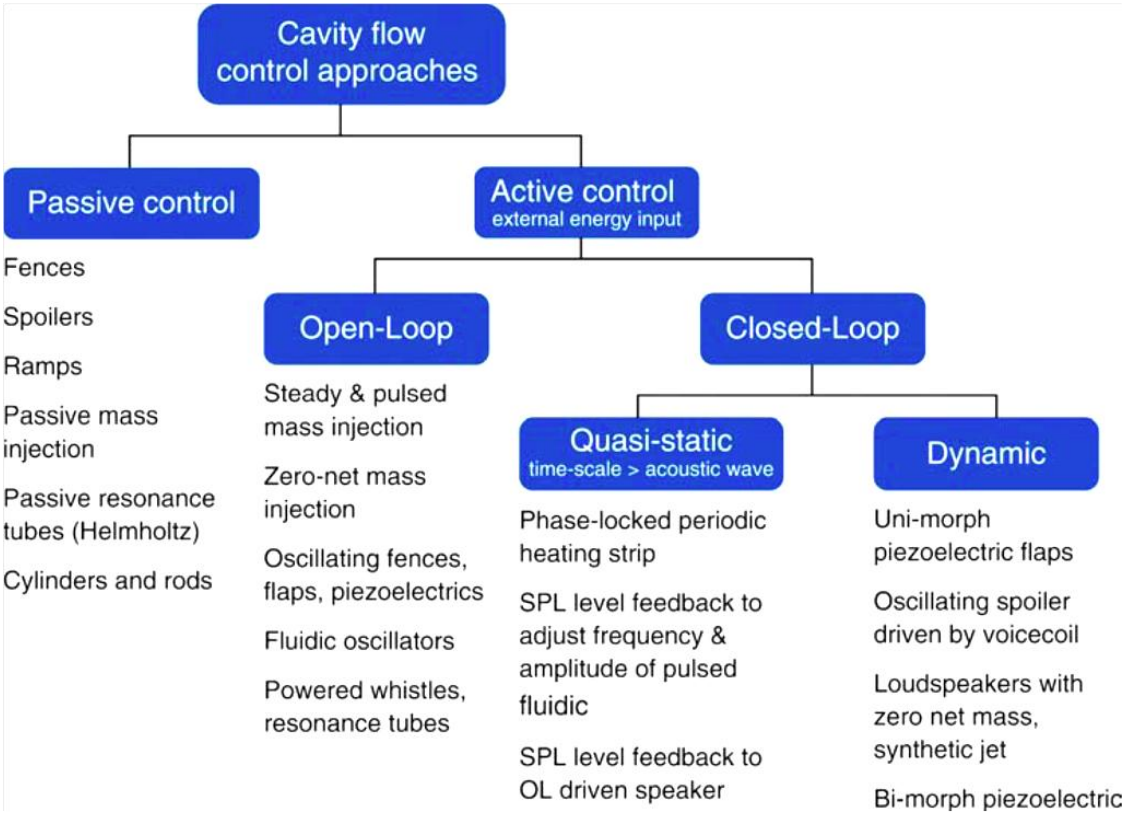

Figure 2-1:categorization of suppression methods originally from ***(Cattafesta and Williams, 2003)*** *and modified by* ***(Rowley and Williams, 2006)***

2.1. Cavity geometry

Modifying the cavity geometry by chamfering or rounding the edges has been a subject of many studies. Ethembabaoglu (1973) studied different upstream edges effect on the fluid dynamic oscillations which does not involve acoustic excitation, and found that all

of the edges can attenuate the oscillations as illustrated in Figure 2-2. Chamfering the cavity edges were investigated by many researchers, Franke and Carr (1975) investigated wide range of edges including chamfered edges installed upstream and/or downstream in rectangular cavities in water channel and air tunnel, the configurations were initially tested on the water channel and then the effective configurations in mitigating the pressure oscillations were tested in the air tunnel. In the air flow study, the experiments were conducted in supersonic flows over cavities with aspect ratios of 2, 3.5, and 4.25 and some configurations were found to be effective on attenuating the fluid resonant effects. Franke and Carr (1975) found that the effectiveness of the double chamfered edges is a subject of the flow separation point, and they were only effective when the separation is near the upstream chamfered edge.

The effect of the different cavity geometries on the fluid resonant oscillations was investigated by Heller and Bliss (1975) in shallow rectangular cavities in flows with Mach number of 0.8 and 2.0. The cavities investigated had aspect ratios of 2.3 and 5.5. Heller and Bliss (1975) intensively studied the physics behind the pressure fluctuations and provided an analytical model for the phenomena, according to this understanding they investigated several geometries that were able to significantly mitigate the pressure oscillations in shallow rectangular cavities. Heller and Bliss (1975) postulated that one of the basic principles of the cavity oscillations is the mass exchange resulting from the interaction at the downstream edge of the cavity. Hence, they suggested that the pressure oscillations in a cavity can be mitigated by preventing this mass exchange by changing the cavity geometry, or by increasing the instability of the shear layer which can be achieved by introducing a spoiler upstream of the cavity. According to this, a chamfered downstream edge was investigated combined with/without a spoiler in the upstream and with/without a detached cowl at the downstream edge as shown in Figure 2-3. The downstream edge was chamfered to alter the downstream interaction characteristics and the detached cowl was attached to prevent the mass exchange process. Both configurations of chamfered downstream edge with a spoiler and a chamfered downstream edge with a detached cowl were found to be effective and able to reduce the pressure by around 20 dB.

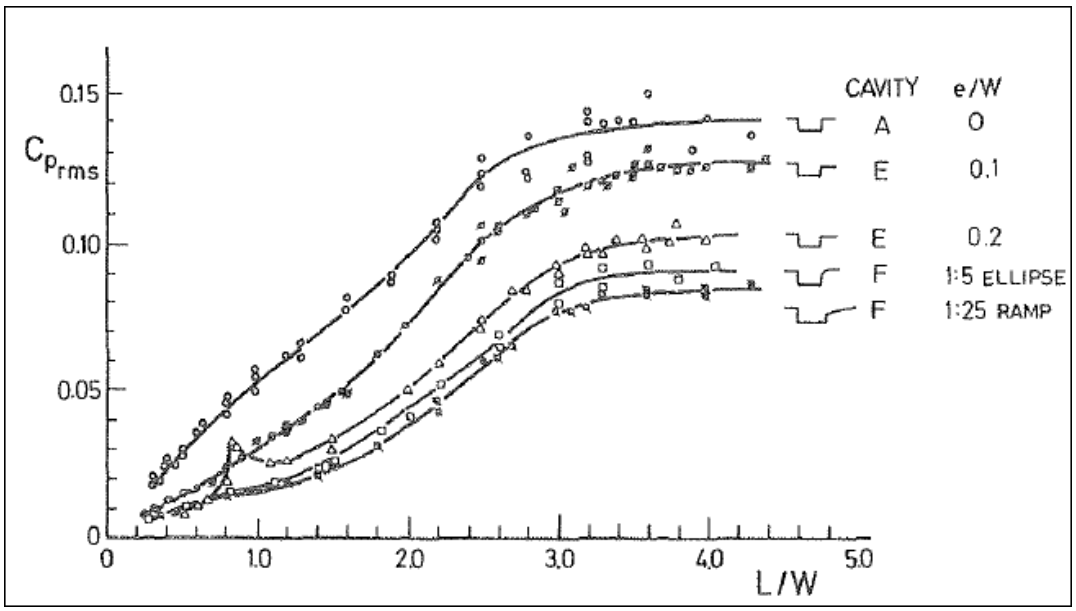

Figure 2-2: fluctuation pressure coefficient for different cavity geometry ***(Rockwell and Naudascher, 1978)***

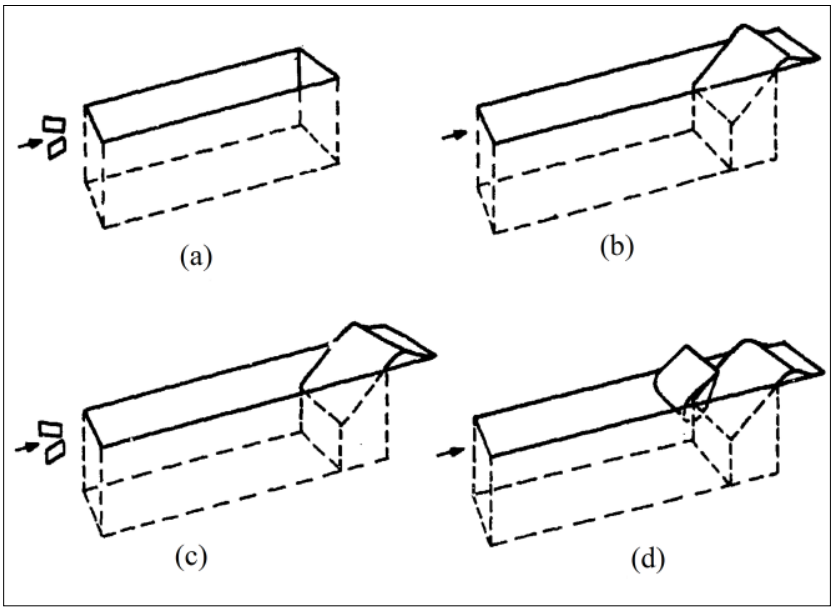

Figure 2-3: (a) cavity with spoilers (b) cavity with chamfered downstream edge (c) cavity with spoilers and chamfered downstream edge (d) cavity with detached cowl and chamfered downstream edge

One of the investigations on safety relief valves was done by Baldwin and Simmons (1986). They studied the flow induced vibration that occurs in safety relief valves, which may cause the failure of the valves in piping systems. They noticed that the pressure pulsation is significantly magnified when the acoustic resonance is excited. One of the

solutions suggested by Baldwin and Simmons (1986) was to round or chamfer the edges of the safety relief valve by an angle of 45°, this is illustrated in Figure 2-4.

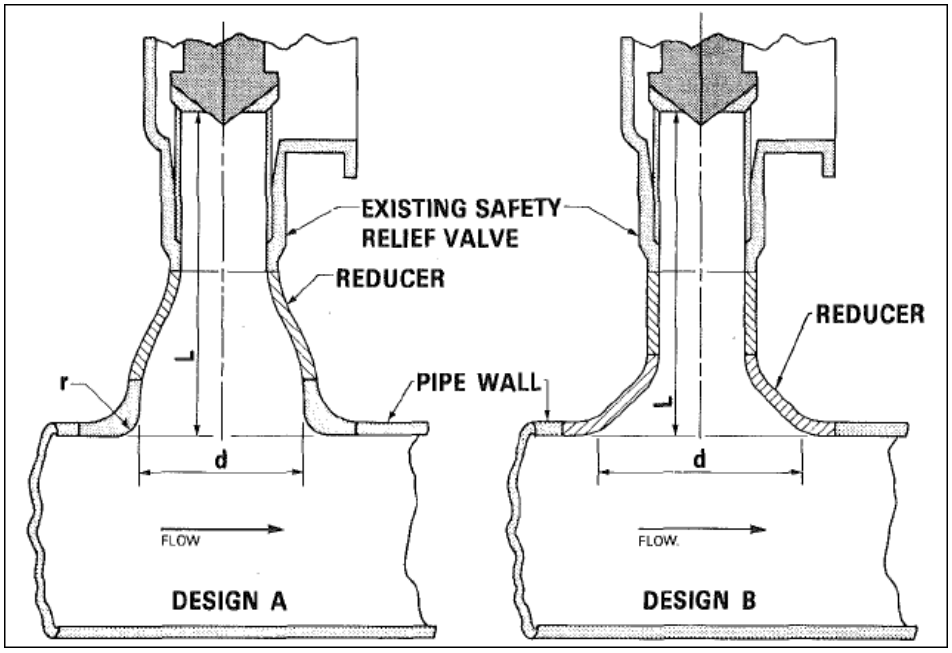

Figure 2-4: designs introduced by ***(Baldwin and Simmons, 1986)*** *to mitigate vortex generation*

Knotts and Selamet (2003) compared ramp, chamfered, and round edges with different dimensions to the normal sharp edge in side branches with different depths. The chamfered and rounded edges were installed in both upstream and downstream, while ramps were installed only in the upstream edge. The experiments were conducted in a test section with a piston that can yield different depths and the flow Mach number was less than 0.3. They concluded that the ramp which directs the flow away from the cavity has the best performance between the other tested edges. However, as illustrated in Figure 2-5 some ramped edges with specific dimensions were observed to introduce other peaks in the spectra.

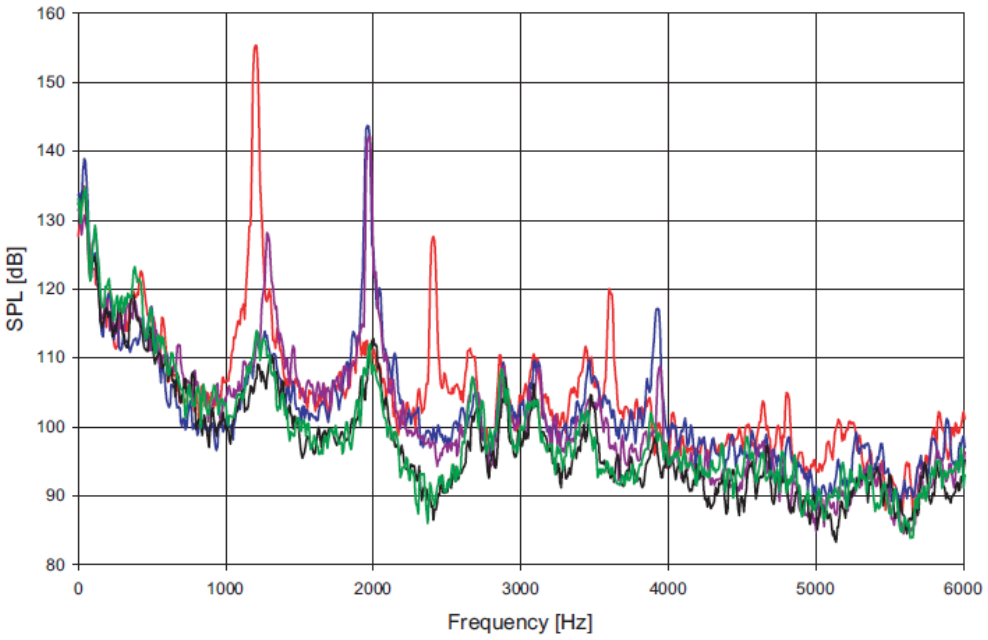

Figure 2-5: SPL versus Frequency; comparison of square and upstream ramp Red: Square edge, ramp edge with h/d=(1/8 blue), (¼ purple), (½ black), (3/4 green) ***(Knotts and Selamet, 2003)***

2.2. Spoilers and vortex generators

Spoilers and vortex generators are known to have an effective performance in mitigating the cavity oscillations. Bruggeman et al. (1991) investigated different spoilers and rounded edges in side branches. The study concentrated on the edge effect in cases of single and multiple side branches. Moreover, they introduced a theoretical model that explains the acoustic resonance on side branches. According to this model, they developed spoilers that were able to significantly mitigate the resonance pulsations. Despite the commonly known assumption that rounding off the side branches edges suppresses the pulsations, Bruggman et al. (1991) found that this effect is dependent on the configuration, where in the single side branch it was found to be suppressive to round the edges while in multiple side branches rounding the edges may actually enhance the resonance pulsation as show in Figure 2-6. The spoilers investigated, shown in Figure 2-7, were found to be effective in suppressing the resonance pulsation and this effect was attributed to the shear layer stabilization introduced by the spoilers as they increase the shear layer momentum thickness.

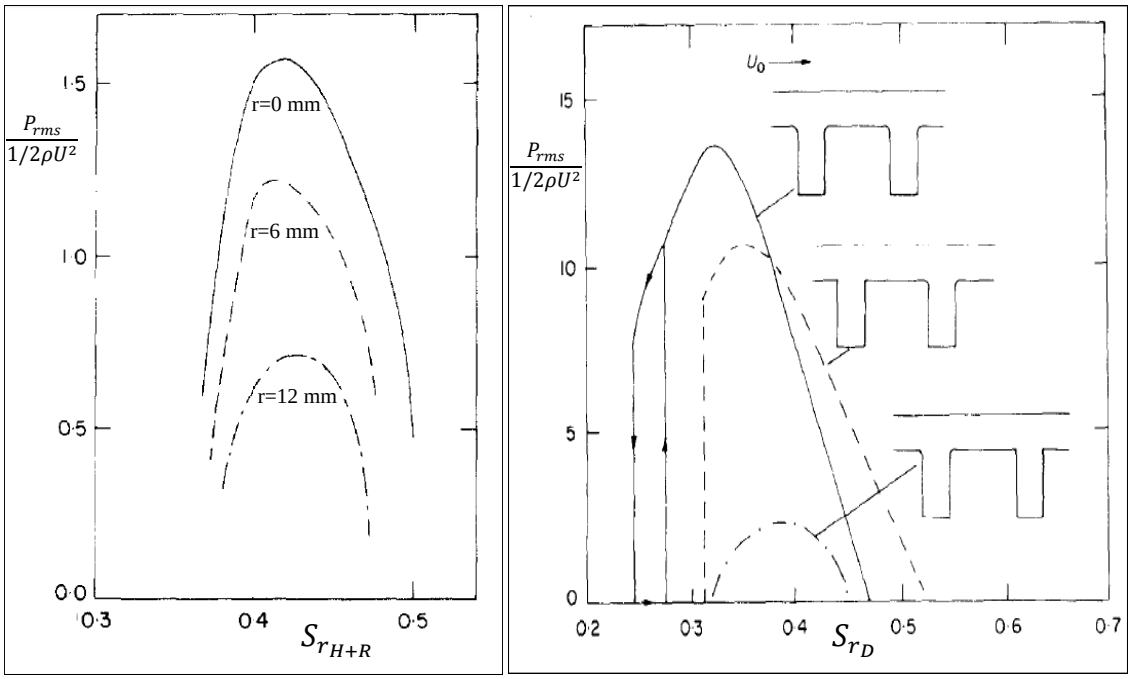

Figure 2-6: effect of rounding edges on the pressure pulsation (left) effect of rounding edges on pressure pulsation in tandem side branches (right) ***(Bruggeman et al., 1991)***

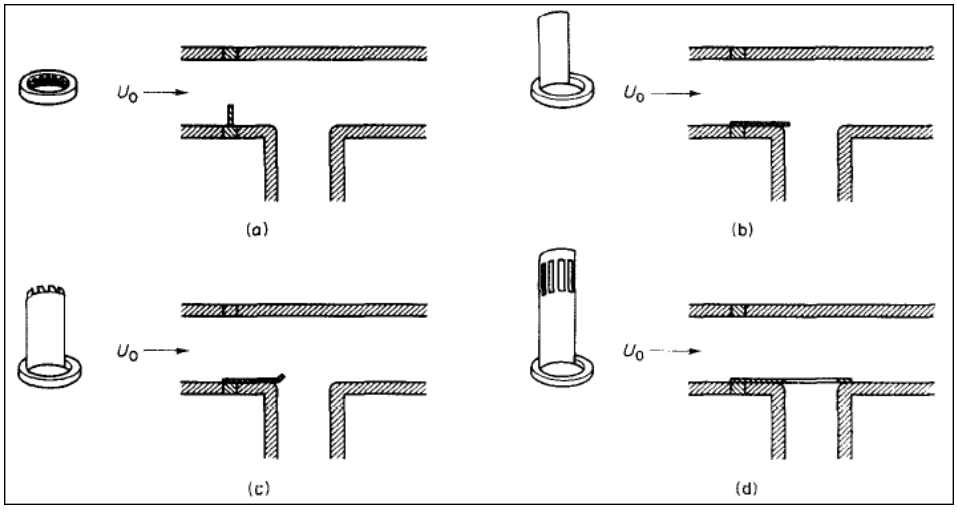

Figure 2-7: spoilers investigated by ***(Bruggeman et al., 1991)***

Shaw (1979) investigated the effect of spoilers and deflectors installed in the upstream edge of a shallow rectangular cavity in subsonic and supersonic flows, the spoilers and the deflectors were tested with/without a chamfered and deflector edges installed at the downstream edge. A 20 dB reduction of the pressure oscillations were observed when the upstream spoiler is combined with a trailing edge ramp. Shaw found that the effective combinations remain effective on both subsonic and supersonic flows, also, observed that the suppression edges investigated result in increasing the cavity temperature and reducing its static pressure.

One of the very successful methods in suppressing the resonance excitation was introduced by Karadogan and Rockwell (1983), the main concept was to introduce a stream wise vorticity orthogonal to the main vortices develop at the cavity mouth due to the boundary layer separation. Introducing these orthogonal vortices result in preventing the main vortices at the cavity mouth from developing. These stream wise vorticity were introduced by means of vortex generator as illustrated in Figure 2-8. It was found that the vortex generators are able to significantly suppress the resonance excitation by generating the stream wise vorticity, nevertheless, they found that the height of the vortex generator should be at least double the momentum thickness of the shear layer and with incident angle of more than 30 degrees, this is illustrated in Figure 2-9.

Several other edge geometries have been investigated by Dix and Bauer (2000) in subsonic, transonic, and supersonic flows. Several spoilers were investigated including saw-tooth spoilers with fine and coarse pitch solid spoilers, and what they called flap-type spoilers that direct the flow out of the cavity. The heights of the spoilers investigated were selected upon the thickness of the boundary layer which was estimated to be 3.81 mm at Mach number of 5. The heights investigated were 1δ, 2δ, and 3δ, where δ is the boundary layer thickness. The spoilers investigated were found to be effective in suppressing the acoustic pressure and the reason was suggested to be the increase of the boundary layer downstream of the spoilers.

Schmit et al. (2005) investigated several types of suppression methods, the methods were classified to high and low frequency devices. The high frequency technique depends on suppressing the turbulence in the shear layer while the low frequency enhances the turbulence, and both methods distract the normal cavity oscillations. All suppression

methods were tested at Mach number of 0.85 and 1.19. Some of the investigated geometries were saw-tooth spoilers, a cylinder, and a cylinder with a wire wrapped around it, as shown in Figure 2-10, to change the vortex shedding characteristics. Schmit et al. (2005) found that the rod and the wire wrapped rod is slightly effective in suppressing the acoustic pressure for the flow with Mach number of 0.85, for the flow with Mach number of 1.19, the method was found to be not effective. The saw-tooth spoiler was also found to be effective only with the subsonic flow, and a reduction of 6 dB was observed in the tonal peak while at Mach number of 1.19 the tonal peak increased by 1 dB.

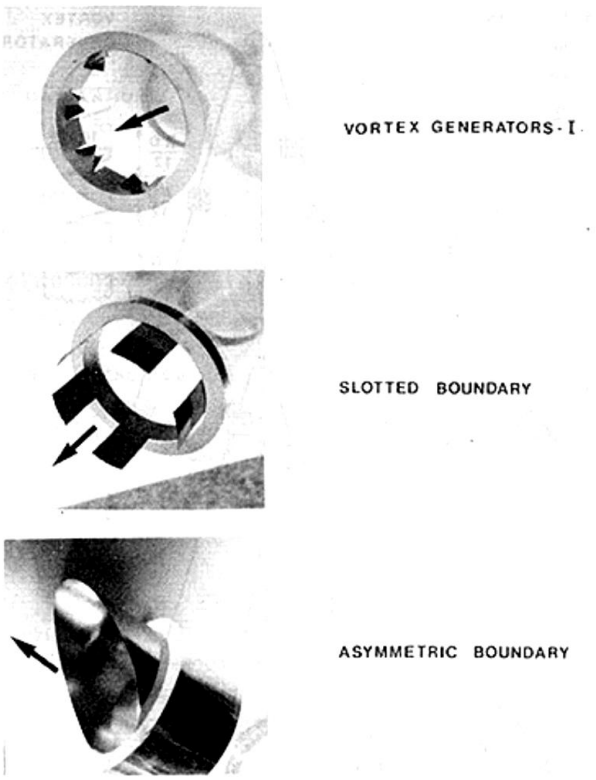

Figure 2-8: pressure pulsation attenuators investigated by ***(Karadogan and Rockwell, 1983)***

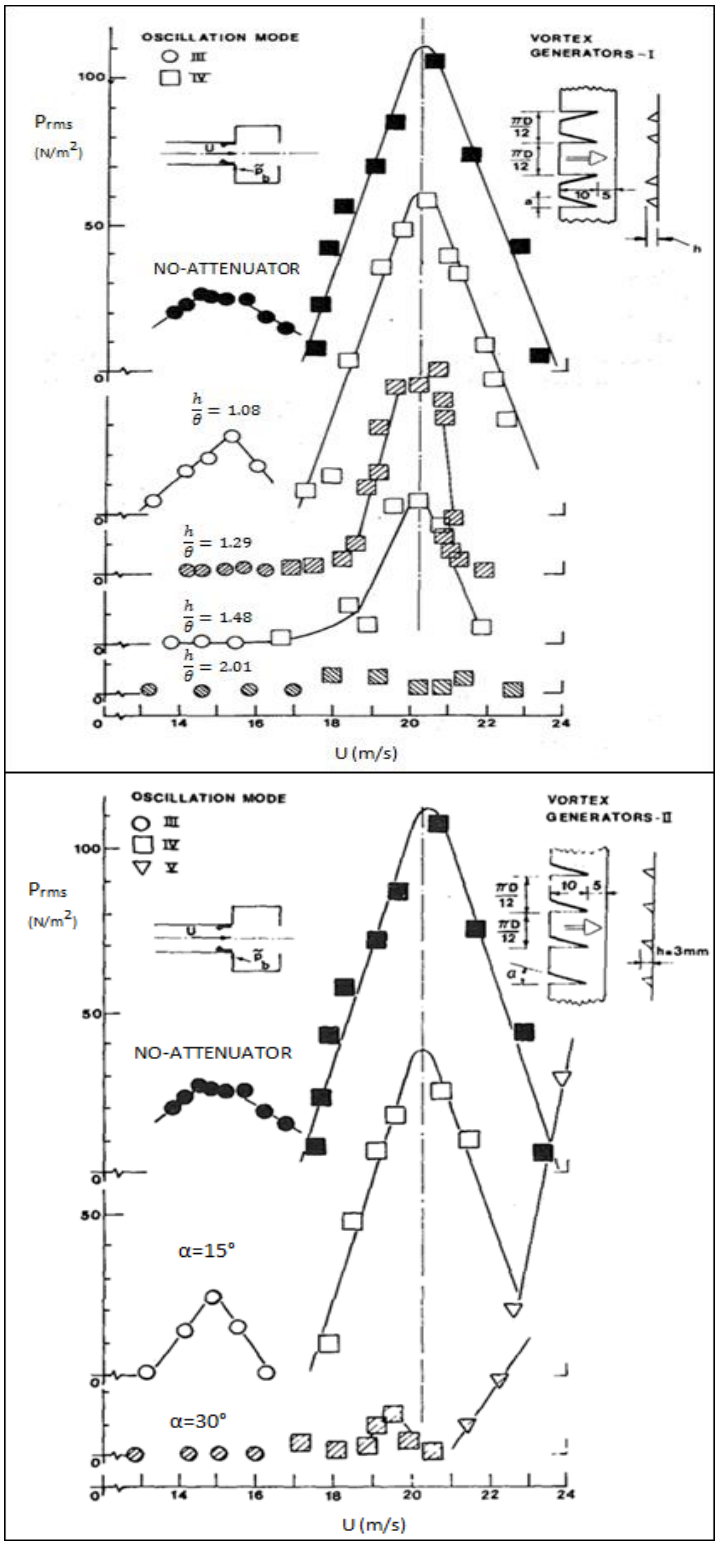

Figure 2-9: effect of vortex generator height on the pressure pulsation(left) effect of the vortex generator angle on the pressure pulsation(right) ***(Karadogan and Rockwell, 1983)***

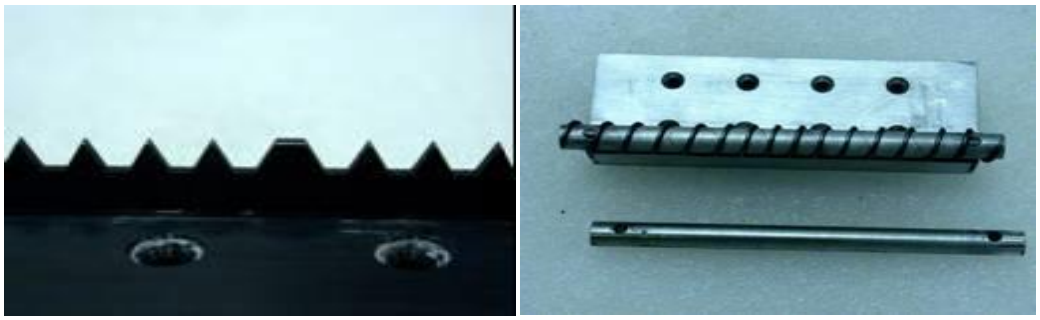

Figure 2-10: saw tooth spoiler (left) cylinder with/without a wire wrap (right) (Schmit et al., 2005)

More recently, Bolduc et al. (2013) studied the effect of the upstream edge geometry on the acoustic resonance excitation in axisymmetric cavities. The tested edges were round edges, chamfered edges, ramp and delta spoilers (i.e. spoilers that are converging together as shown in Figure 2-11) which were inspired by the vortex generator developed by Karadogan and Rockwell (1983). Among the investigated edges, Bolduc et al. (2013) found that the delta spoilers have the best performance in suppressing the acoustic resonance. However, only specific dimensions of the delta spoilers were investigated in the axisymmetric cavity and it is not clear whether these dimensions are the most effective or not.

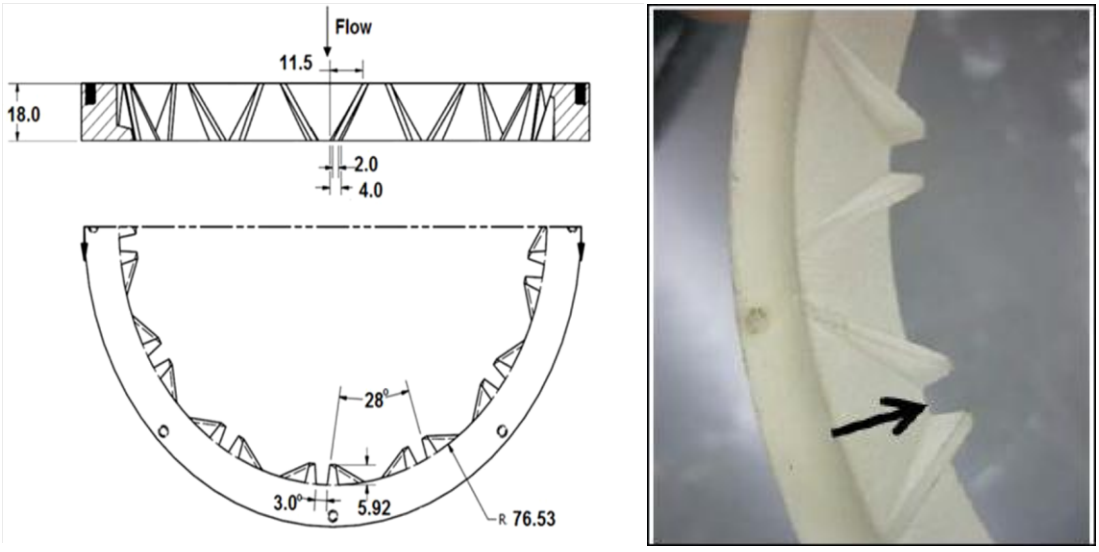

Figure 2-11: delta spoilers developed by ***(Bolduc et al., 2013)***

2.3. High frequency vortex generator (control cylinder)

Another passive method that was proven to be effective is placing a cylinder nearby the upstream edge of a cavity as shown in Figure 2-12. The vortex shedding created by the cylinder interferes with the shear layer develops in the cavity; this interference can damp the shear layer in the cavity and hence suppresses the acoustic resonance excitation. This method was also applied in suppressing the vortex shedding developed by a cylinder; this was applied by placing a relatively small control cylinder in the wake of the main cylinder subject to the suppression. The method was found to be effective and many studies including Strykowski and Sreenivasan (1989), Chen and Shao (2013), Mittal and Raghuvanshi (2001) found that the control cylinder can significantly suppresses the vortex shedding from the main cylinder within specific range of Reynolds number if the control cylinder is placed in a proper location.

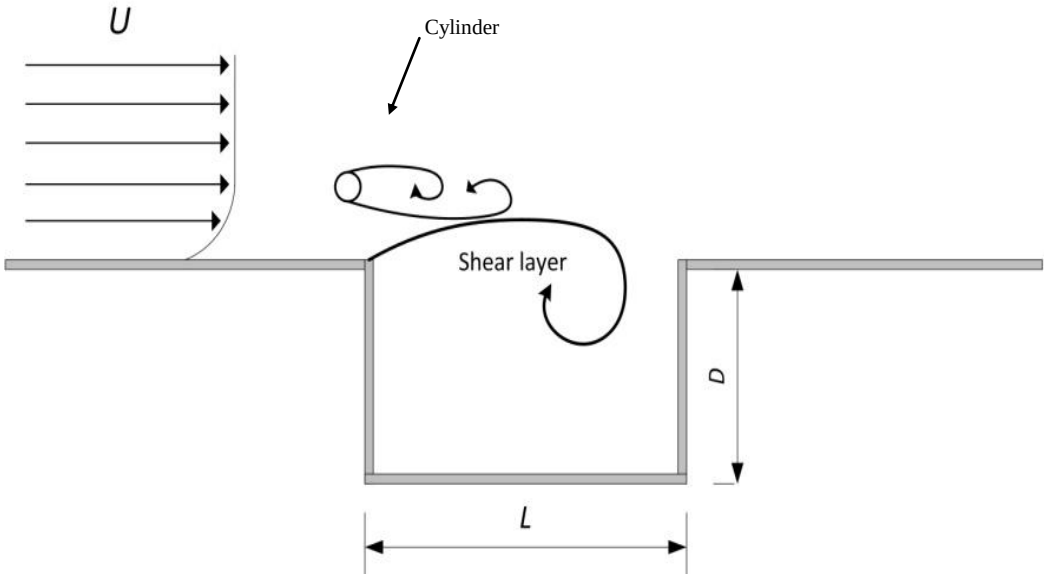

Figure 2-12: Schematic of flow over cavity with a cylinder located upstream

The effect of the cylinder on the cavity instabilities was also the subject of many studies. This method was first considered by McGarth and Shaw (1996), they investigated the effect of adding a cylinder in flow with Mach number of 0.6 and 0.8, a cylinder with diameter of 1.57 mm was tested in three different heights from the upstream edge for shallow rectangular cavities with aspect ratio of 2.56, 3.73, and 6.83. The method was found to be effective in attenuating the acoustic pressure and a reduction up to 30 dB was

observed. They also suggested that the reason behind the suppressive effect of the cylinder is the interaction between the cylinder vortex shedding and the shear layer in the cavity.

Illy et al. (2008) investigated the effect of a 2.5 mm diameter cylinder at locations with different heights near to the upstream edge of a shallow cavity with Mach number of 0.6 and in a deep cavity with Mach number of 0.78. Illy et al. (2008) also introduced visualization for the problem to understand the suppression mechanism. They found that the method is effective in suppressing the acoustic resonance with poor dependence on the flow boundary layer within the range investigated. The effectiveness of the mechanism can be seen in Figure 2-13, where the pressure amplitudes are highly reduced when the cylinder is located at a height equal to 1.2 of the cylinder diameter. Moreover, they found that the height between the cylinder and the bottom wall can control the mixing layer at the cavity and using very small height actually lifts the mixing layer upward slightly. Illy et al. (2008) concluded that the best performance can be achieved by placing the cylinder with a ratio between the height and the diameter of 0.5-0.7 and 1.6-2.2. However, they concluded that the mechanism of the suppression is yet not clear and no consistent assumption can be provided to interpret the physics behind the suppression.

Comte et al. (2008) studied numerically the effect of the cylinder suppression method on a cavity with aspect ratio of 0.42 with a cylinder of diameter 2.5 mm. They used a hybrid between URANS and LES models for the simulation. The results obtained were compared to Illy et al. (2004) results. Comte et al. (2008) suggested that the suppression effect of the control cylinder is due to the interaction between the cylinder vortex shedding and the cavity shear layer.

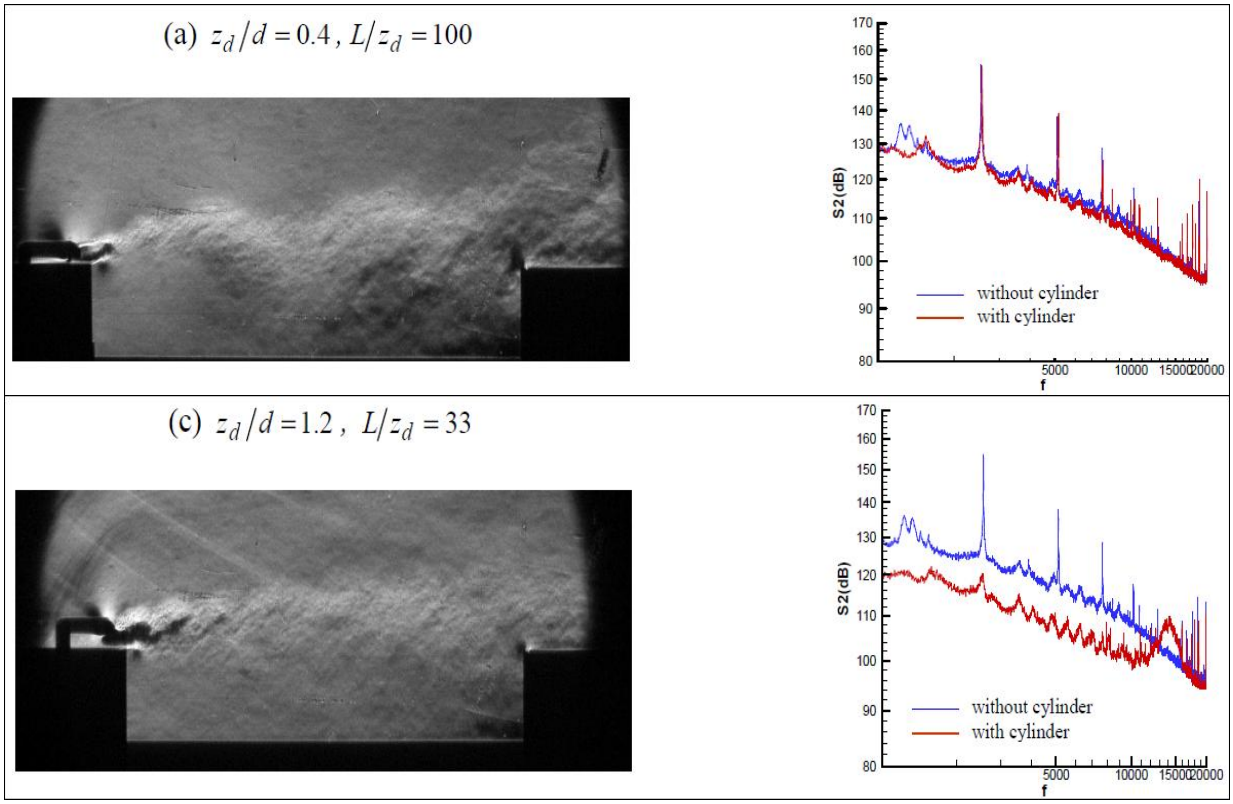

Figure 2-13: suppression effect of two different locations in shallow rectangular cavity ***(Illy et al., 2008)***

Keirsbulck et al. (2008) investigated the effect of a cylinder in deep cavities of aspect ratios of 0.2 and 0.41. The experiments were conducted on relatively low velocity with Mach number around 0.17 and the different heights from the bottom wall were tested. They found that the method can achieve a suppression of 36 dB if the cylinder is located at a height of 10 mm from the upstream edge. However, by testing a cylinder with a special shape as shown in Figure 2-14 that reduces the vortex shedding generation in the wake, Keirsbulck et al. (2008) found that the special shape cylinder is able to suppress the SPL as shown in Figure 2-15, hence, they concluded that the mechanism of the suppression is attributed to the increase in the thickness of the mixing layer due to the interaction between the cylinder wake and the shear layer and not the vortex shedding developed by the cylinder.

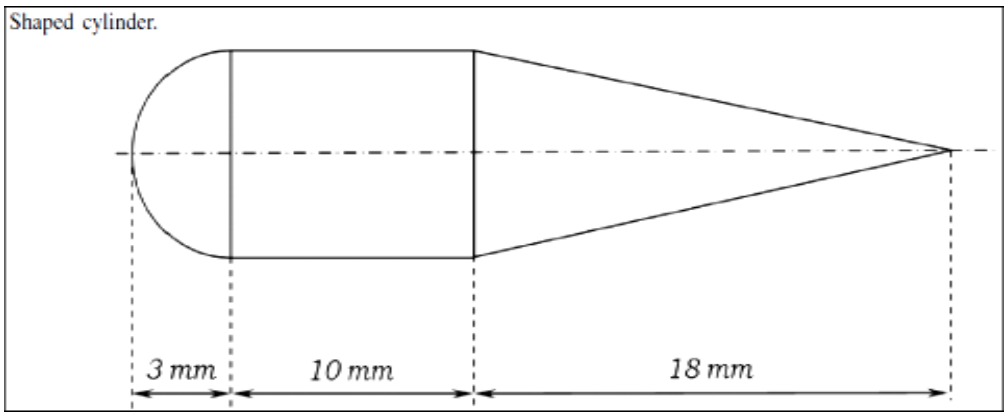

Figure 2-14: cylinder with special shape investigated by ***(Keirsbulck et al., 2008)***

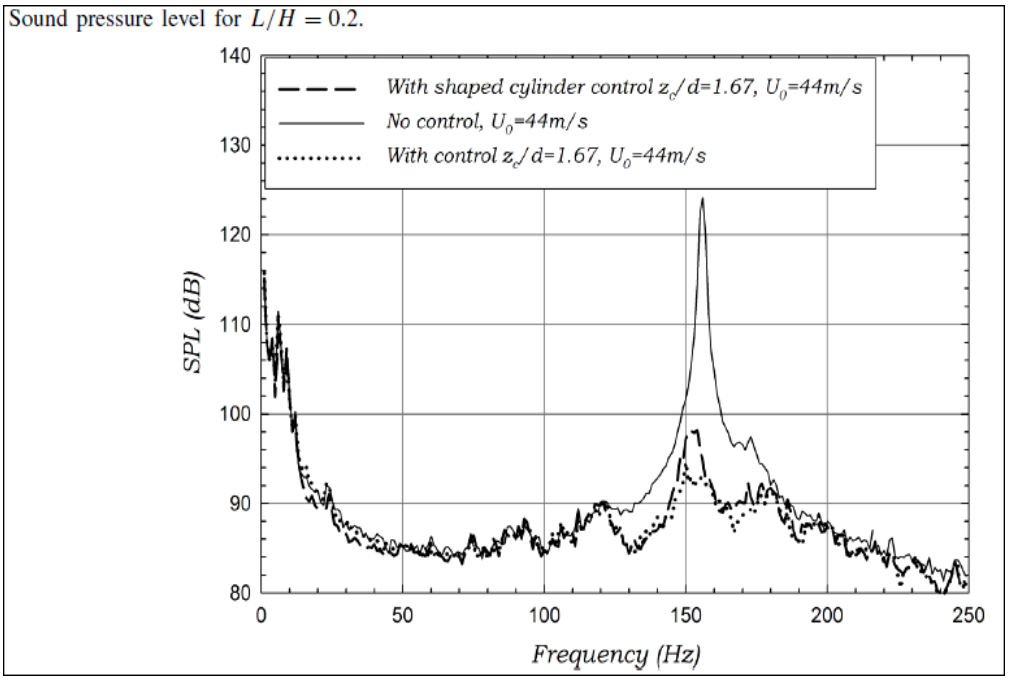

Figure 2-15: comparison between no cylinder case, normal cylinder and the specially shaped cylinder ***(Keirsbulck et al., 2008)***

Ukeiley et al. (2004) investigated the effect of a spoiler and a control cylinder at the upstream edge in shallow cavities with aspect ratios of 5.6 and 9.0. The experiments were conducted in flows with Mach number of 0.6, 0.75, and 1.4. The spoiler proposed by Ukeiley et al. (2004) was designed to lift the shear layer above the normal level in the base cavity without a spoiler installed. The shear layer lift was suggested to change the interaction at the downstream edge, and hence, reduce the oscillations in the cavity. The spoiler was able to significantly reduce the pressure oscillations specifically near to the

downstream edge as the shear layer lift affects the downstream interaction. The control cylinder was observed to introduce more suppression compared to the spoiler when located at specific locations. Ukeiley et al. (2004) found that the optimum location for the cylinder is inside the shear layer with the top of the cylinder approximately at the top of the shear layer. Similar to the suppression of the spoiler, Ukeiley et al. (2004) suggested that the suppression mechanism of the cylinder is lifting the shear layer at the cavity.

The physics behind the suppression of the pressure oscillations in cavities by the mean of placing a cylinder near the upstream edge remains unclear. Recently, Martinez et al. (2012) investigated this method using particle image velocimetry to visualize the problem. The experiments were conducted in a cavity with an aspect ratio of 3 in flow with Reynolds number of 9300. The results of the experiments contradicted two assumptions about the suppression mechanism, the first assumption attribute the suppression to lifting the shear layer in the cavity upward and hence changing the impingement at the downstream edge and the second assumption assume that the cylinder introduce stability to the shear layer by changing its characteristics. Martinez et al. (2012) concluded that the mechanism of the suppression is the direct interaction between the vortex shedding and the shear layer and an interruption to the organized grow of the vortices in the shear layer which lead to random vorticity in the shear layer.

Up till today, the concept behind the suppression of the acoustic resonance excitation in a cavity by using a cylinder is not yet fully understood.

2.4. Numerical studies of flow over cavities

The fast improvement on the capability of the computational methods and the high cost of the experimental investigations raise the dependency on the numerical simulation, and several studies have been conducted for flow over cavities with very satisfactory results that agree with the experimental findings. Some of the well-known methods used to simulate this type of flow in relatively high Reynolds numbers are Reynolds-Averaged Navier-Stokes (RANS), Large Eddy Simulation (LES), and Detached Eddy Simulation (DES).

RANS method is based on the concept of separating the turbulent flow components into mean and fluctuating components. The averaged components are obtained by solving a set of equations derived from Navier-Stokes equations while a turbulence model is used to account for the fluctuating components. Despite that the RANS model is known to be the most cost appropriate, however, its capability to predict flows with large separation regions is limited.

LES method is based on segregating the flow upon the size of the turbulence eddies. The large size eddies are solved using the normal grid, while for small eddies, with more isotropic behavior, they are solved using a sub-grid. Despite the very good predictions for flows with large separation regions, this method is known to be cost expensive as the near wall areas where the small scale eddies intensively exist demand a high computational power that is comparable with the computational power needed for a Direct Numerical Simulation (DNS). Hence, come the idea of a hybrid model between LES and RANS.

Hybrid models of LES and RANS proved to have good agreement with experimental results with less cost compared to the pure LES method and with more reliable results compared to the RANS. The hybrid method uses LES model for the detached area flows and the RANS for the near walls regions. One of the successful hybrid models is the Detached Eddy Simulation (DES) which was introduced by Spalart et al. (1997) , the method is known to provide good results with high agreement with the experimental results. DES was first introduced in 1997 and then used in 1999. The DES method overcomes the high cost associated with the pure LES method, which requires comparatively high numbers of grid points and time steps. RANS model as mentioned earlier is known to be efficient for relatively small boundary layer separation; this model fails to give good results with large separation regions, hence, the DES limits the use of the RANS model to the near wall region, and the LES model to the separation regions, resulting in very good prediction with relatively less cost.

Some of the DES studies that involved flow over cavities and found to be effective is a study done by Peng and Leicher (2008), they studied flow over rectangular cavity with aspect ratio of 5.0 in flow with Mach number of 0.85 using a DES and algebraic hybrid model of RANS and LES. The study was concerned with the pressure fluctuations in the cavity and the results of the two models were compared with experimental results

obtained by Stanek et al. (2000) and LES results obtained by Larchevêque et al. (2004). The grid used was unstructured with more than 6 million nodes. The results obtained from both models were compared to the work done by Stanek et al. (2000) in terms of the sound pressure level at different locations. Generally the results highly agreed with the experimental results, this is show in Figure 2-16.

Spalart (2009) used URANS and DES to predict the pressure oscillations produced in landing gear cavity, the results were compared with experimental results of wind tunnel measurements done by Boeing. The simulation was done on a coarse mesh with a 5.0 million nodes and a fine mesh with 12 million nodes to exclude the effect of the mesh refinement on the results. The results obtained from the numerical simulation highly agreed with the experimental results in terms of the sound pressure level and the frequency. The error in the sound pressure level was around 4 dB from the experimental values, which considered an acceptable error, while the frequency obtained from the simulation was 17 Hz compared to 15 Hz from the experiments.

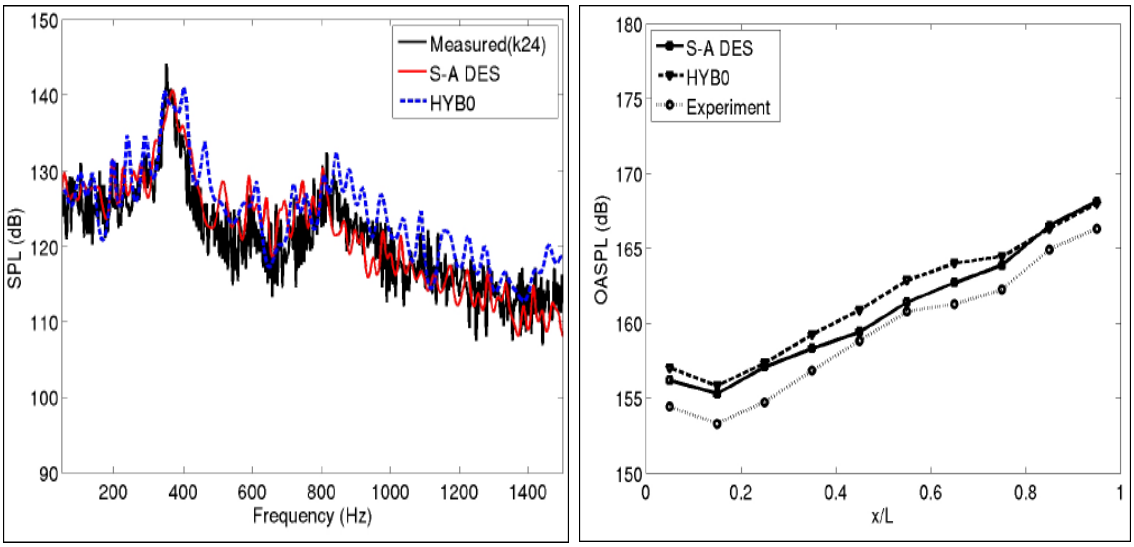

Figure 2-16: sound pressure level comparison between two numerical methods and the experimental results at specific location (left) and at different location along the cavity floor (right) (Peng and Leicher, 2008)

2.5. Summary of the literature and research needs

As explained in the literature, several attenuation techniques including spoilers and control cylinders have been investigated to suppress the undesirable effects associated with the flow-excited acoustic resonance phenomenon. However, the mechanism behind the suppressive effect of these methods is not completely understood, also the configurations and the dimensions of the spoilers including the height of the spoilers, the spacing, angles, and the thickness are not fully addressed. For the control cylinder, not all locations are investigated, and the effect of the horizontal distance remains not clear. Moreover, some of the techniques are used for axi-symmetric cavities, side branches, and deep cavities, and it is not clear whether they will be effective in shallow rectangular cavities or not. It is also noteworthy that most of the studies done before investigated the phenomenon in specific velocities, by investigating specific velocities, the occurrence of any shift in the phenomenon cannot be observed. Up till today, intensive research efforts are undergoing to understand the complex flows over cavities and the mechanisms of the suppression methods. Therefore, the main objectives of this thesis are:

- To investigate the effect of the cavity edge geometry including different dimensions and configurations on suppressing the acoustic resonance excitation in shallow rectangular cavities
- To enrich the understanding of the acoustic resonance suppression mechanism and the flow structure downstream of the spoilers by performing localized velocity measurements
- To investigate the effect of high frequency vortex generator (control cylinder) on suppressing the acoustic resonance excitation in shallow rectangular cavities with respect to the cylinder location and diameter
- To contribute to the understanding of the interaction between the control cylinder wake and the cavity shear layer by performing numerical simulation

3. Experimental setup

In this chapter, the experimental setup used is described. This chapter includes the experimental approach for both the upstream edge geometry experiments and the high frequency vortex generator (control cylinder) experiments. Both passive methods were experimented in the same test section and the same instrumentations were used.

3.1. Wind tunnel setup

The experiments were conducted in an open loop wind tunnel consisting of a ***bellmouth*** at the entrance of the wind tunnel, acrylic ***test section***, wooden ***diffuser*** connected with a flexible connector, and a ***centrifugal blower*** connected to an electric motor.

The ***bellmouth*** was made of wood, the rectangle dimensions of the bellmouth were 254 x 127 mm. The bellmouth is attached to help reducing the pressure drop at the inlet while maintaining a uniform flow inside the duct.

The ***test section*** used was 254 mm high and 127 mm wide test section made of 25.4 mm thick acrylic. As illustrated in Figure 3-1, a cavity with aspect ratio of 1.0 is attached at 330 mm from the inlet. The cavity dimensions are 127 x 127 x 127 mm. The base of the cavity is adjustable and can give a depth of 76.2 mm that yield an aspect ratio of 1.67. The cavity was designed with the ability to change both the upstream and the downstream edges independently. At the mid of the test section there are windows that give accessibility to change the edges. Along the sides of the test section, an O-ring with a diameter of 2.6 mm was placed between the acrylic pieces for sealing purposes to avoid any air leakage problems. The acrylic test section is connected with the bellmouth and the diffuser using Aluminum L-brackets, and a foam sealing strips were attached between the acrylic and the wood sides for sealing. In the test section, some holes were made to allow entrance for the: pitot tube, the hot-wire probe, the pressure tabs, and the microphone at the cavity floor. All these holes were closed and sealed when they are not in use. The test section is supported with two wooden supports attached at the two sides of the cavity. The pressure measurements were taken from the cavity floor by the microphone, further details about the measurements are provided in the instrumentation section.

The ***diffuser*** is connected to the end of the acrylic test section. The diffuser is built out of wood and it spreads gradually with an angle of 7° till connects with a circular flexible connector to isolate the vibration from the centrifugal blower. The test section is also supported by wooden supports. Along all the edges of the diffuser a silicone sealant is used for sealing.

The ***centrifugal blower*** is made by Sheldons engineering company of type 9019 XB, the blower has a suctions side with a diameter of 266 mm. The blower is driven by a 75 horsepower motor made by Baldor Company, the electric motor is 3 phase and can achieve a 1780 RPM and a maximum flow velocity of 155 m/s in the test section installed. The electric motor is controlled by a variable frequency drive made by Danfoss Company. The centrifugal blower and the electric motor are fixed in a proper foundation that can absorb any vibration.

3.2. Upstream edge experiments

As mentioned earlier, the upstream edge is interchangeable. The upstream edge block shown in Figure 3-1 is changed with different blocks for each edge geometry experiment. Four bolts fix the edge block to the test section to ensure firmness. The edges tested were installed upstream and/or downstream. The dimensions of the spoilers investigated were selected to be comparable with the thickness of the shear layer to ensure that the spoilers can significantly influence the shear layer development in the cavity. The edges investigated were:

Sharp rectangular edge which considered as the base case and all other edges are compared to it. The thickness of the acrylic block of the sharp edge is 25.4 mm.

Round edges: round edges were made of acrylic. The thickness of the acrylic block of the round edge is 25.4 mm. The edges have two different radii; 25.4 mm and 12.7 mm.

Chamfered edges: chamfered edges were made of acrylic with a chamfer length of 25.4 mm. To address the effect of the chamfer angle, different chamfer angles were investigated; 107°, 120°, 135° and 150°.

Saw-tooth edge: saw-tooth edge was also made of acrylic and it has a special configuration as described in Figure 3-5. The thickness of the acrylic block of the saw-tooth edge is 25.4 mm

Curved spoilers: curved spoilers were 3D printed, they were designed to direct the flow towards the test section side walls, and prevent the development of the shear layer at the cavity mouth. To address the effect of the height of the spoilers, four different heights of curved spoilers were investigated; 5.9, 8.2, 12 and 16 mm.

In order to study the effect of the delta spoilers developed by Bolduc et al. [16] on the acoustic resonance excitation in shallow rectangular cavities, several spoilers with different heights, thickness, spacing, and converging angles were investigated. Four ***straight spoilers*** with different spacing (type (A) spacing s= 4mm and type (B) spacing s=16 mm) were investigated, the height of the straight spoilers was also investigated by testing two different heights; 5.9 mm and 8.2 mm.

Delta spoilers with different spoilers thickness were investigated. The spoilers converging angle was 60° and the thicknesses investigated were 2 mm and 3 mm spoilers thickness. These two thicknesses were tested at two spoilers heights: 12 mm and 16 mm. To understand the effect of the converging angle of the spoilers; delta spoilers with three different converging angles were investigated. The angles investigated were: 60°, 65°, and 70°. These angles were tested at two different heights of 12 mm and 16 mm, and a thickness of 2 mm. The effect of the height of the delta spoilers is investigated by using spoilers with heights of 5.9, 8.2,12, and 16 mm. These spoilers have a thickness of 2 mm and converging angle of 60°. Summary of the straight, curved, and delta spoilers dimensions are provided in Table 3-1. The dimensions and configurations of the edges are illustrated in Figure 3-3 to Figure 3-5.

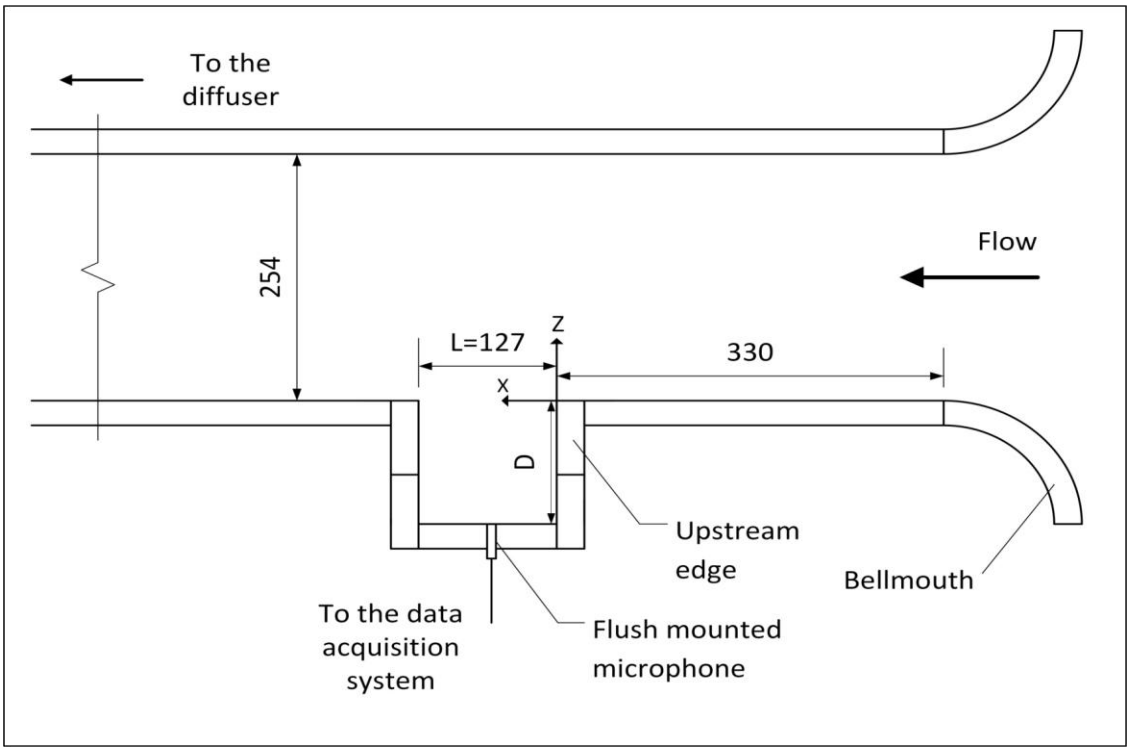

Figure 3-1: Schematic drawing of the test section

Figure 3-2: acrylic test section with the cavity of the aspect ratio of 1.0 is attached, and the microphone installed at the cavity floor.

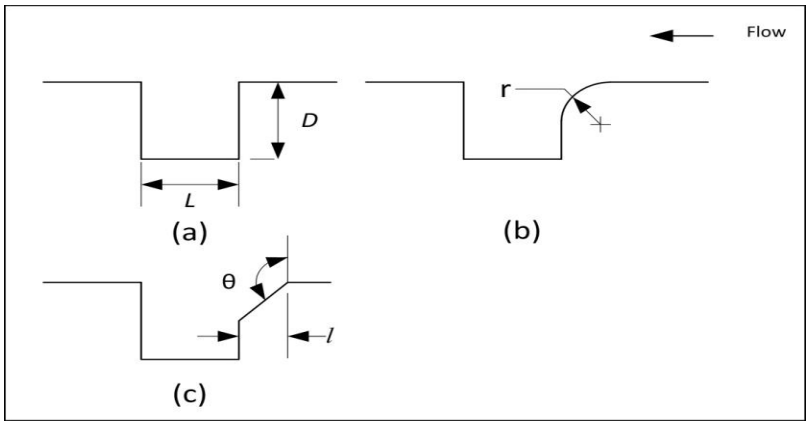

Figure 3-3: (a) sharp edge (b) round edge (c) chamfered edge

Table 3-1 : details of delta and straight spoilers investigated

	Thickness	**Converging angle**	**Height**	**Spacing**
Delta spoilers	2	60	5.9	-
	2	60	8.2	-
	2	60	12	-
	2	60	16	-
	3	60	12	-
	3	60	16	-
	2	65	12	-
	2	65	16	-
	2	70	12	-
	2	70	16	-
Straight spoilers	2	-	5.9	4
	2	-	5.9	4
	2	-	8.2	16
	2	-	8.2	16
Curved spoilers	2	-	5.9	-
	2	-	8.2	-
	2	-	12	-
	2	-	16	-

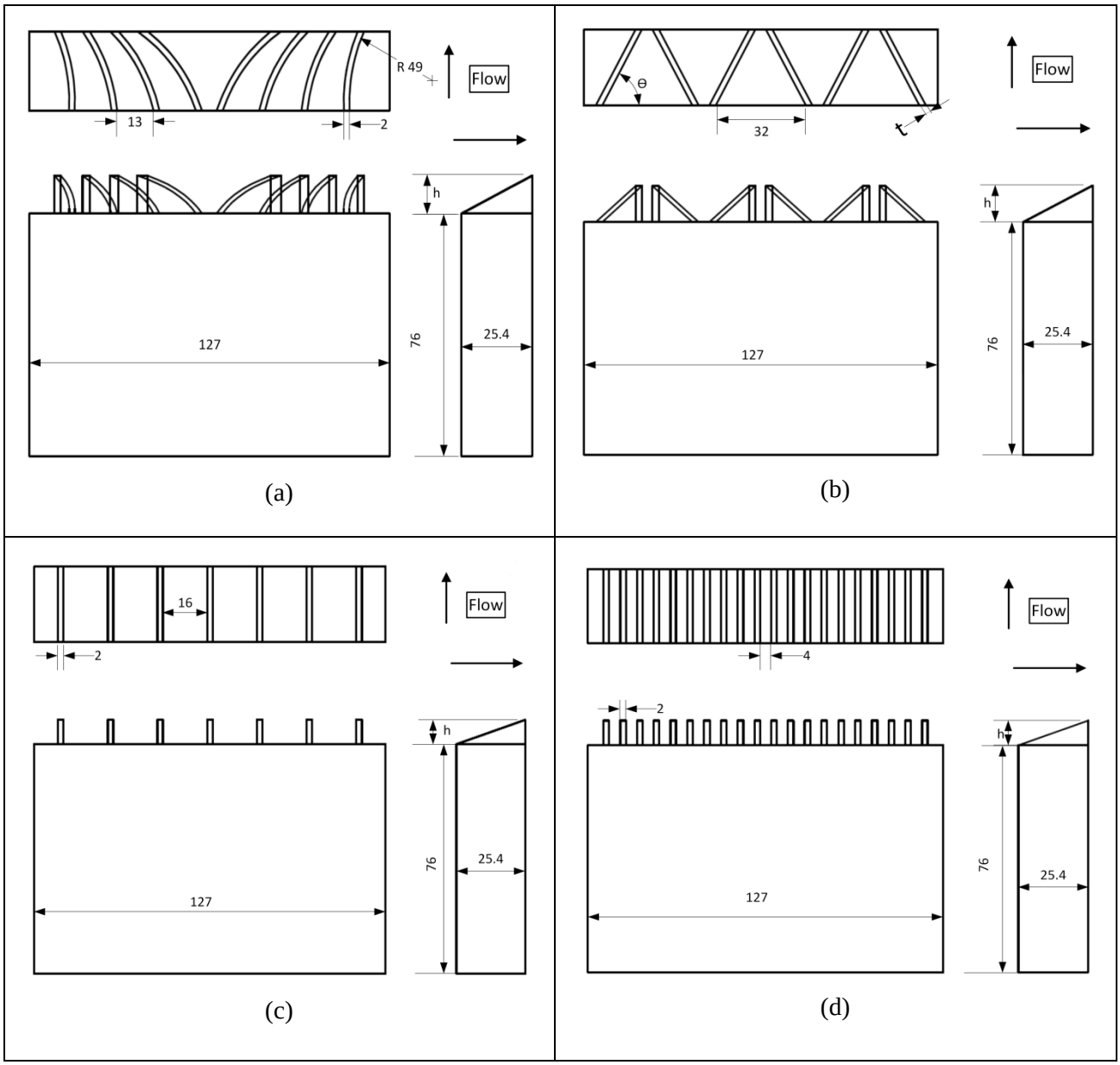

Figure 3-4: (a) Curved spoilers, (b) Delta spoilers, (c) Straight spoilers type (B) spacing 16mm, (d) Straight spoilers type (A) spacing 4 mm.

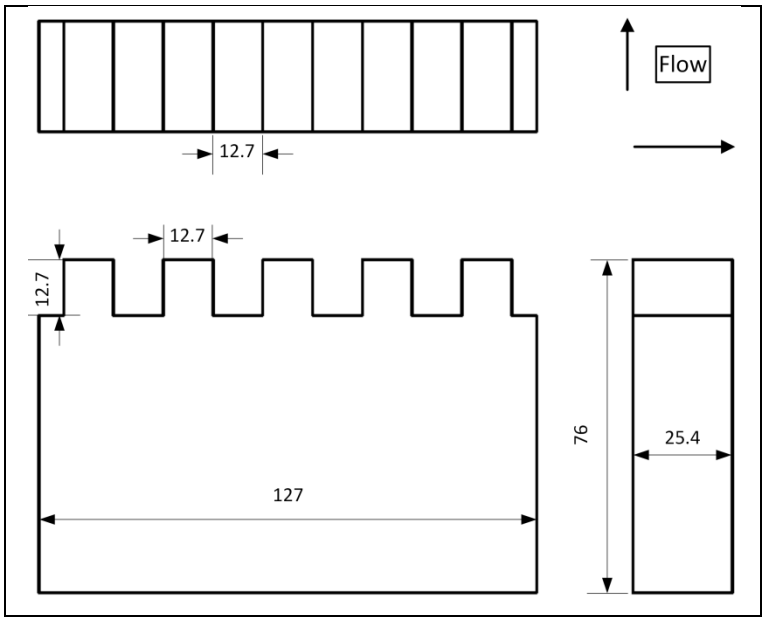

Figure 3-5: Saw-tooth edge

3.3. High frequency vortex generator experiments

The high frequency vortex generator experiments are performed in the same test section. A cylinder with a diameter of 4.57 mm which yields a ratio *L/d* of 27.78, where *L* is the cavity length and *d* is the cylinder diameter, was installed in different locations near the upstream edge of the cavity. Different locations in terms of vertical and horizontal distances were tested as illustrated in Figure 3-6 and Figure 3-7. The cylinders were attached to the acrylic test section using a plastic suction cups at each side, that were able to firmly fix the cylinders without any noticeable vibration during the experiments. In the results chapter the locations will be identified with the Cartesian coordinates assuming the tip of the sharp edge is the (0.0, 0.0) point, and the upstream direction is the negative X direction, while the downstream is the positive X direction, as shown in Figure 3-6.

Another two cylinders with diameters of 3.81 mm and 6.35 which yield *L/d* ratios of 33.33 and 20 respectively were tested in some of the effective locations obtained from testing the cylinder with the diameter of 4.57 mm.

Measurements of the acoustic pressure are taken from the base of the cavity by means of a flush mounted microphone and delivered to a data acquisition system for the spectral analysis as in the edge geometry study.

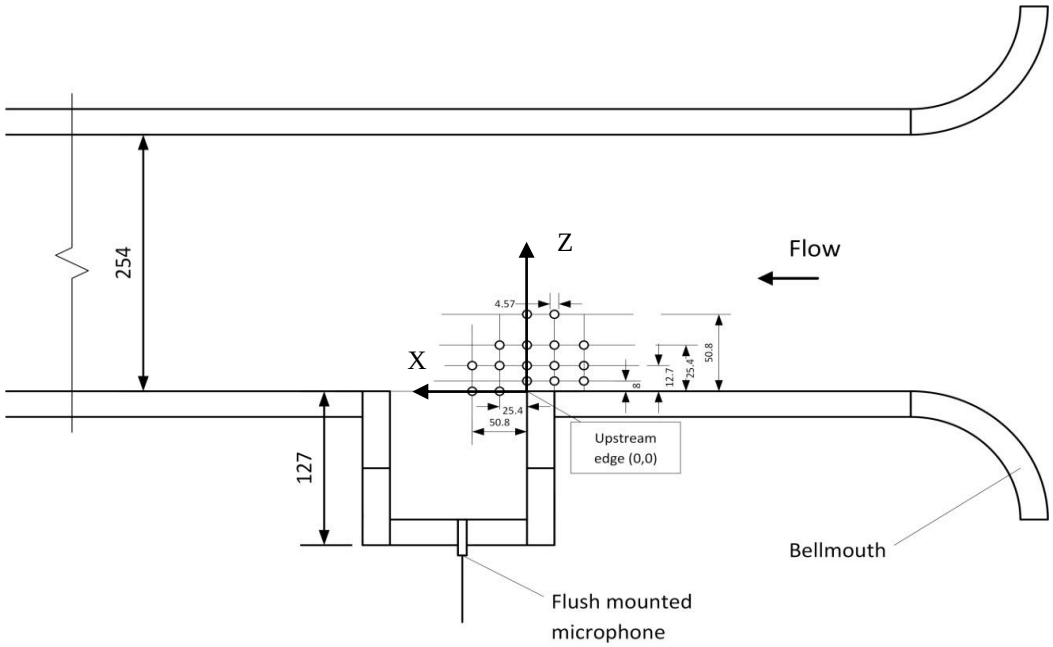

Figure 3-6: schematic of the test section and the investigated locations of the control cylinder

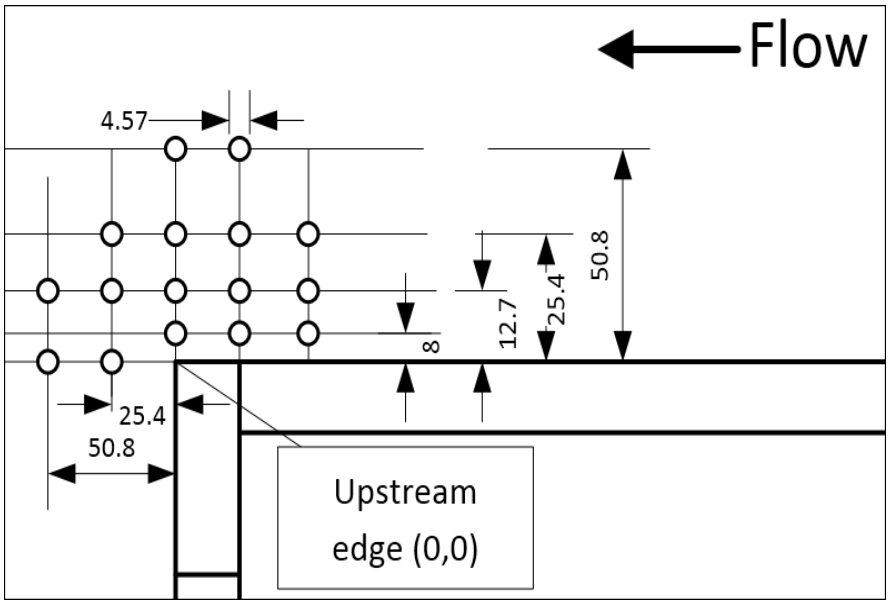

Figure 3-7 : locations investigated of the control cylinder with detailed dimensions

3.4. Instrumentation and data acquisition

In the experiments several instrumentation devices were used including, microphone for acoustic pressure measurements, Pitot tube for flow velocity measurements, hot-wire probe for flow velocity measurements, and a digital manometer for differential pressure measurements.

Pressure microphone: the microphone used was made by PCB PIEZOTRONICS (model: 377A12) and it is flush mounted to the base of the cavity. The microphone is connected with a preamplifier from PCB PIEZOTRONICS (model:426B03). The microphone was calibrated before the experiments to ensure the high accuracy of the measurements using a sound calibrator from G.R.A.S. Sound & Vibration. The microphone signal is transferred to the data acquisition system through a PCB PIEZOTRONICS signal conditioner (model: 482C). The output signal from the signal conditioner is transferred to a BNC connector made by National Instruments (model: BNC-2110). Both real time signal and the FFT spectrum are acquired by the software Labview as r.m.s amplitudes. The sampling rate used to acquire the data was 10 KHz with sampling time of 100 seconds for the edge effect experiments and 60 seconds for the cylinder effect experiments.

Hot-wire mechanism: to measure local velocity and velocity perturbations a 2D traverse mechanism was attached to the test section as shown in Figure 3-8 and Figure 3-9. The hot-wire probe was only used before the onset of acoustic resonance to avoid the interaction between the acoustic particle movement and the air flow when the resonance is excited, as a single probe hotwire takes only unidirectional measurements and gives no data about the direction. The hot wire measurements were conducted to obtain the velocity fluctuations along different spoilers and the shear layer thickness at the cavity. Moreover, measurements were taken for the velocity profile in the cavity. Some of the velocity profile measurements were obtained in order to validate the simulation results as will be discussed later. The traverse mechanism has a step of 1.27 mm which can generate a very precise velocity profile in both vertical and stream wise direction.

Digital manometer (HT-1890): the manometer was used to obtain the differential pressure between upstream and downstream the cavity. Each side of the manometer was

connected to four pressure tab points in the same plane upstream and downstream. The pressure tabs were connected to the manometer through plastic tubes. The differential pressure was recorded for the base case at different flow velocities, same measurements were taken with some of the most effective edges and cylinders to address the drop in the pressure.

Pitot tube: a pitot tube was used to calibrate the electric motor with the flow velocity in the test section. The pitot tube was connected to the digital manometer to acquire the difference in the pressure between the total and the static pressure. The Pitot tube was installed after the bellmouth and upstream of the cavity. The electric motor was able to achieve a velocity of 155 m/s. This range from 0 m/s to 155 m/s was divided into 60 steps by the electric motor control panel. After acquiring the calibration chart for the motor step with the flow velocity the pitot tube was removed.

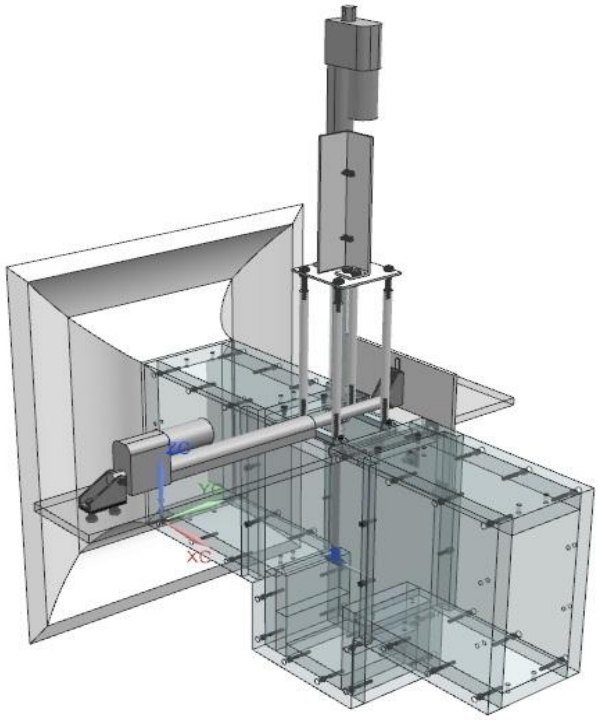

Figure 3-8: Isometric drawing of the hot-wire mechanism connected to the test section

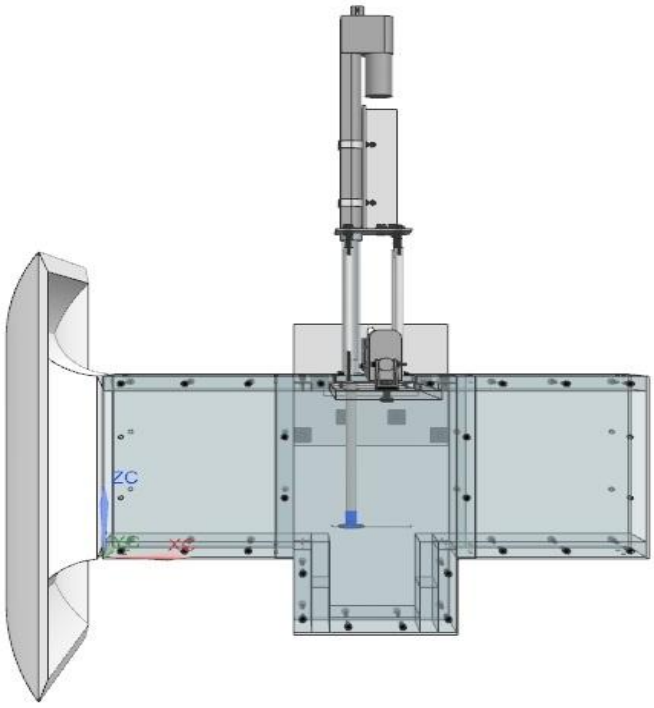

Figure 3-9: side view of the hot-wire mechanism connected to the test section

4. Results

In this chapter the results of the experiments are presented. For the edge geometry effect, the acoustic pressure recorded with each edge is compared to the base case where the sharp edge is installed upstream and downstream. The performance of the edge is assessed upon the mitigation of the acoustic pressure values. Another parameter that can affect the performance of the edge geometry is the pressure drop produced by the geometry. To assess the pressure drop produced by the edge, differential pressure measurements were taken upstream and downstream of the cavity, the measurements were taken for some of the edges that were found to be effective in suppressing the acoustic resonance excitation. For the edge geometry effect, hotwire measurements are also presented. These measurements are provided for better understanding of the suppression mechanism. The effect of placing a high frequency vortex generator (control cylinder) is also presented and compared to the base cavity case, each location and diameter investigated is assessed upon the reduction of the acoustic pressure compared to the base case. The numerical simulation is provided in order to enrich the understanding of the effect of the cylinder on the acoustic resonance excitation.

4.1. Edge geometry effect

In this section the performance of each edge in suppressing the acoustic resonance excitation is presented. The edges were tested for two cavity aspect ratios, 1.0 and 1.67, in order to study the edges effectiveness with respect to the cavity depth.

4.1.1. Results of cavity with aspect ratio of 1.0

- **Base case**

The base case, which is the sharp edges installed upstream and downstream is considered the reference line for all experiments. For each experiment the acoustic pressure was taken at different speeds starting from 0 to 155 m/s divided into 60 steps. At each flow velocity real time signal and FFT spectrum is acquired. A typical pressure spectrum acquired with the base case at flow velocity of 133.6 m/s is shown in Figure 4-1. The

figure depicts a peak at frequency of 465 Hz which represents the acoustic resonance phenomena, while the peak at 930 Hz is the harmonics of the first peak. Figure 4-2, shows a 3D waterfall plot, this figure combines the entire pressure spectrum obtained at each flow velocity investigated. It can be seen how the pressure is intensified when the acoustic resonance is excited.

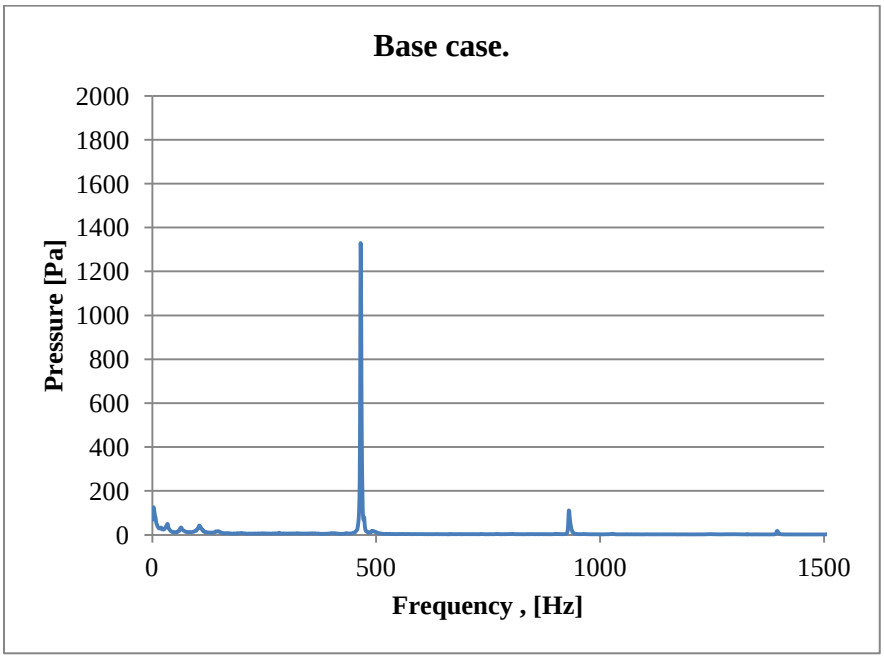

Figure 4-1: pressure spectrum for the base case at flow velocity of 133.6 m/s

For better illustration, Figure 4-3 shows a 2D waterfall plot of the pressure spectra for the base case, the three shear layer modes developed in the cavity are illustrated by the dotted lines. The lines of the shear layer modes are also illustrated in Figure 4-4(a), the slopes of these lines follow Strouhal number of each shear layer mode. The values of Strouhal number obtained from the experiments are summarized in Table 4-1.Figure 4-4 is constructed from the waterfall plot shown in Figure 4-3. Each point in Figure 4-4 represents the amplitude and frequency of the vortex shedding component taken from the pressure spectra. In addition, it can be seen from Figure 4-3 and Figure 4-4 that when the frequency of the shear layer mode comes close to the acoustic resonance mode, the process of flow-excited acoustic resonance is initiated and a lock-in region is observed.

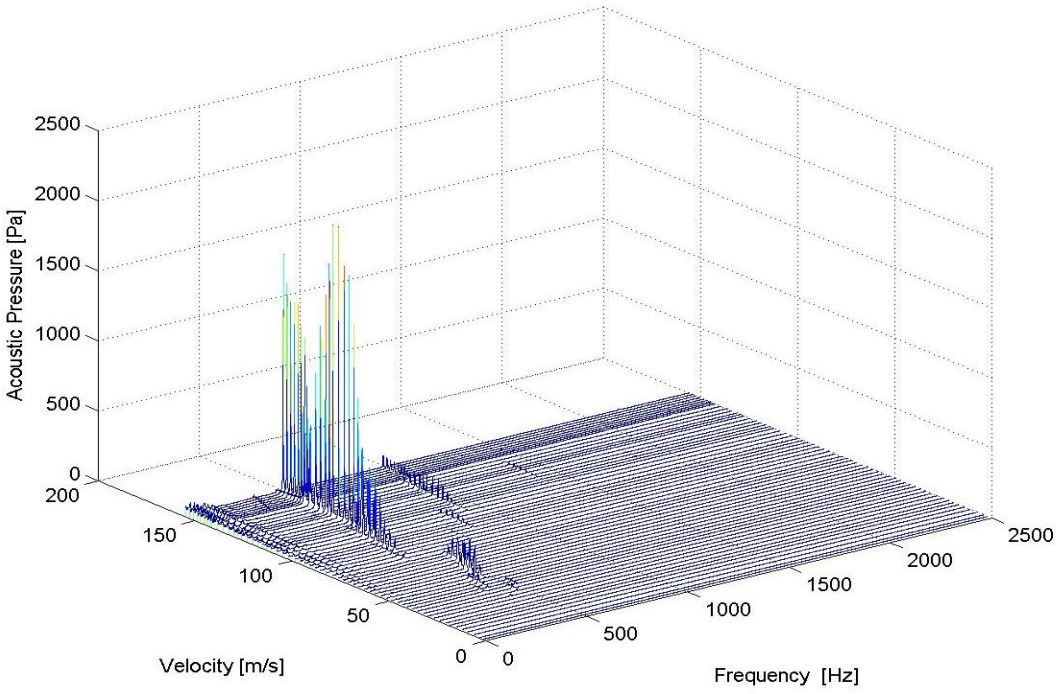

Figure 4-2: 3D waterfall plot for the base case with aspect ratio of 1.0

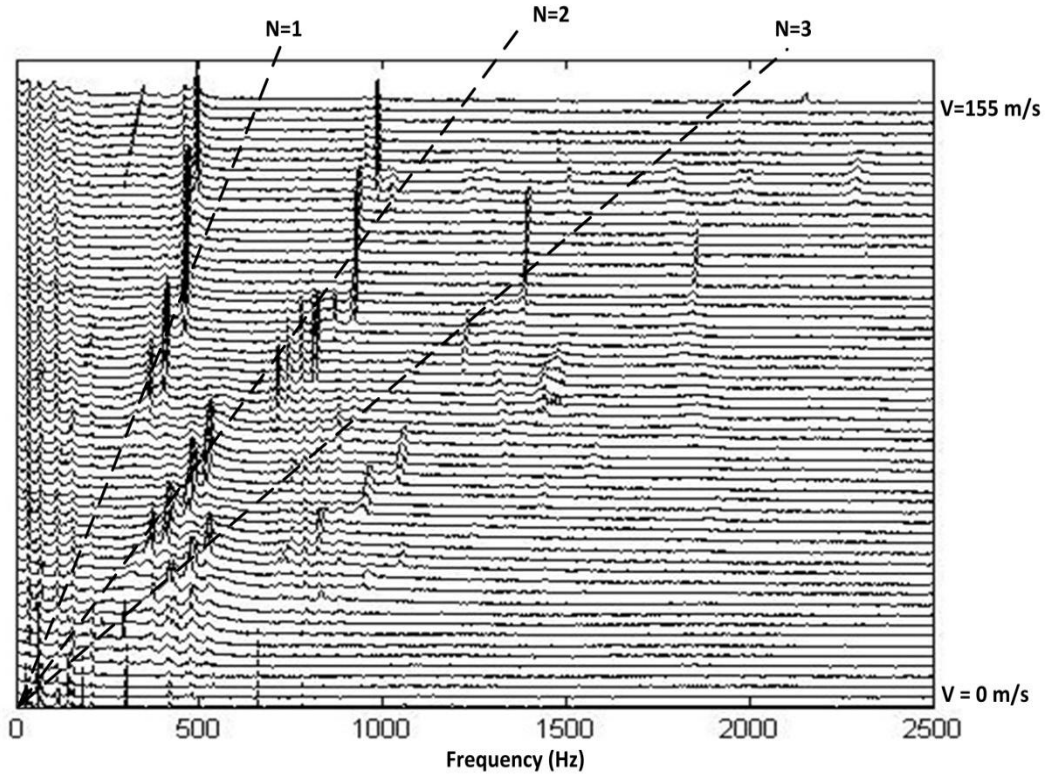

Figure 4-3: 2d waterfall plot for base case (sharp edge) with aspect ratio of 1.0

The frequency of the acoustic mode can be predicted from the formula (Kinsler et al., 2000)

$$f_a = \frac{nc}{2H} \qquad (4)$$

where c is the speed of sound, n the number of the acoustic mode excited and H is the total height of the test section. Figure 4-3 and Figure 4-4 show that the first acoustic mode is excited by the first three shear layer modes. The first resonance occurs when the third shear layer mode excite the first acoustic mode at around 488 Hz and starts at flow velocity of 36 m/s. The second shear layer mode excites the first acoustic mode at around 480 Hz and starts at flow velocity of 50 m/s. The first shear layer mode excites the first acoustic mode at around 100 m/s and produces the highest acoustic pressure amplitudes as can be seen in Figure 4-4. Since the coincidence between the first three shear layer modes and the first acoustic mode produce the highest acoustic pressure, the performance of each edge is assessed and compared with respect to the first acoustic mode.

Table 4-1: Strouhal number values obtained from experiments for the aspect ratio of 1.0

Shear layer mode	St
N=1	0.48
N=2	0.96
N=3	1.44

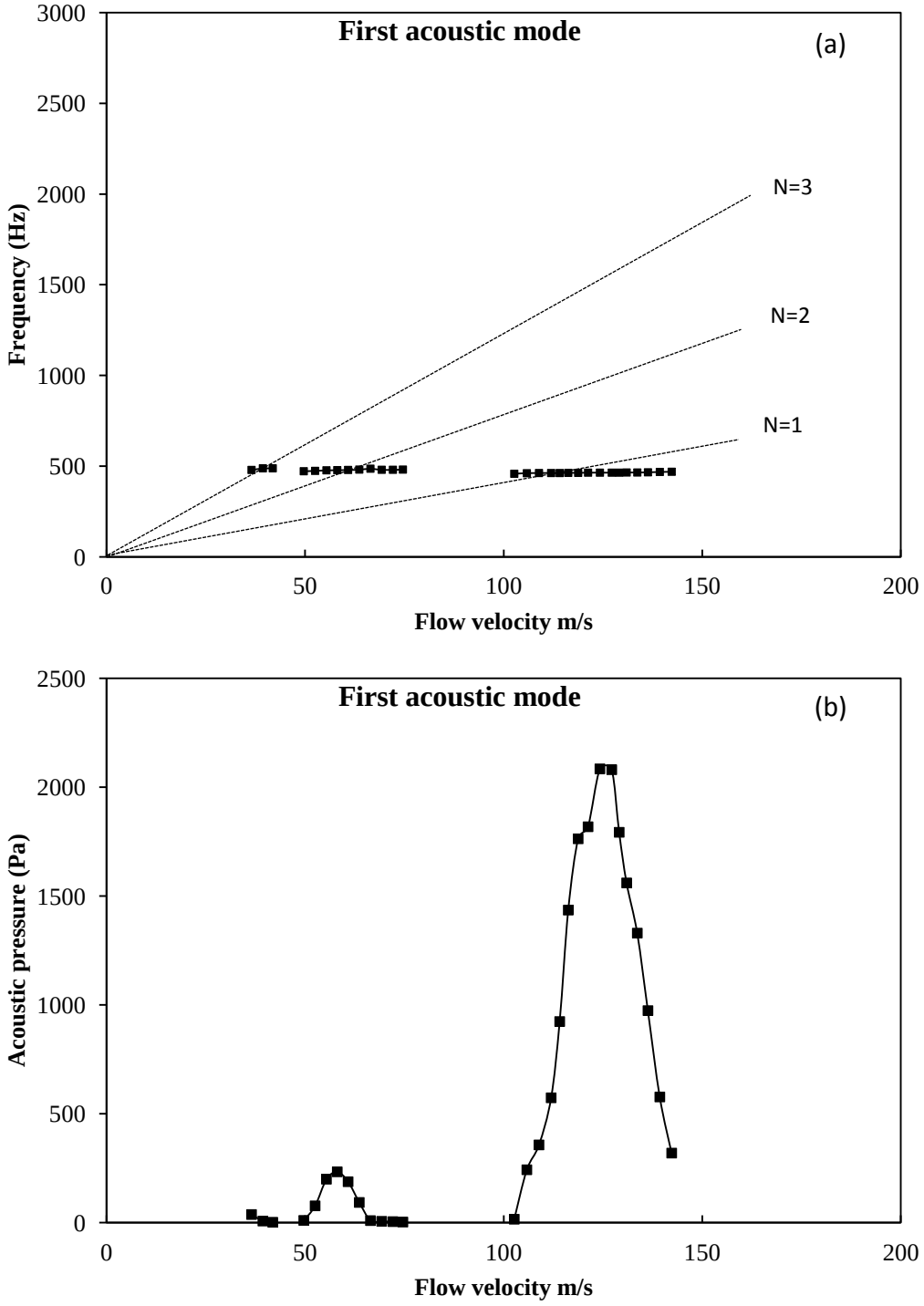

Figure 4-4: first acoustic mode excited in the base case with aspect ratio of 1.0. (a) shows the frequency with the flow velocity, (b) shows the acoustic pressure with the flow velocity

- **Round edges**

The radii of the round edges tested are 12.7 and 25.4 mm. The edges are tested upstream and/or downstream. Figure 4-5 shows the 2D waterfall plot for the round edge with diameter of 12.7 mm installed upstream. Figure 4-6 shows a comparison of the acoustic pressure extracted from the waterfall plot for the first acoustic mode between the round edges and the sharp edge when the round edge is installed upstream. It can be seen that the round edges delay the onset of acoustic resonance to higher velocities, moreover, the increase of the radius of the round edge results in increasing the delay of the onset of acoustic resonance. This was expected as the effective length used in Strouhal number increased by the radius of the round upstream edge as suggested by Bruggeman et al. (1991). This delay of the onset of acoustic resonance is observed in both aspect ratios 1.0 and 1.67. Nevertheless, the delay in the onset of acoustic resonance is found to be proportional to the increase in the cavity length which agrees with the constant values of Strouhal number for the cavity. Moreover, the acoustic pressure is also amplified with values exceeding 4000 Pa.

Figure 4-7 and Figure 4-8 show comparison between the effects of the round edges when installed upstream and/or downstream for both radii investigated. The figures show that rounding the upstream edge shifts the occurrence of the acoustic resonance excitation to higher velocities and intensify the acoustic pressure, however, rounding the downstream edge has no significant shift on the resonance excitation and the acoustic pressure is reduced. From the figures it can be concluded that the shift in the acoustic resonance excitation is introduced by the upstream edge, hence, when calculating the Strouhal number the increase in the characteristic length introduced by the upstream edge should be considered. This conclusion agrees with the results of Bruggeman et al. (1991) in terms of the shift introduced only by the upstream edge geometry.

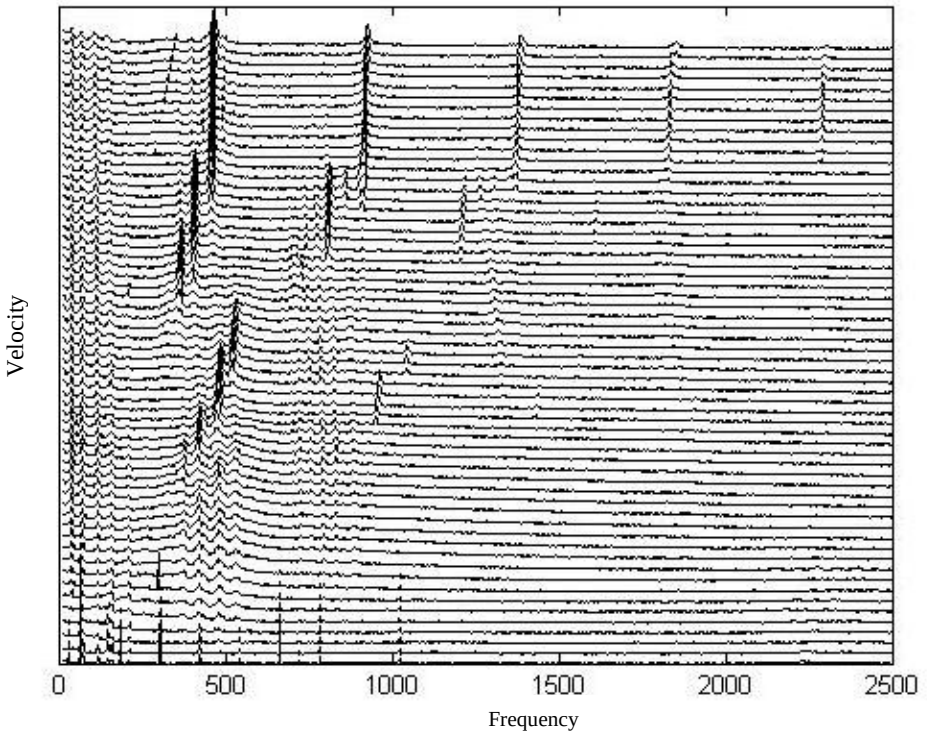

Figure 4-5: 2D waterfall plot for round edge (r=12.7mm) installed upstream

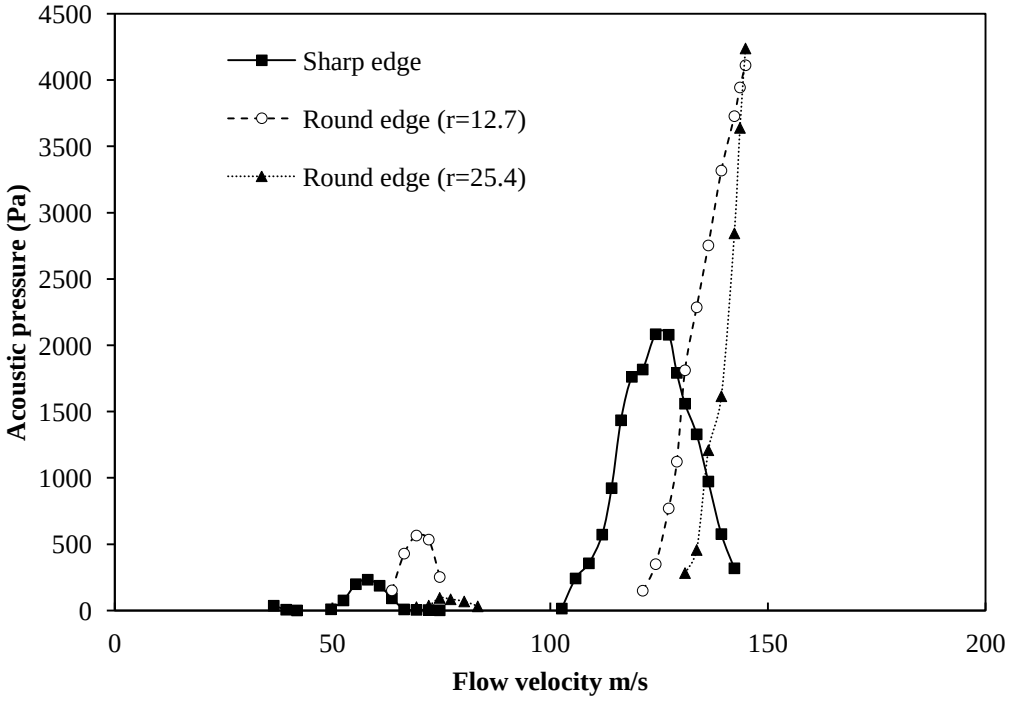

Figure 4-6: comparison between sharp edge and round edge installed upstream

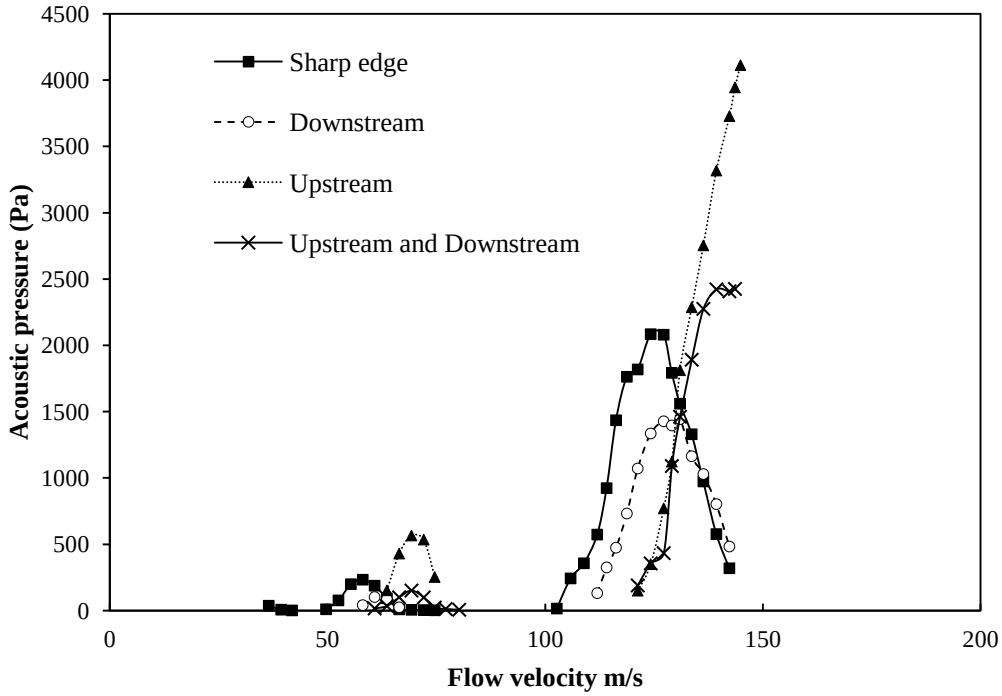

Figure 4-7: comparison between sharp edge and round edge (r=12.7 mm) installed upstream and/or downstream

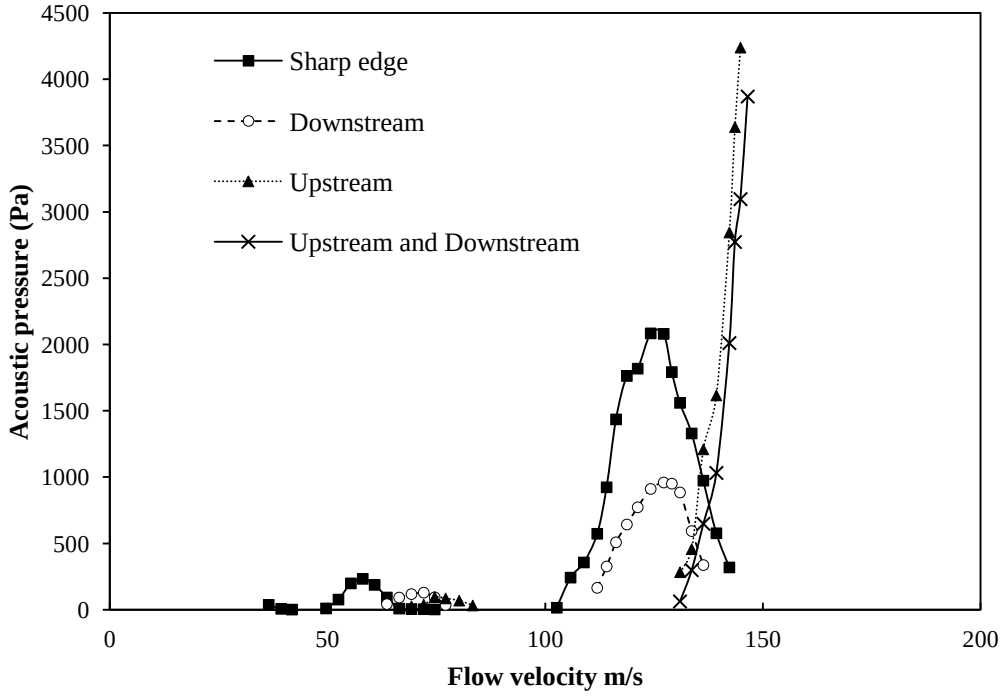

Figure 4-8: comparison between sharp edge and round edge (r=25.4 mm) installed upstream and/or downstream

- **Chamfered edge**

Chamfered edges with different four angles are investigated. The edges are installed upstream, while sharp edge is installed downstream. The angles investigated are: 107°, 120°, 135°, and 150°. Figure 4-9 shows the 2D waterfall plot for the chamfered edge with an angle of 135°. Figure 4-10 shows the effect of the chamfered edges on acoustic resonance excitation. The chamfered edges delay the onset of acoustic resonance to higher velocities as observed with the round edges. This delay is also found to be proportional with the increase of the cavity length by the distance *l* (length of the chamfer) which yields the same Strouhal number for the base case except for the chamfered edge with the angle of 107°, which is known in the literature to be the most effective angle (Ziada and Lafon, 2013), with this angle the second and third shear layer modes effect is completely suppressed but when the resonance is excited by the first shear layer mode the acoustic pressure is intensified with a slight shift that results in slight difference in Strouhal number.

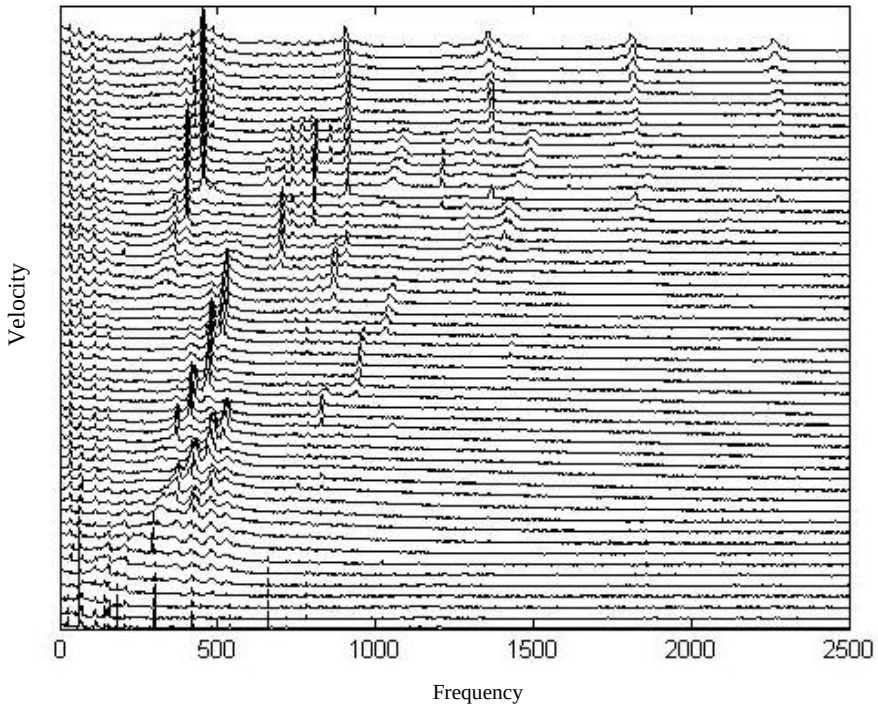

Figure 4-9: 2D waterfall plot for chamfered edge with angle of 135° installed upstream

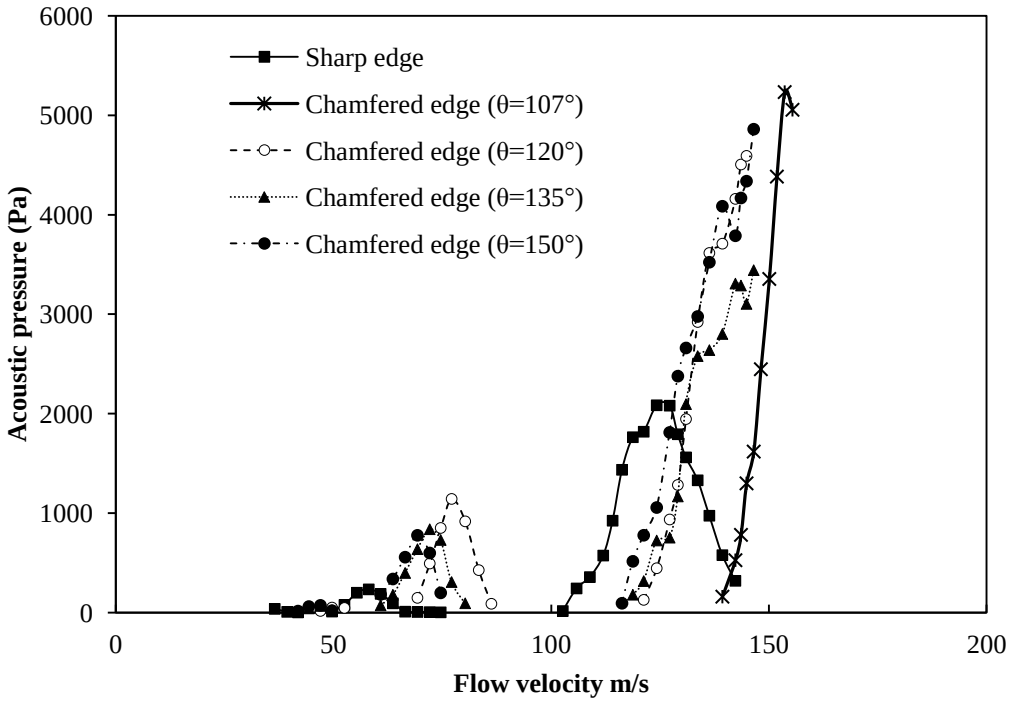

Figure 4-10: comparison between sharp edge and chamfered edges

To illustrate the effect of the chamfered and round edges on resonance excitation, the data are normalized in Figure 4-11 and Figure 4-12 by using the Strouhal number and the dimensionless pressure given by:

$$Dimensionless\ pressure = P/0.5\rho U^2 \qquad (5)$$

where ρ is the fluid density, U is the main flow velocity and P is the r.m.s amplitude of the acoustic pressure. Figure 4-11 and Figure 4-12 show the normalized values, it can be seen that the Strouhal number values are overlapping when the modified cavity length is used ($L+r$ for round edge and $L+l$ for chamfered edge).

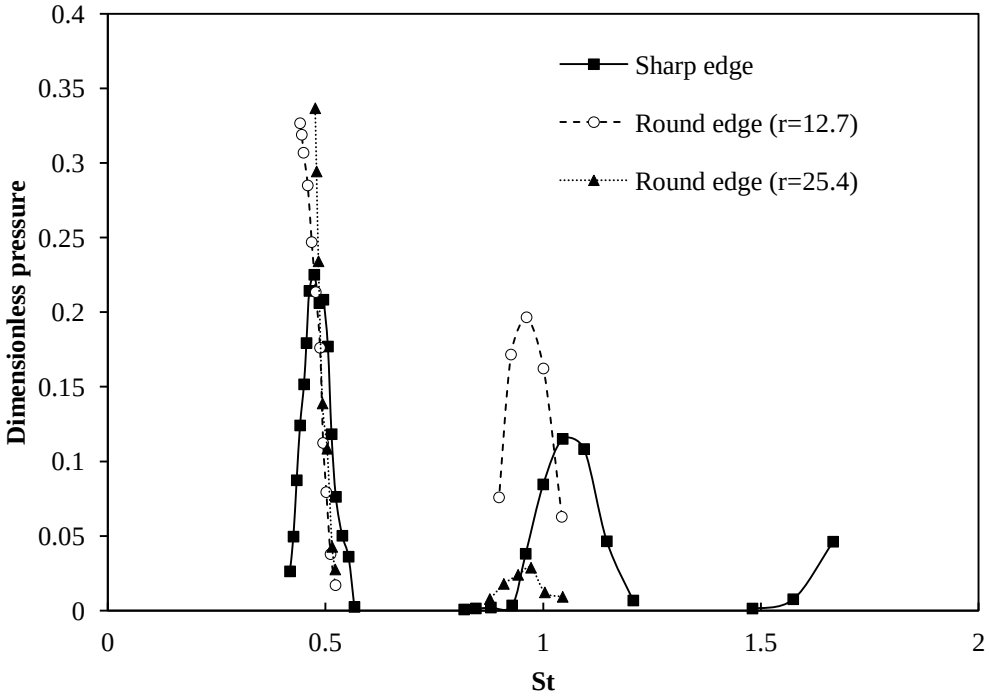

Figure 4-11: comparison between normalized values for sharp and round edges

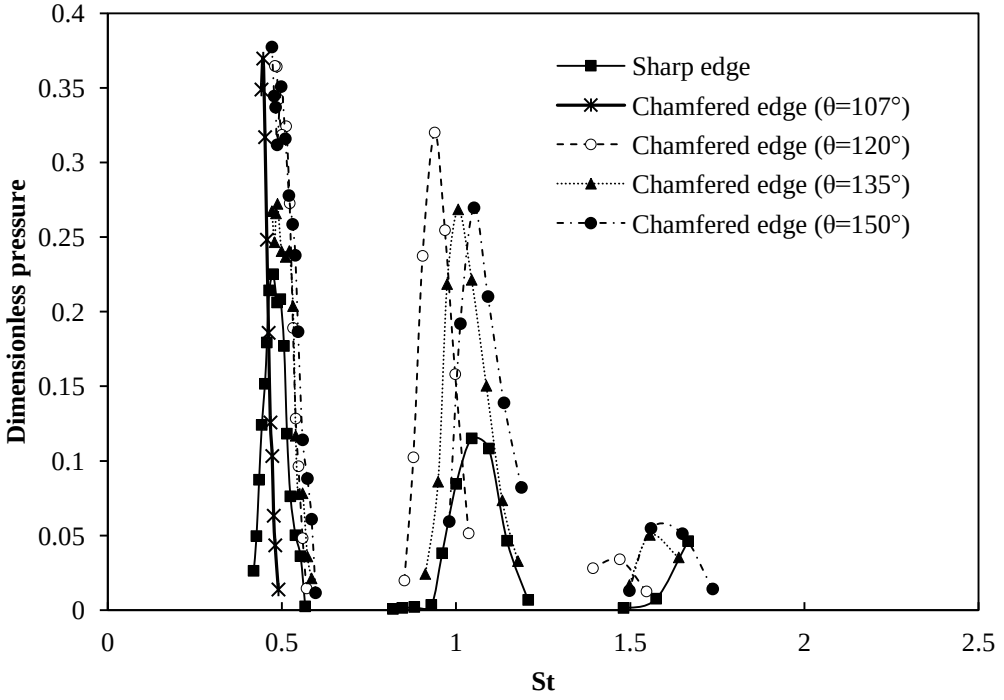

Figure 4-12: comparison between normalized values for sharp and chamfered edges

- **Saw-tooth edge**

The saw-tooth edge effect is illustrated in the 2Dwaterfall plot in Figure 4-13.The saw-tooth edge was installed upstream while sharp edge was installed downstream of the cavity. The effect of the saw-tooth edge on acoustic resonance excitation, as show in Figure 4-14, is observed to be similar to the chamfered and round edges where the resonance excitation is shifted to higher velocities and intensified to values reaching 4000 Pa.

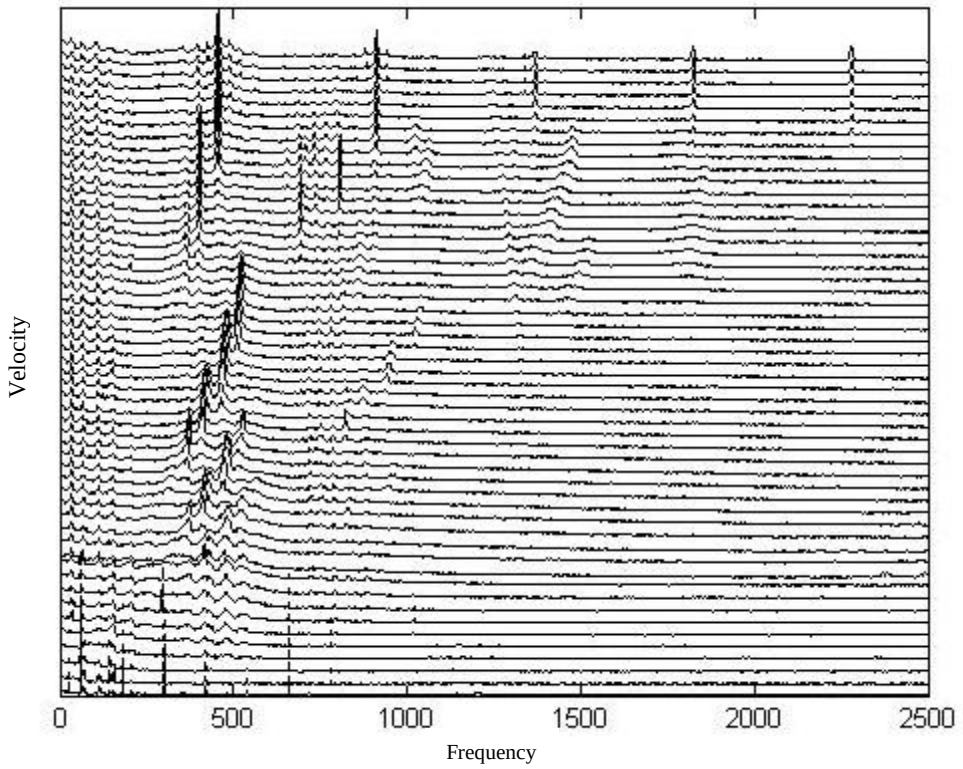

Figure 4-13: 2D waterfall plot for saw-tooth edge

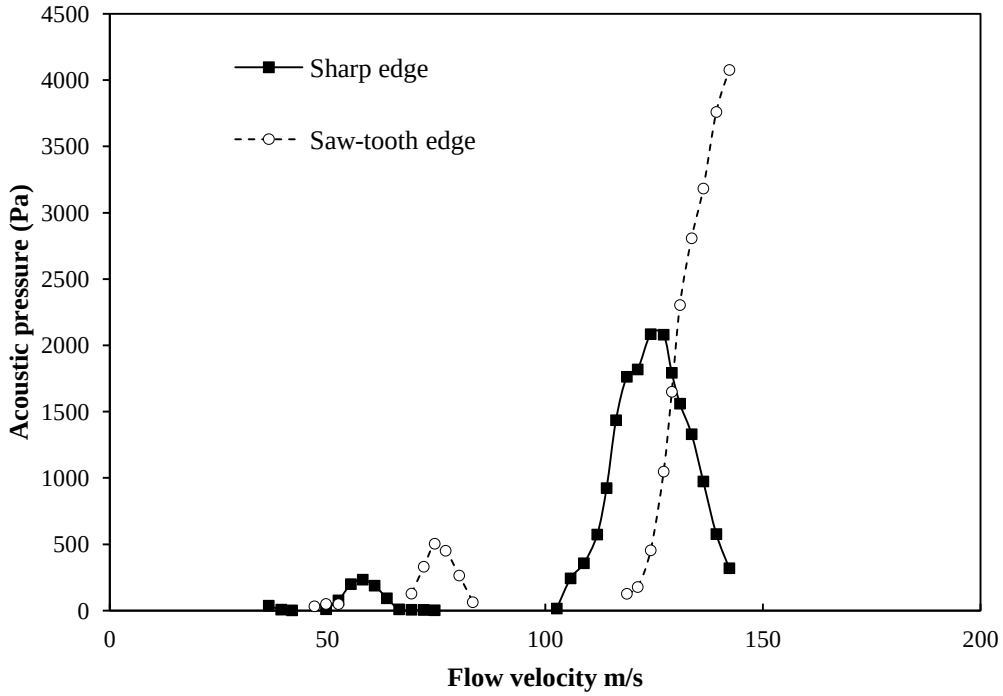

Figure 4-14: comparison between sharp edge and saw tooth edge

Generally the round, chamfered, and saw tooth edges are observed to shift the occurrence of the acoustic resonance excitation to higher velocities, this method can be utilized in the industry by shifting the acoustic resonance excitation out of the operation range. However it should be applied carefully as the acoustic pressure observed when the acoustic resonance is excited is highly magnified compared to the base case with the sharp edges.

- **Delta spoilers**

The delta spoilers are found to be suppressive. The spoilers are able to completely suppress the second and third shear layer modes, and significantly mitigate the acoustic pressure of the first acoustic mode when excited by the first shear layer mode. Four delta spoilers with different heights (5.9, 8.2, 12, and 16) were investigated. Figure 4-15 shows a 2D waterfall plot when the delta spoilers with height of 12 mm is installed upstream of the cavity. Figure 4-16 shows the effect of the delta spoilers on suppressing the acoustic resonance, it is clearly seen that the delta spoilers are able to keep the acoustic pressure

below 300 Pa. It is also observed that increasing the height for the delta spoilers has no significant effect on the acoustic resonance excitation. The effect of the converging angle and the thickness of the delta spoilers on the acoustic resonance mechanism is also investigated for a constant height of 16 mm. The investigated converging angles of the delta spoilers, as shown in Figure 4-17, are: 60°, 65°, and 70°. Figure 4-18 shows that using larger converging angles (i.e. 65° and 70°) can still be suppressive and all the acoustic pressure values were kept less than 150 Pa. Having this suppressive performance with different angles can be useful in designing a spoiler that causes the least amount of pressure drop as will be discussed later.

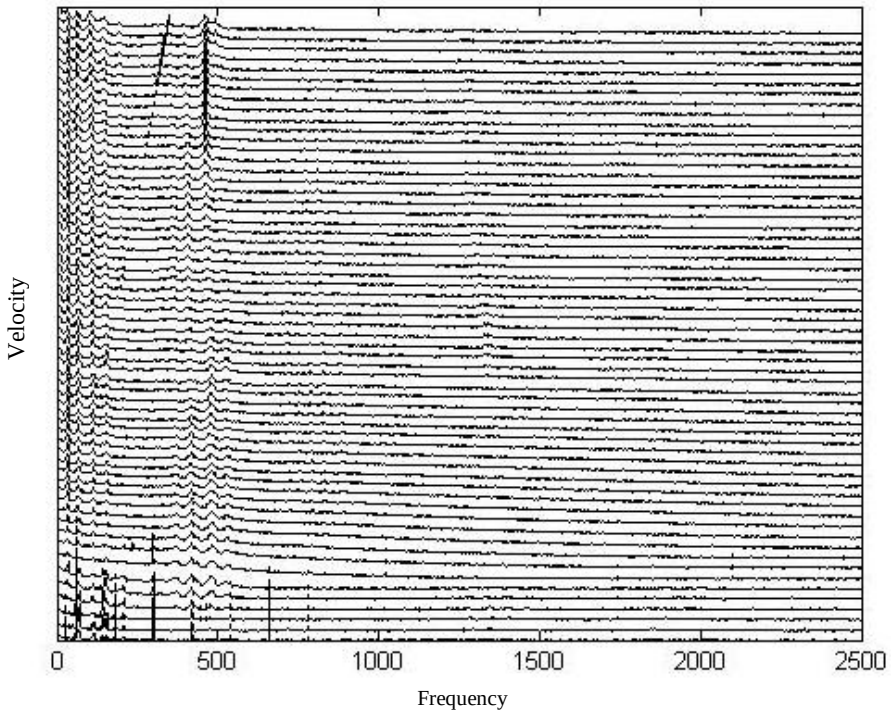

Figure 4-15: 2D waterfall plot for delta spoilers with height of 12 mm.

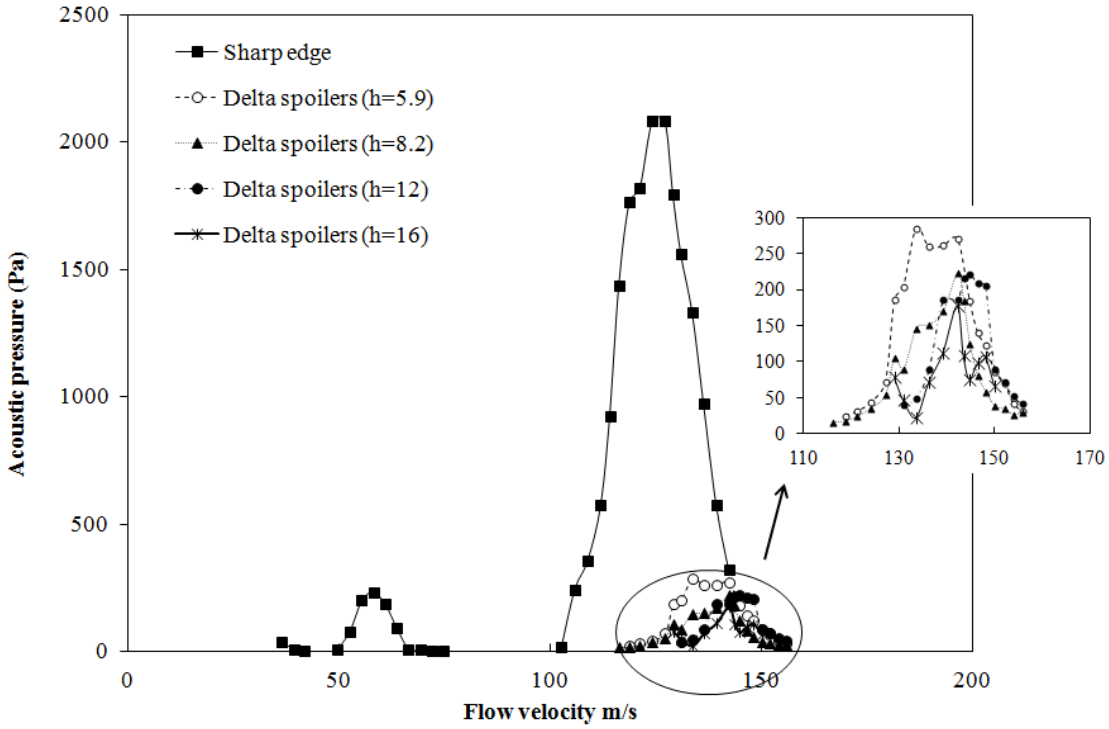

Figure 4-16: comparison between sharp edge and delta spoilers

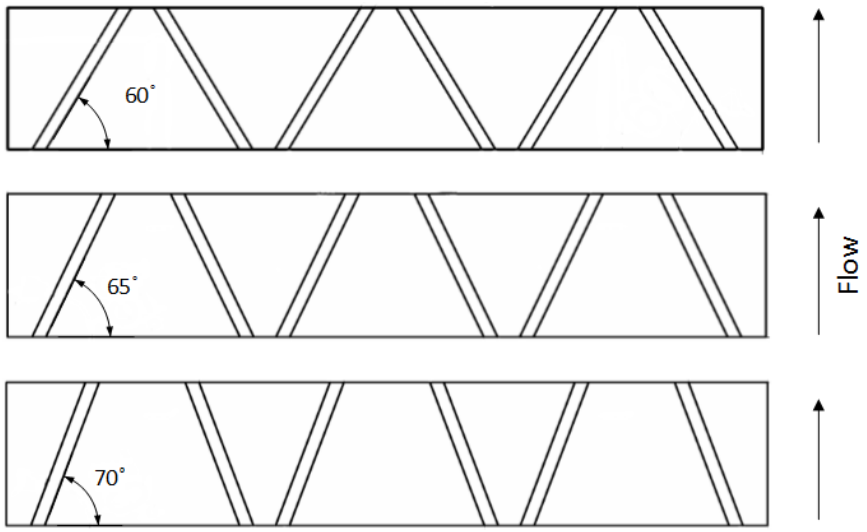

Figure 4-17: delta spoilers converging angles investigated

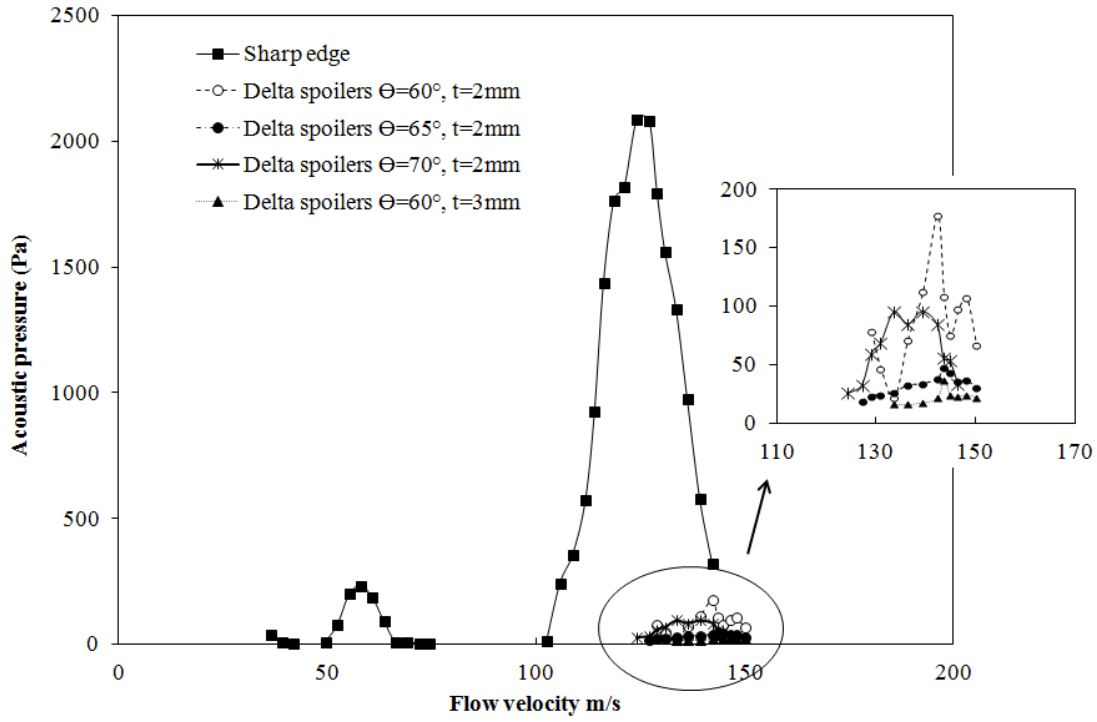

Figure 4-18: comparison between delta spoilers with different angles and thickness at height of 16 mm.

- **Curved spoilers**

Another edge geometry that is found to have suppressive effect is the curved spoilers, which direct the flow towards the side walls of the test section. 2D waterfall plot for curved spoilers with height of 12 mm is illustrated in Figure 4-19. Figure 4-20 shows the effect of the curved spoilers on suppressing the acoustic resonance excitation. When the first acoustic mode is excited by the first shear layer mode, the curved spoilers with a height of 5.9 mm suppress the acoustic pressure to less than 1260 Pa. Nevertheless, the curved spoilers with the height of 8.2 and 12 mm are not able to suppress more than the spoilers with the height of 5.9 mm. However further increase in the height of the spoilers to 16 mm results in better effect with amplitudes below 500 Pa.

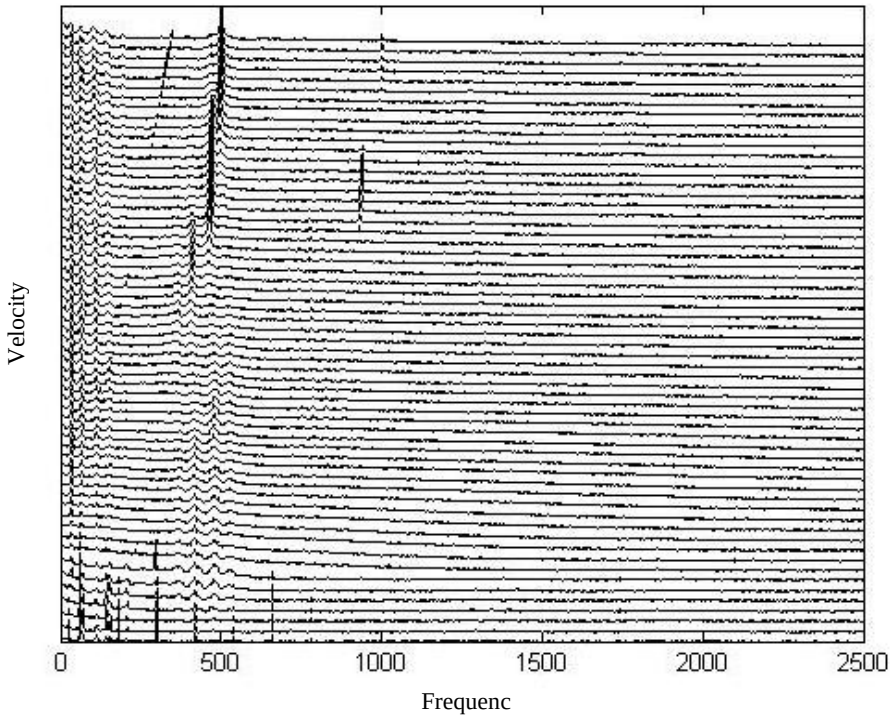

Figure 4-19: 2D waterfall plot for curved spoilers with height of 12 mm

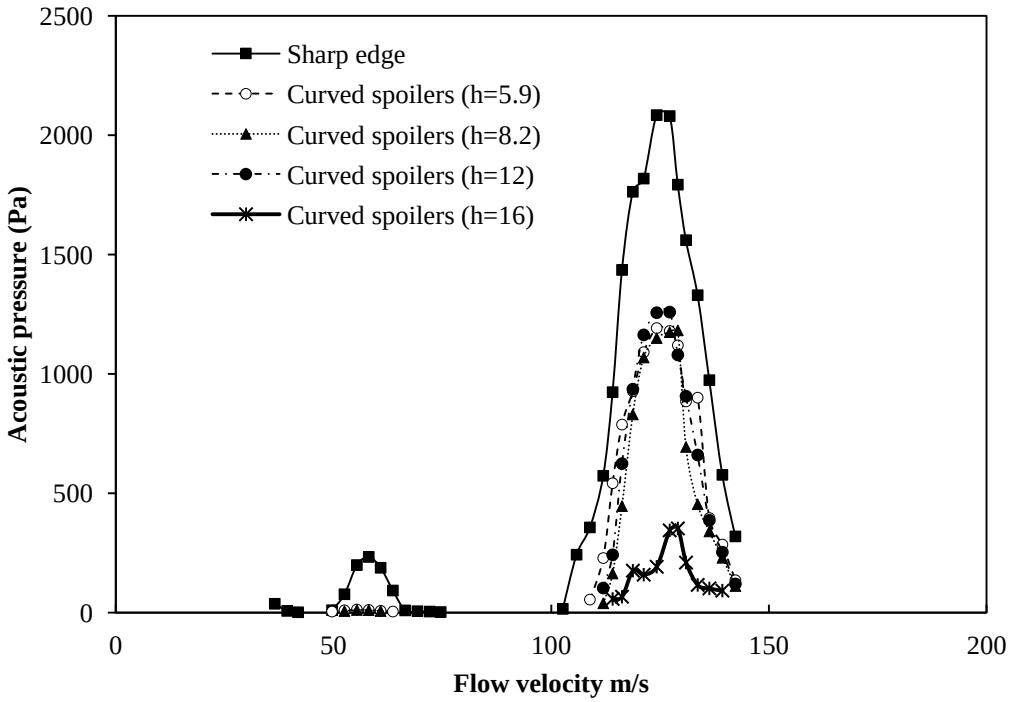

Figure 4-20: comparison between sharp edge and curved spoilers

- **Straight spoilers**

The straight spoilers which represent delta spoilers with angle of 90° and with different two spacing are found to have a minor effect on the acoustic resonance excitation. Figure 4-21 shows a 2D waterfall plot for straight spoilers with spacing of 4 mm and height of 5.2 mm. The effect of the straight spoilers on the acoustic resonance excitation is illustrated in Figure 4-22. The straight spoilers are not able to change the acoustic pressure significantly. The spacing between the spoilers and the height of the spoilers has no major effect on the acoustic resonance excitation.

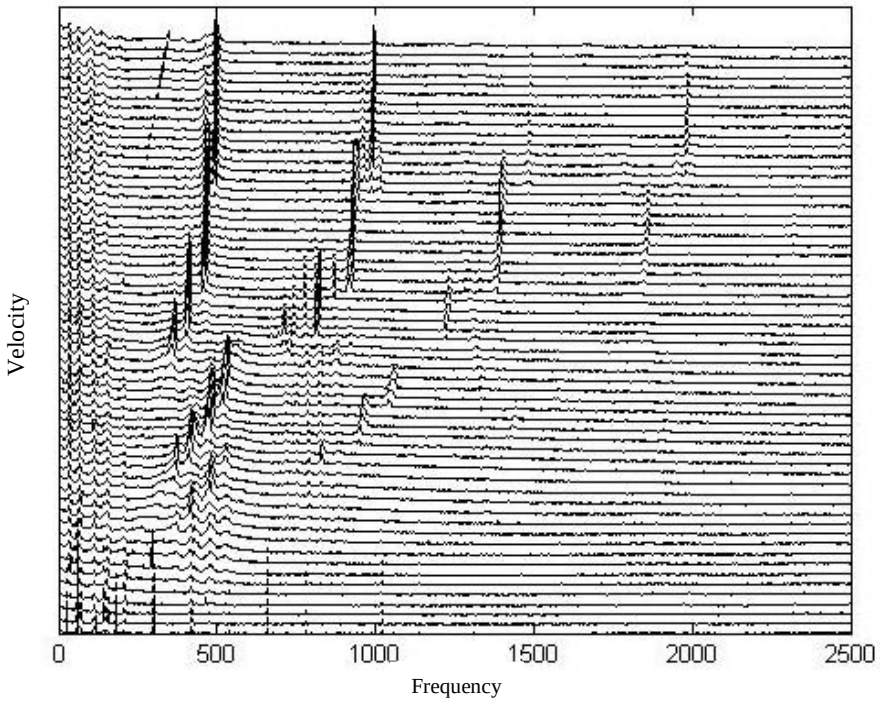

Figure 4-21: 2D waterfall plot for straight spoilers with spacing of 4 mm and height of 5.2 mm

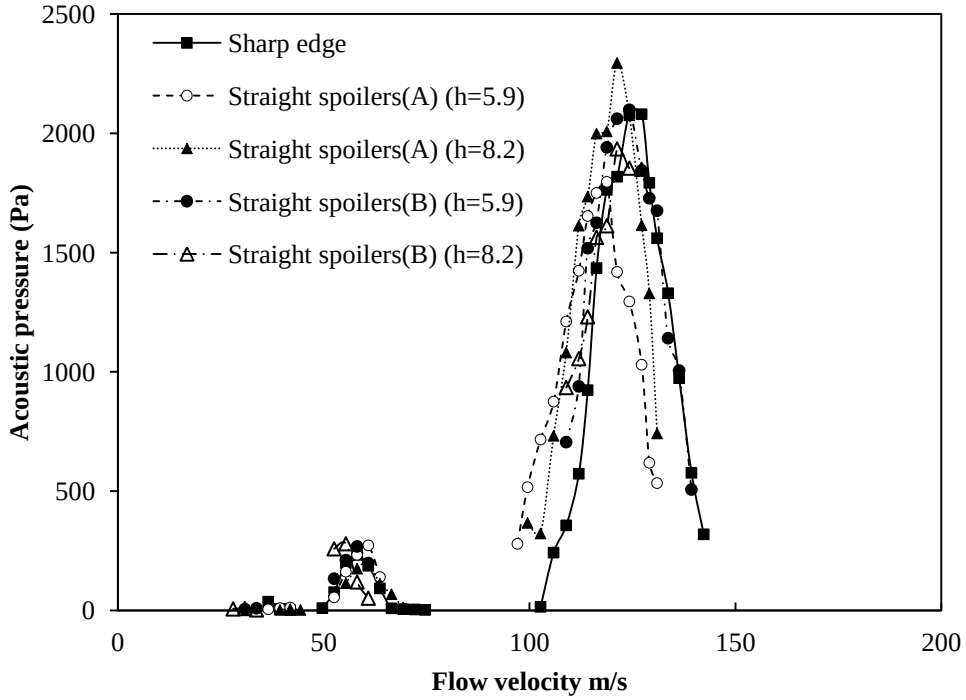

Figure 4-22: comparison between sharp edge and straight spoilers

4.1.1.1. Delta and curved spoilers height effect

The effect of the spoilers height on the acoustic resonance for both curved and delta spoilers is illustrated in Figure 4-23. The figure shows the maximum acoustic pressure recorded for the first acoustic mode. It can be seen that the increase of the spoilers height has no significant effect on the performance of the curved spoilers except for the height of 16 mm, which indicates that there is an optimum height for the spoilers to be effective and below that height the spoilers can't achieve the best performance.

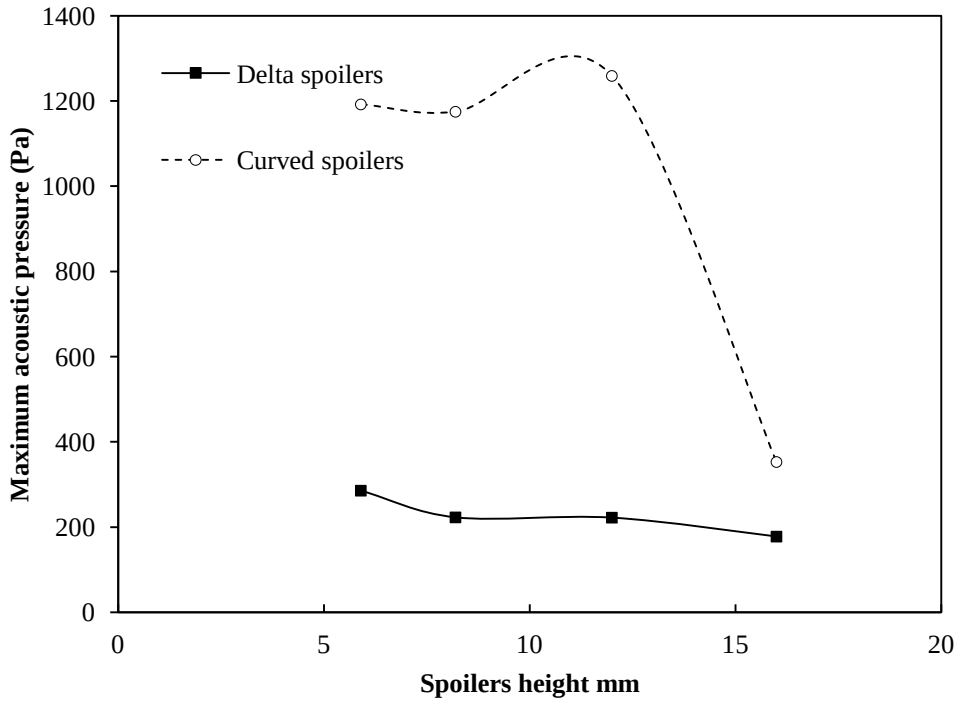

Figure 4-23: comparison between delta and curved spoilers (the maximum acoustic pressure of the first acoustic mode)

For the cavity with aspect ratio of 1.0 it can be concluded that the chamfered, round, and saw-tooth edge are not able to mitigate the acoustic resonance excitation, alternatively these edges were able to shift the acoustic resonance excitation to higher velocities. This shift was found to be dependent on the increase of the cavity length. The straight spoilers have no effect on the acoustic resonance excitation and almost same trends and values were obtained. The best performance was observed by the delta and curved spoilers and the acoustic pressure was significantly reduced. The increase of the delta spoilers converging angle to 70° has still good performance on the acoustic resonance excitation, the advantage of this suppressive performance will be discussed in the pressure drop and the hot wire measurements sections.

4.1.1.2. Pressure drop produced by edges – aspect ratio of 1.0

Pressure drop is an essential matter on designing spoilers. The main objective is to develop spoilers that can effectively suppress the acoustic resonance excitation with the least amount of pressure drop. To assess the pressure drop, differential pressure measurements were taken upstream and downstream the cavity. The differential pressure measurements were taken at various flow velocities up to 155 m/s. Figure 4-24 shows the pressure drop for the delta spoilers with the angles of 60° and 70° and the curved spoilers with a height of 16 mm compared to the base case. It can be seen that the curved and delta spoilers with angle of 60° produce the highest pressure drop with values reaching 2300 Pa at the velocity of 155 m/s, compared to the 1250 Pa at the base case. This pressure drop is significantly reduced when using the delta spoilers with an angle of 70°. The dimensionless pressure values obtained from equation (5) for each case are summarized in Table 4-2. From these values it can be concluded that the delta spoilers with the angle of 70° can reduce the pressure drop by around 35% compared to the delta spoilers with angle of 60°.

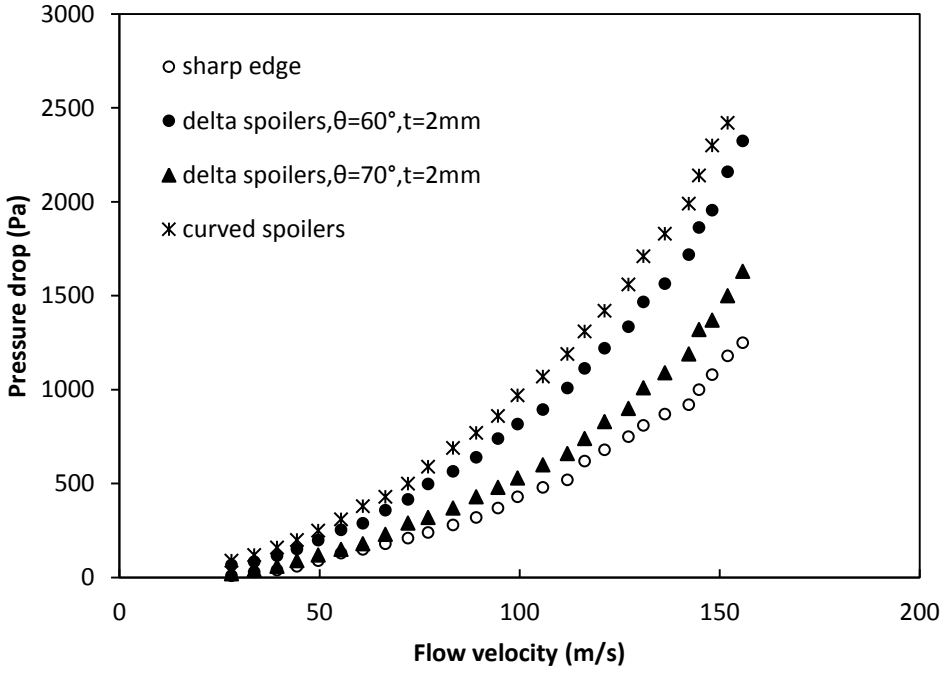

Figure 4-24 : comparison of pressure drop for some of the effective spoilers

Table 4-2: dimensionless pressure drop values

Edge geometry	Dimensionless pressure drop
Base case	0.07
Delta spoilers – angle 60°	0.14
Delta spoilers – angle 70°	0.09
Curved spoilers	0.15

4.1.2. Results of Cavity with aspect ratio of 1.67

- **Base case**

The same method of analysis used in the cavity with the aspect ratio of 1.0 is used for this cavity. Figure 4-25 shows the 3D waterfall plot for the base case. In this cavity only the first and second shear layer modes are developed. The Strouhal number values for the shear layer modes are summarized in Table 4-3 .The second shear layer mode excites the first acoustic mode at 585 Hz as seen in Figure 4-26 and Figure 4-27 starting around flow velocity of 66 m/s. It is observed that the resonance in this cavity occurs at higher frequency compared to the cavity with aspect ratio of 1.0, this is consistent with the predicted resonance frequency obtained from equation (4), and this equation governs the selection of the cavity aspect ratio, where shallower cavities will result in sending the resonance excitation out of the operating range. When the flow velocity reaches 120 m/s the first shear layer mode excites the first acoustic mode at frequency of 530 Hz. The effectiveness of the edges on suppressing acoustic resonance excitation is assessed with respect to the first acoustic mode.

Table 4-3: Strouhal number values for cavity with aspect ratio of 1.67

Shear layer mode	St
N=1	0.48
N=2	0.94

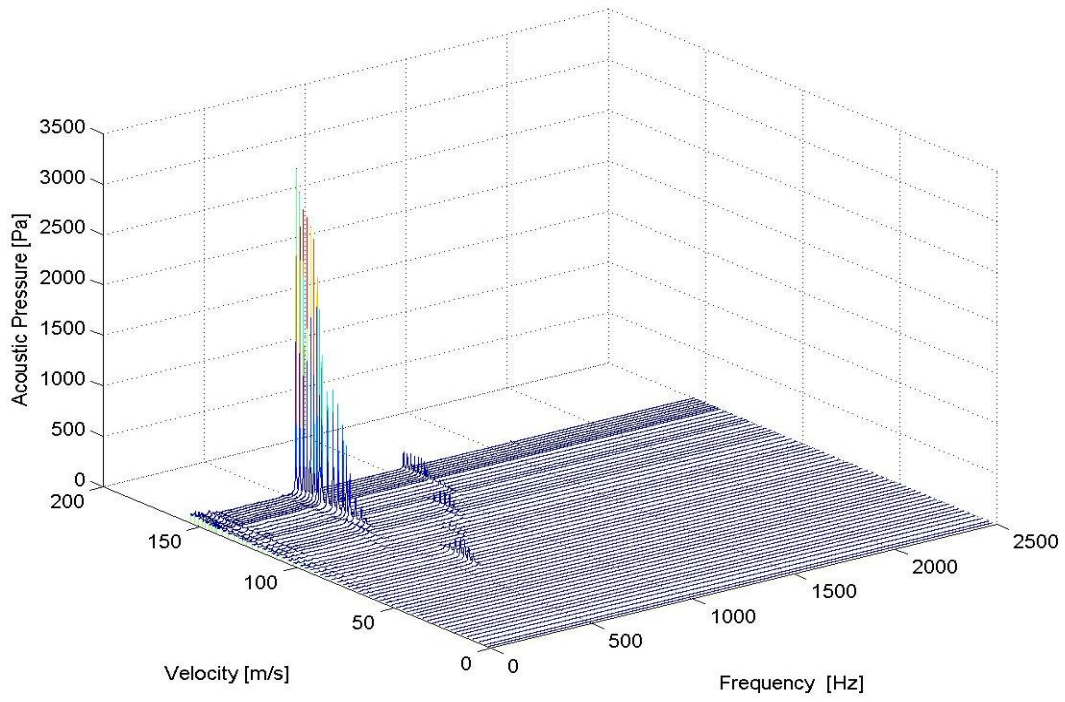

Figure 4-25: 3D waterfall plot for base case, aspect ratio of 1.67

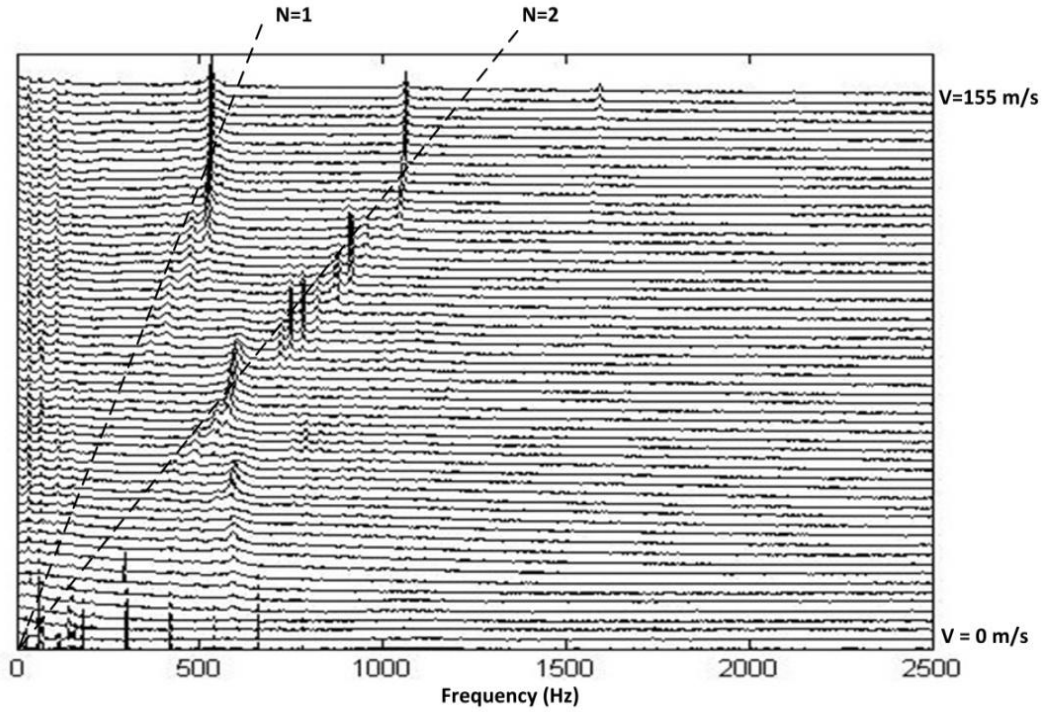

Figure 4-26: 2d waterfall plot for base case (sharp edge) with aspect ratio of 1.67

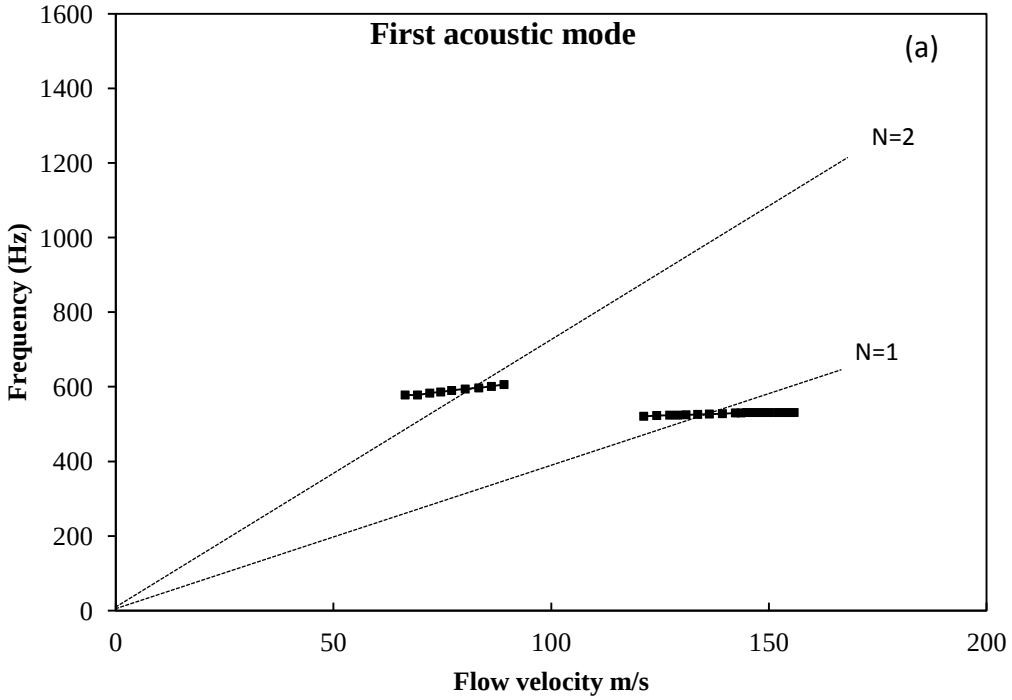

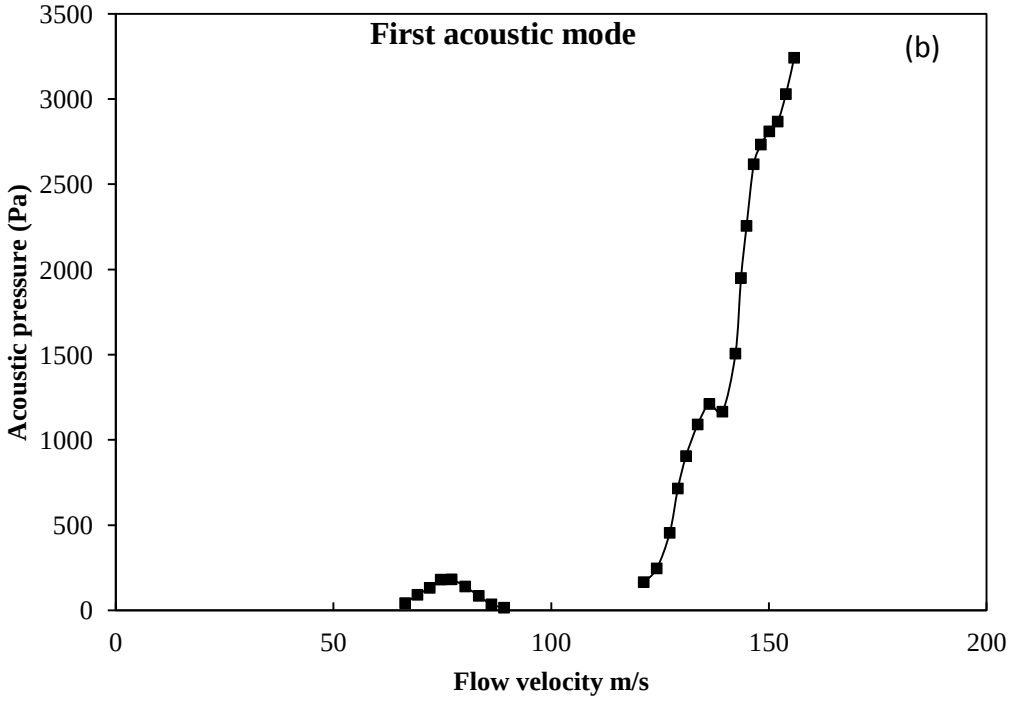

Figure 4-27: first acoustic mode excited in the base case with aspect ratio of 1.67. (a) shows the frequency with the flow velocity, (b) shows the acoustic pressure with the flow velocity

- **Round edges**

The radii of the round edges tested are 12.7 and 25.4 mm. The edges are tested upstream and/or downstream. Figure 4-28 shows the 2D waterfall plot for the round edge with diameter of 12.7 mm installed upstream. The effect of the round edges on the acoustic resonance excitation is illustrated in Figure 4-29. The round edge with radius of 12.7 mm suppresses the resonance excited by the second shear layer mode and delays the onset of acoustic resonance to start around flow velocity of 77 m/s, while the round edge with 25.4 mm completely suppresses the first acoustic resonance when it is excited by the second shear layer mode and the resonance excited by the first shear layer mode is delayed to start after flow velocity of 150 m/s. Figure 4-30 and Figure 4-31 show comparison between the effects of the round edges when installed upstream and/or downstream for both radii investigated. As observed with the cavity with aspect ratio of 1.0, the figures show that rounding the upstream edge shifts the occurrence of the acoustic resonance excitation to higher velocities, however, rounding the downstream edge has no significant shift on the resonance excitation. As observed earlier with the cavity with aspect ratio of 1.0 the shift in the acoustic resonance excitation is introduced by the upstream edge.

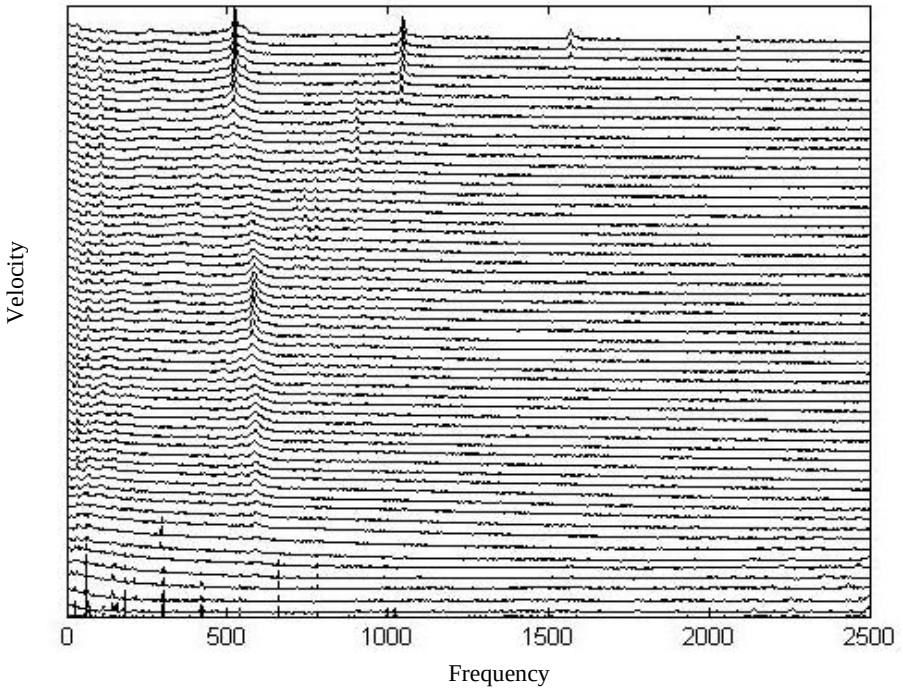

Figure 4-28: 2Dwaterfall plot for the round edge with diameter of 12.7 mm installed upstream

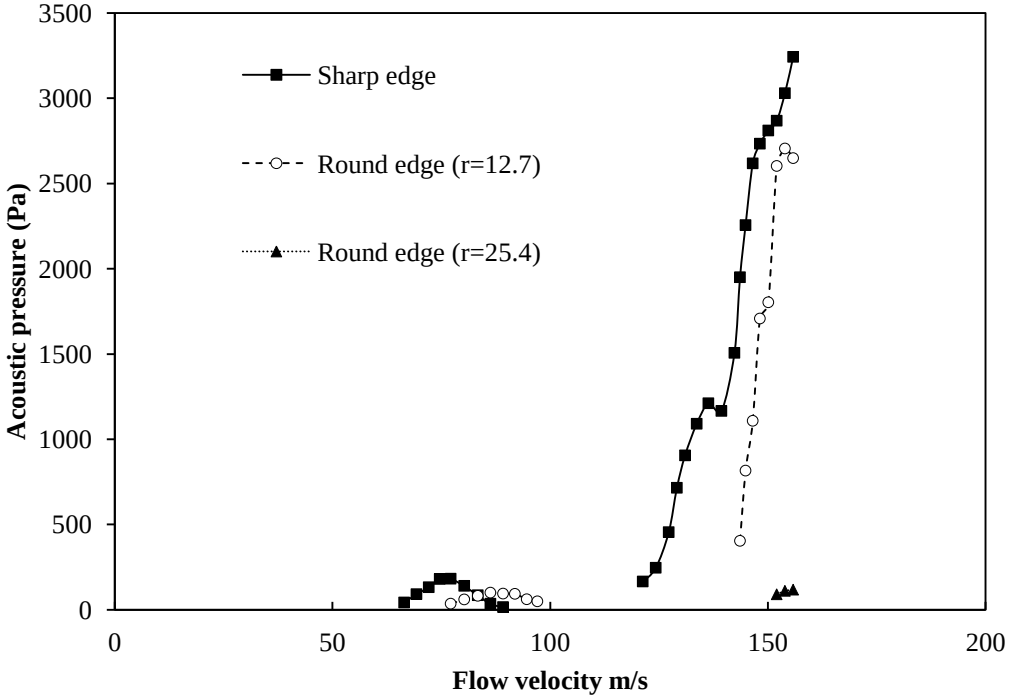

Figure 4-29: comparison between sharp edge and round edge installed upstream

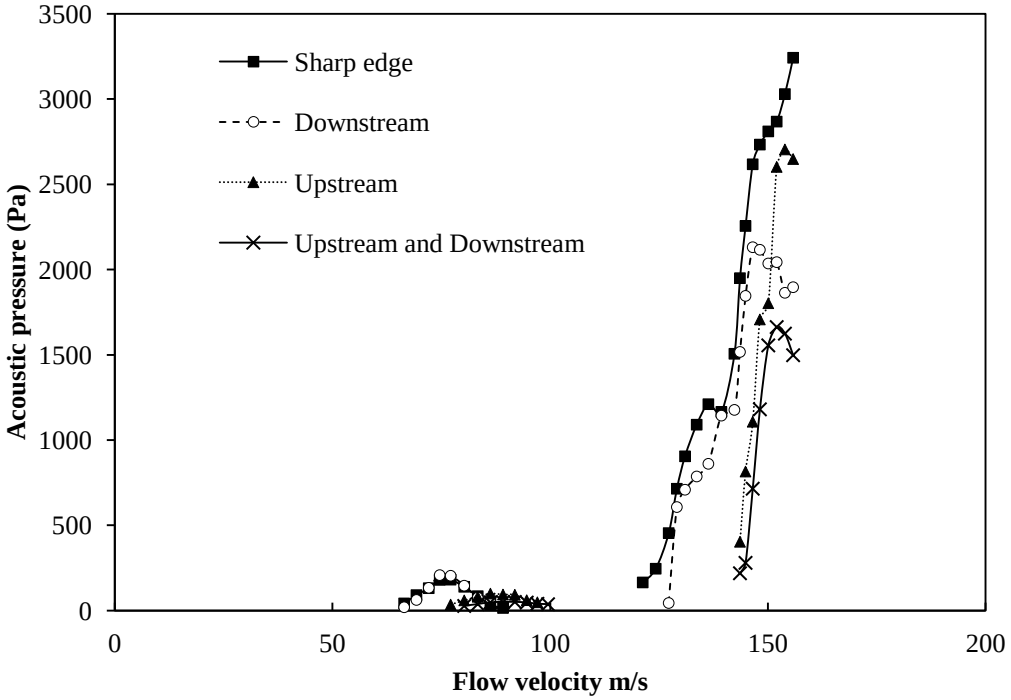

Figure 4-30: comparison between round edge (r=12.7 mm) installed upstream and/or downstream

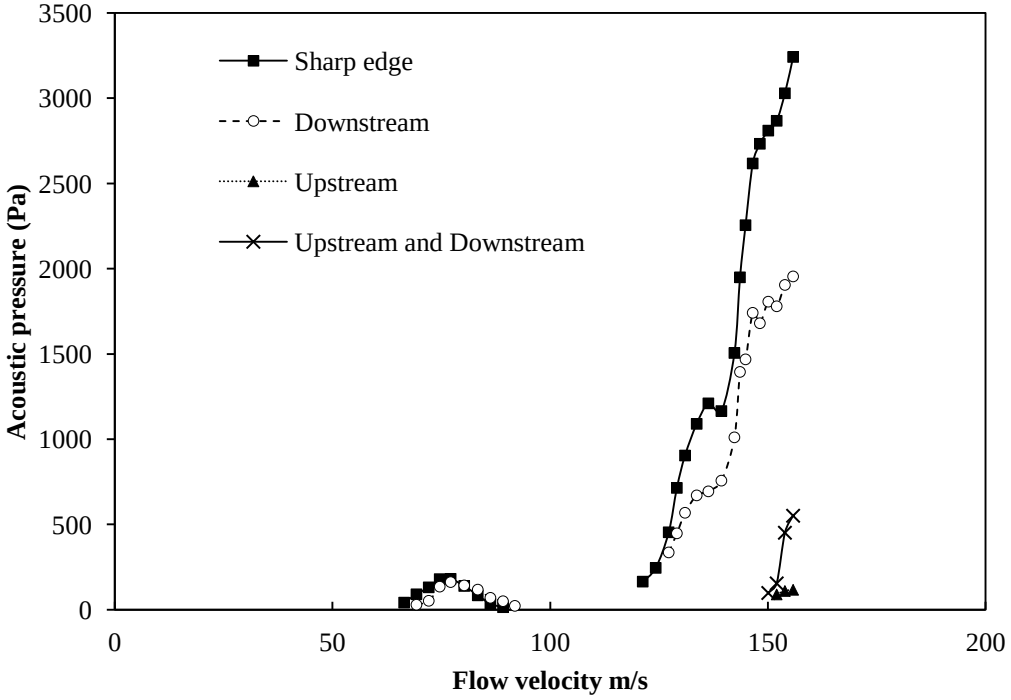

Figure 4-31: comparison between round edge (r=25.4 mm) installed upstream and/or downstream

- **Chamfered edges**

The chamfered edges were installed upstream. The angles of the chamfered edges investigated are: 107°, 120°, 135°, and 150°. Figure 4-32 shows the 2D waterfall plot for chamfered edge with an angle of 120° installed upstream. Figure 4-33 shows the effect of the chamfered edges on the acoustic resonance excitation. It is observed that the onset of the acoustic resonance excited by the second shear layer mode is delayed from 66 m/s to 77 m/s. Moreover, in this acoustic resonance excitation the chamfered edges result in amplifying the acoustic pressure. The resonance excited by the first shear layer mode is also delayed from 121 m/s to 143 m/s. Moreover, the angle of the chamfered edge is observed to have little influence on the acoustic pressure without major difference in the onset of the acoustic resonance. As observed in the cavity with aspect ratio of 1.0, the chamfered edge with angle 107° results in further shift in the onset of acoustic resonance which completely moves the resonance excitation out of the flow range investigated, same behavior is observed with the round edge with radius 25.4 mm.

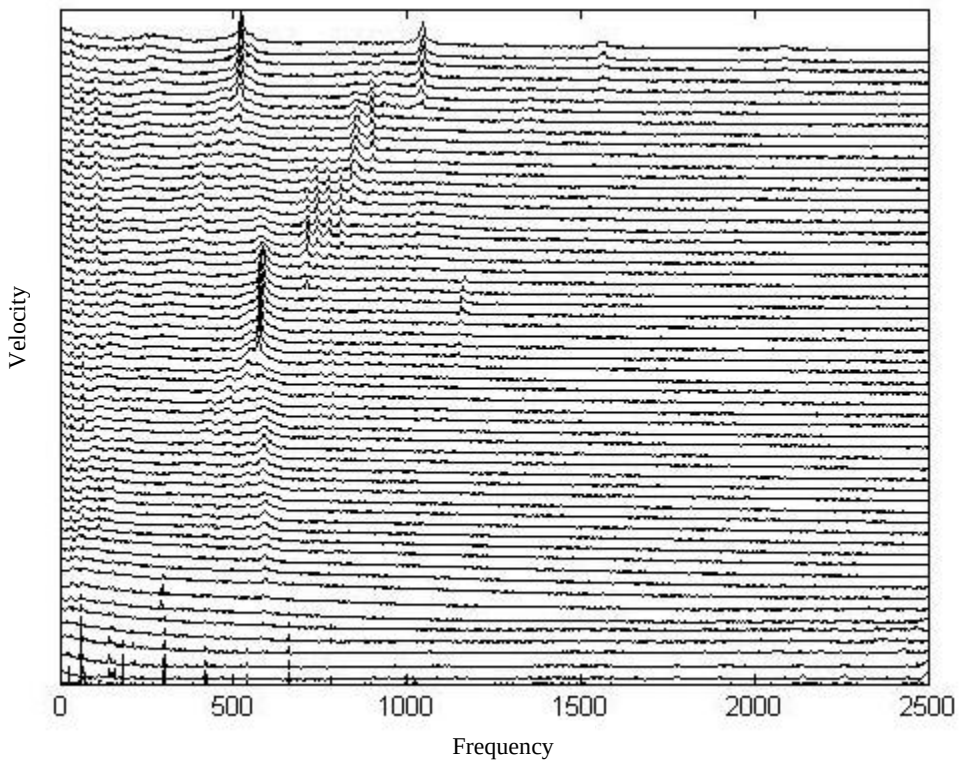

Figure 4-32: 2D waterfall plot for chamfered edge with an angle of 120° installed upstream

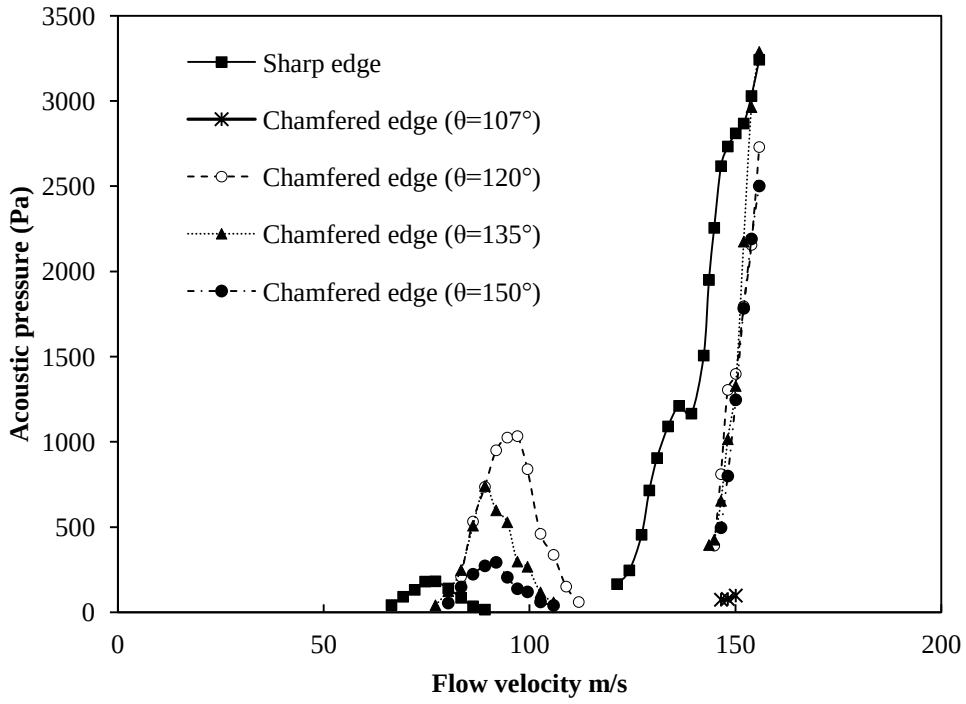

Figure 4-33: comparison between sharp edge and chamfered edges

As in the cavity with aspect ratio of 1.0, the data for the chamfered and round edges are normalized and plotted using dimensionless pressure and Strouhal number, as shown in Figure 4-34 and Figure 4-35. The cavity length in these figures is adjusted to count for the round and the chamfered edges and it is clear that the Strouhal number for the first and second shear layer modes are similar to that reported in the literature.

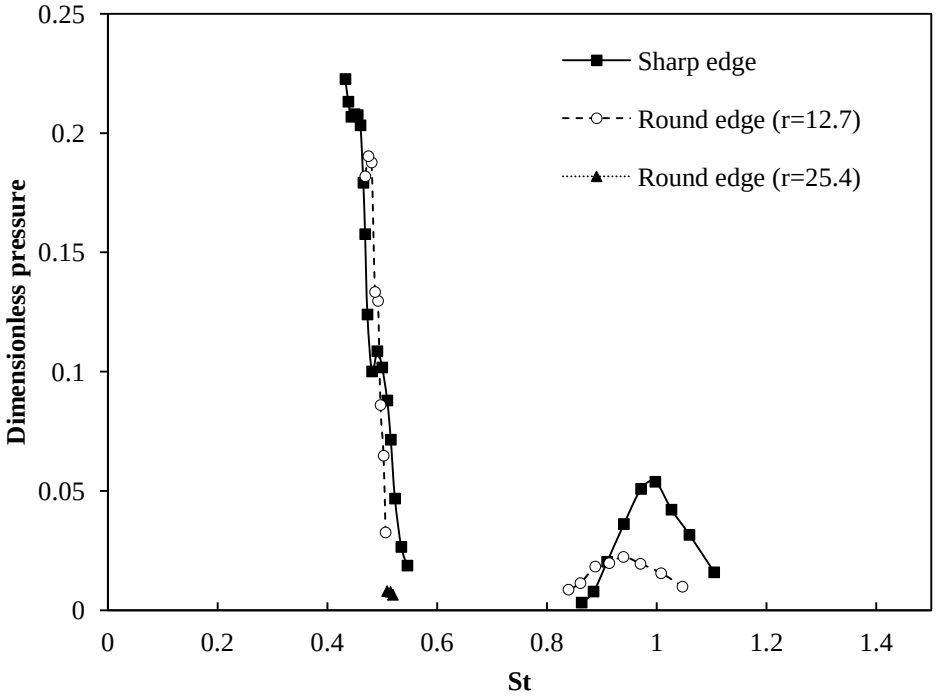

Figure 4-34: comparison between normalized values for sharp and round edges

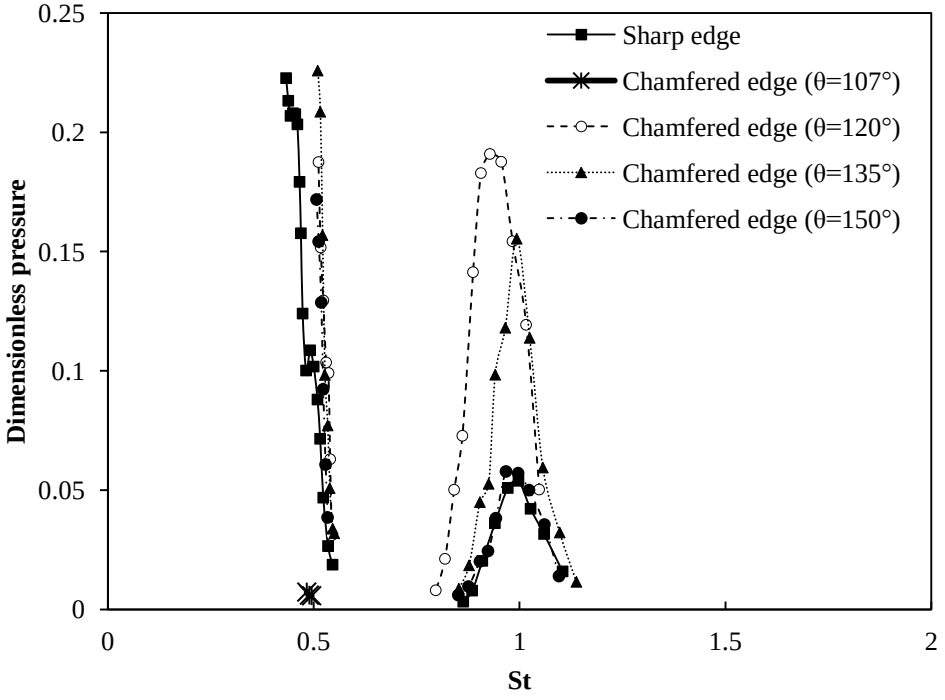

Figure 4-35: comparison between normalized values for sharp and chamfered edges

- **Saw-tooth edge**

The saw-tooth edge results in delaying the onset of acoustic resonance to higher velocities as observed with the chamfered and round edges. Figure 4-36 shows a 2D waterfall plot for saw-tooth edge installed upstream. Figure 4-37 shows the effect of the saw-tooth on the acoustic resonance excitation. This conclusion is consistent with the results obtained from the cavity with aspect ratio of 1.0.

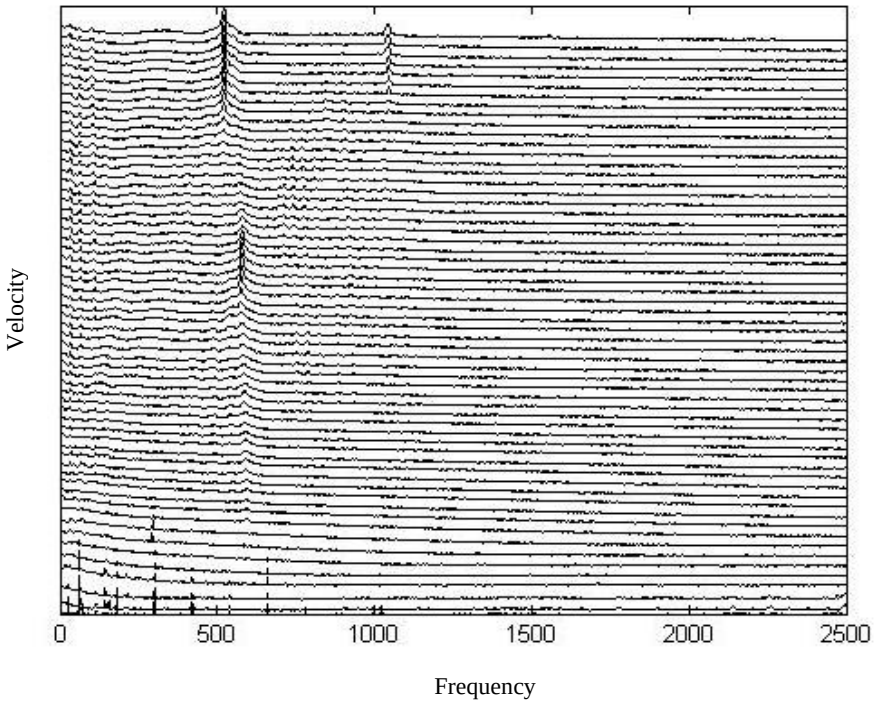

Figure 4-36: 2D waterfall plot for saw-tooth edge installed upstream

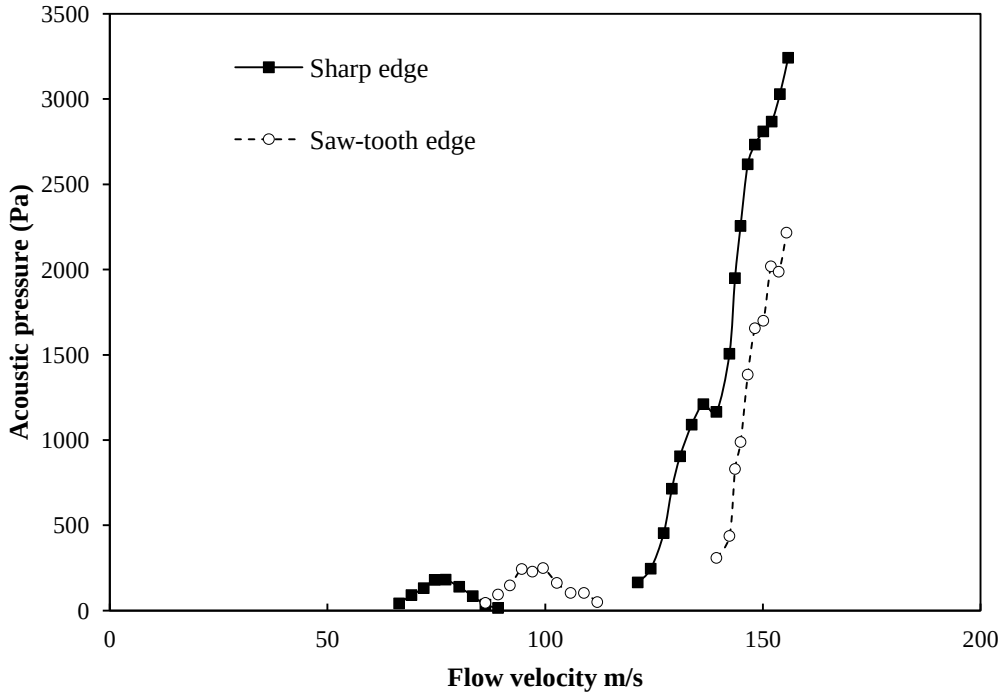

Figure 4-37: comparison between sharp edge and saw tooth edge

- **Delta spoilers**

Delta spoilers with different dimensions are investigated. Figure 4-38 shows 2D waterfall plot for delta spoilers with height of 8.25 mm. The effect of the delta spoilers on the acoustic resonance excitation is illustrated in Figure 4-39. The delta spoilers significantly suppress the pressure amplitudes as seen in the figure. The four delta spoilers are able to completely suppress the excitation of the first acoustic mode caused by the second shear layer mode. The resonance of the first acoustic mode when it is excited by the first shear layer mode is suppressed as well, and it is observed that the increase in the height of the spoilers results in better performance in suppressing the acoustic resonance excitation.

As observed in the cavity with aspect ratio of 1.0, increasing the angle of the delta spoilers still considered suppressive as shown in Figure 4-40. Nevertheless, increasing the thickness of the spoilers to 3 mm can slightly enhance the performance of the spoilers.

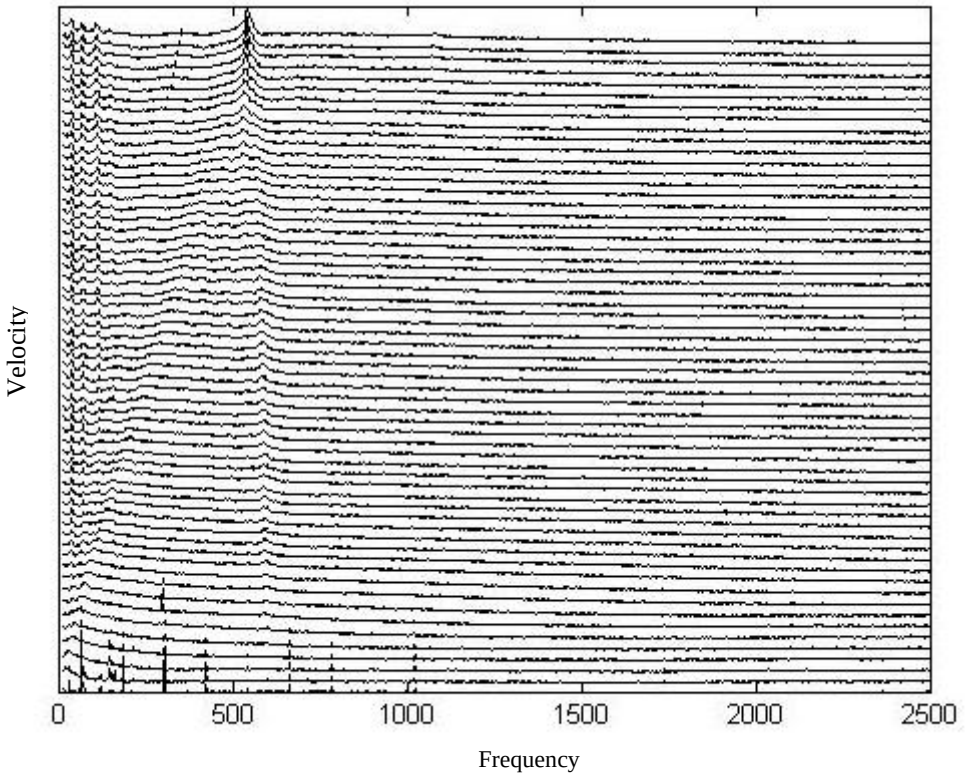

Figure 4-38: 2D waterfall plot for delta spoilers with height of 8.2 mm

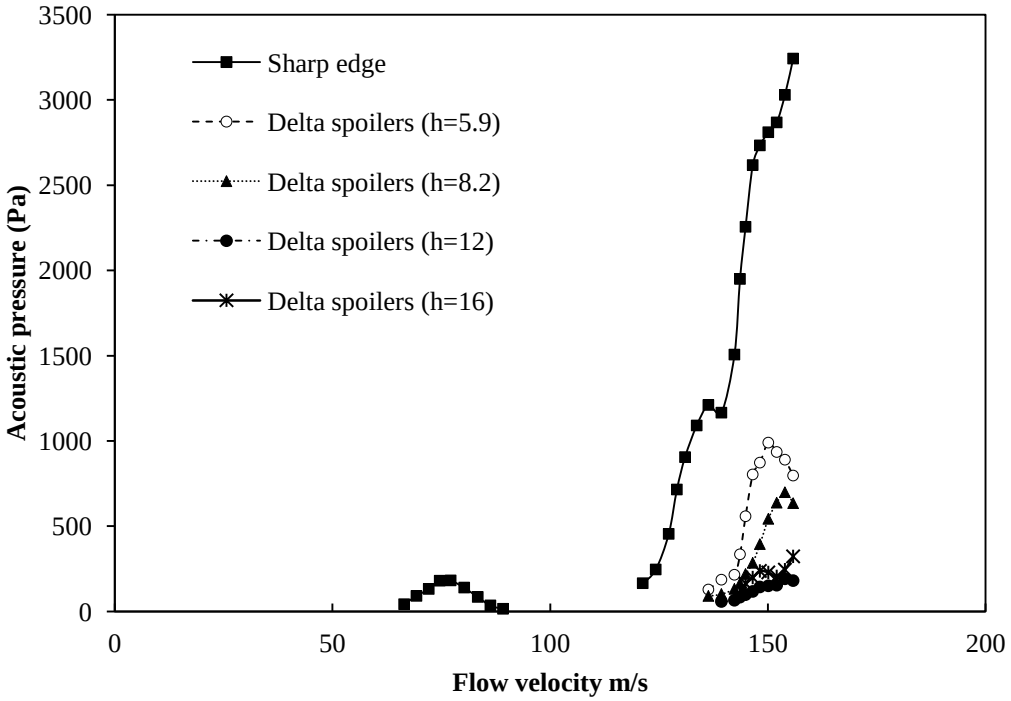

Figure 4-39: comparison between sharp edge and delta spoilers

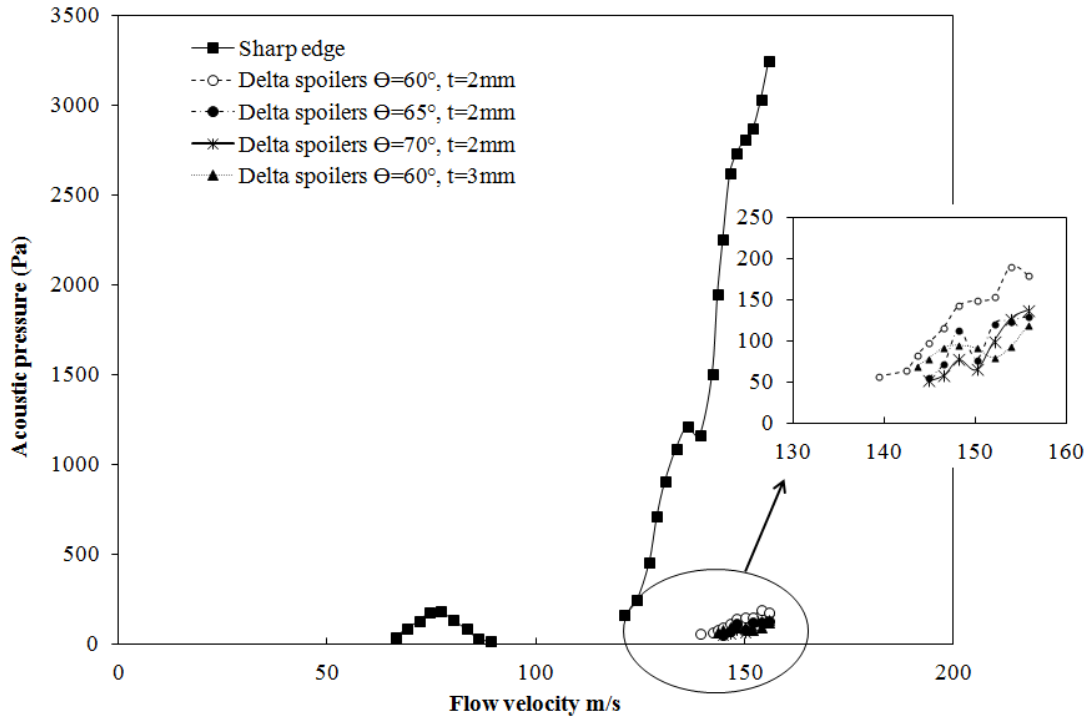

Figure 4-40: Comparison between the base case and the delta spoilers with different converging angles and spoilers thickness (h=12 mm).

- **Curved spoilers**

The curved spoilers are found to be suppressive as well. Figure 4-41 Shows 2D waterfall plot for curved spoilers with height of 8.2 mm. The effect of the curved spoilers on the acoustic resonance excitation is illustrated in Figure 4-42. All curved spoilers are able to completely suppress the effect of the second shear layer mode on exciting the first acoustic mode. For the resonance caused by the first shear layer mode and the first acoustic mode the spoilers are also able to significantly suppress the pressure amplitudes. The increase of the spoilers' height results in better performance, and the curved spoilers with the height of 12 and16 mm suppress the acoustic pressure to less than 150 Pa, which seems to be more effective than the delta spoilers with the same heights.

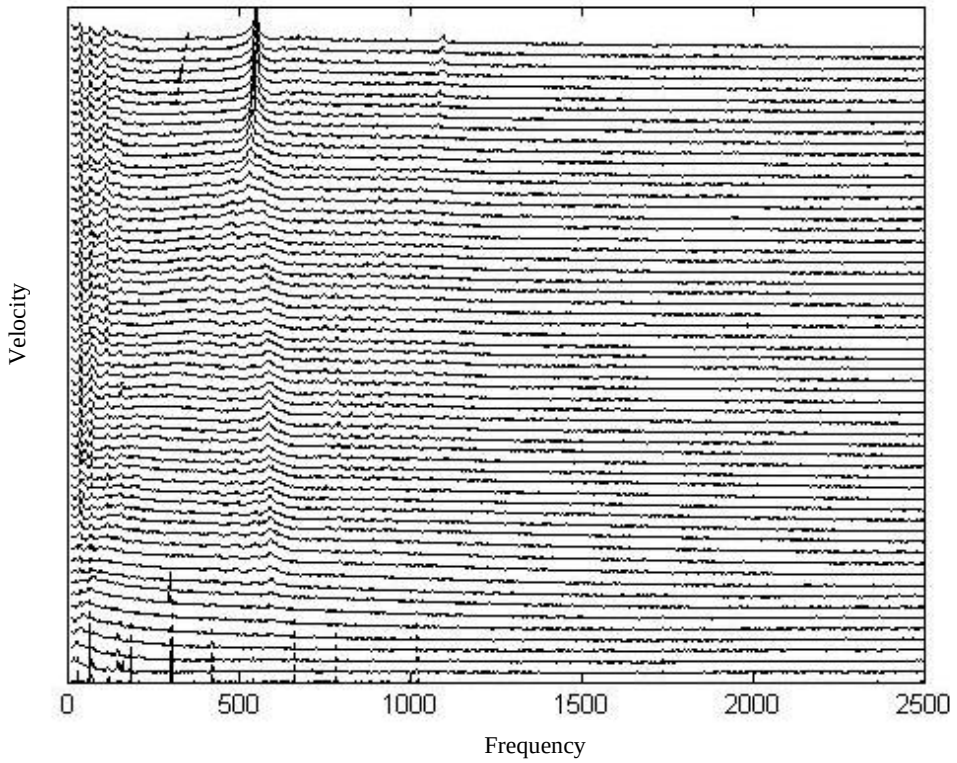

Figure 4-41: 2D waterfall plot for curved spoilers with height of 8.2 mm

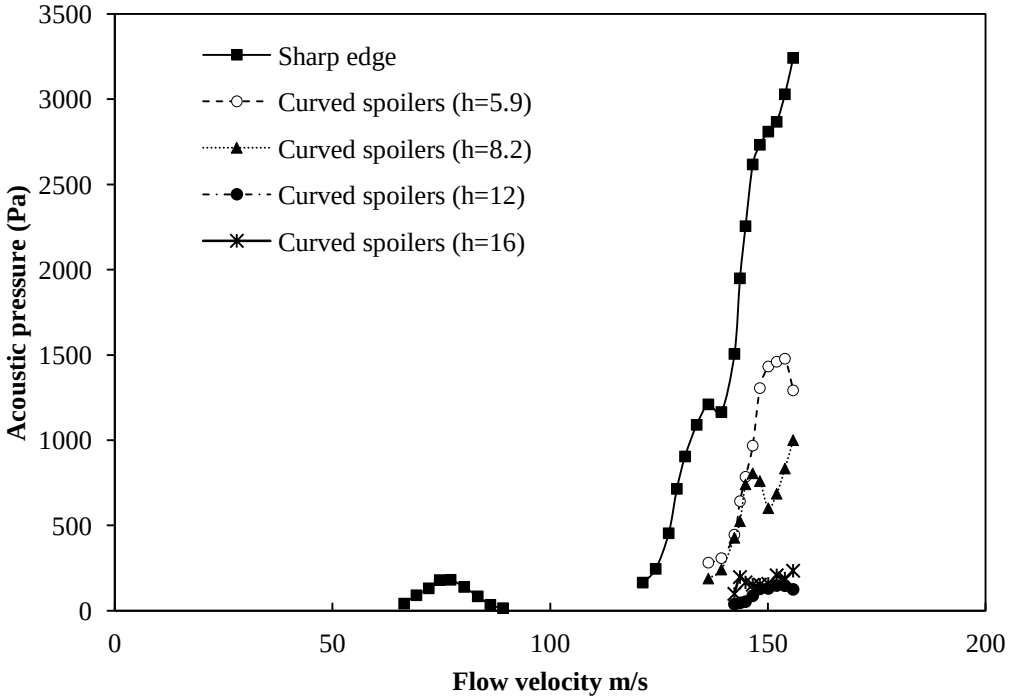

Figure 4-42: comparison between sharp edge and curved spoilers

Straight spoilers

The straight spoilers in this cavity were found to have no significant effect compared to the base case. Figure 4-43 shows a 2D waterfall plot for straight spoilers with spacing of 4 mm and height of 8.2 mm. Figure 4-44 shows the effect of the straight spoilers in the acoustic resonance excitation. The acoustic pressure values generally following the same trend of the base case and the acoustic pressure values are almost the same. This is consistent with the results from the cavity with aspect ratio of 1.0 From these results a conclusion can be driven that the straight spoilers do not affect the resonance excitation mechanism regardless of the spacing and the heights.

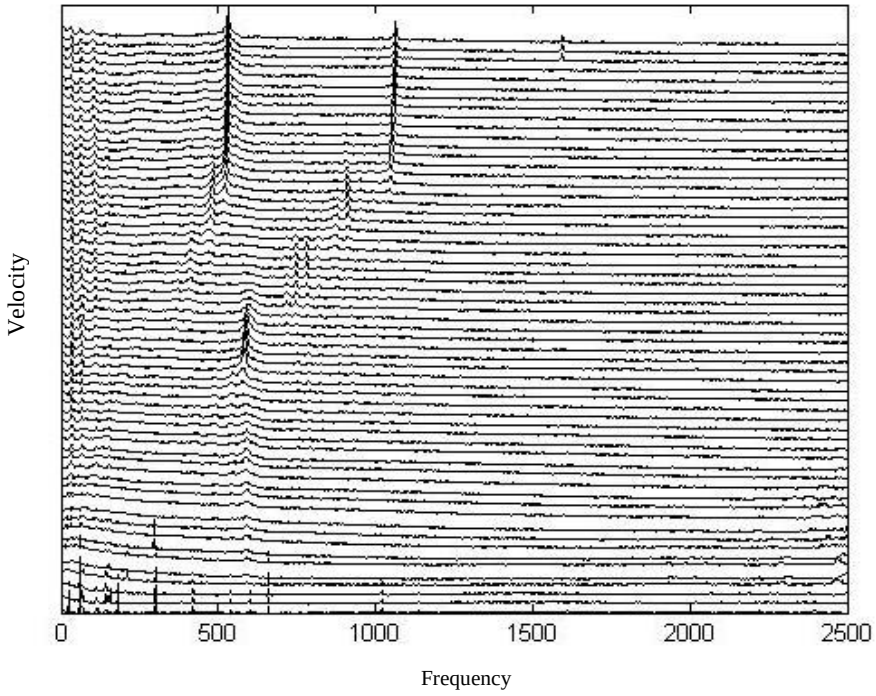

Figure 4-43: 2D waterfall plot for straight spoilers with spacing of 4 mm and height of 8.2 mm

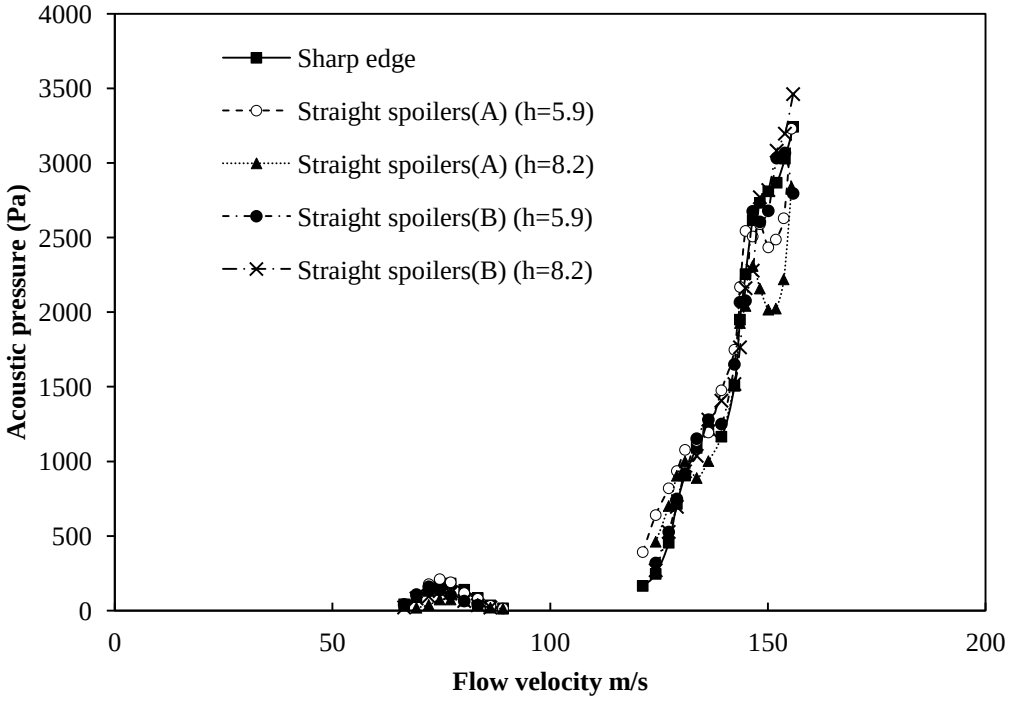

Figure 4-44: comparison between sharp edge and straight spoilers

4.1.2.1. Curved and delta spoilers height effect

The effect of the spoilers' height for the delta and curved spoilers on the acoustic excitation mechanism for this cavity is illustrated in Figure 4-45. Interestingly, the increase of the height for both delta and curved spoilers significantly change the performance on suppressing the acoustic resonance excitation. Moreover, further increase of the height in the curved spoilers to 12 and 16 mm is observed to achieve better performance compared to the delta spoilers.

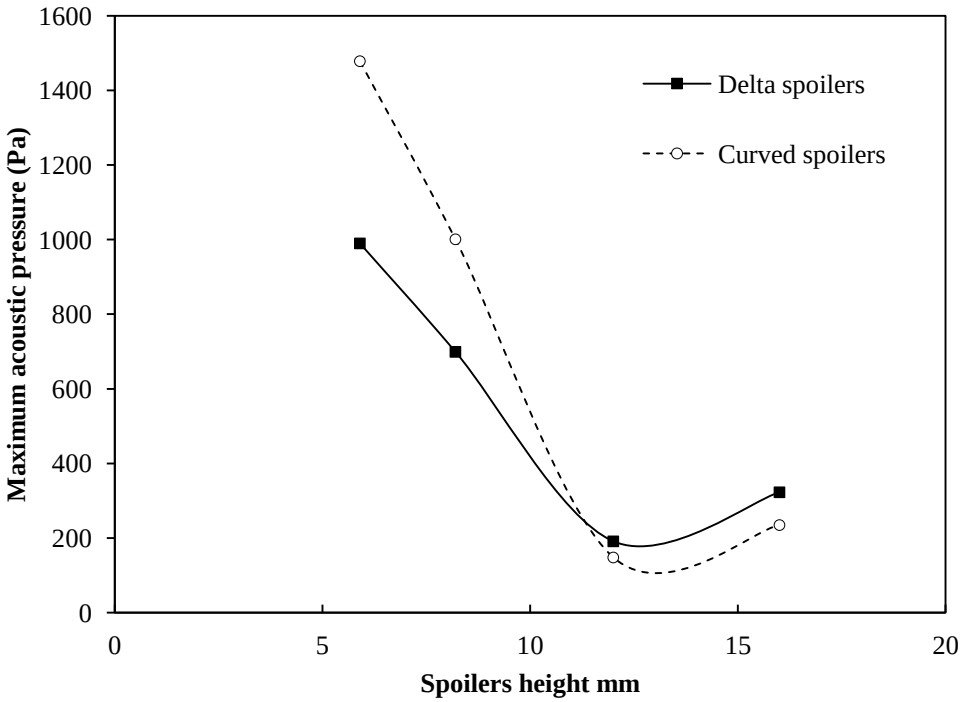

Figure 4-45: comparison between delta and curved spoilers (the maximum acoustic pressure of the first acoustic mode)

The results for the cavity with aspect ratio of 1.67 are consistent with the results obtained from the cavity with the aspect ratio of 1.0. This can be noticed in the shift observed with the chamfered, round, and saw-tooth edges. Moreover, the straight spoilers were observed to have no effect on the acoustic resonance excitation as observed in the cavity with aspect ratio of 1.0. The curved and delta spoilers with different angles were found to be suppressive. However, in contrary to what observed in the cavity with aspect ratio of 1.0, the effect of the spoilers height on the acoustic resonance excitation seems to have proportional relation with the suppression performance as the height of the spoilers increases the suppression performance increases till the height of 12 mm. After the height of 12 mm , the spoilers performance remain on the same level with the acoustic pressure values almost vanished.

4.1.2.2. Pressure drop produced by edges – aspect ratio of 1.67

For this aspect ratio a pressure drop measurements were also obtained. To investigate the effect of the spoilers height on the pressure drop, the measurements were taken for spoilers with different height than in the cavity with aspect ratio of 1.0. Curved, delta spoilers with angle 60, and delta spoilers with angle 70 are compared at height of 12 mm. Figure 4-46 shows the pressure drop for each geometry at different flow velocity, generally, it is observed that the difference in the pressure drop values between all geometries investigated is small compared to the values obtained in the cavity with aspect ratio of 1.0. This is attributed to using spoilers with smaller height (12mm). However, the delta spoilers with the angle of 70° is observed to have the least pressure drop as in the cavity with aspect ratio of 1.0. The dimensionless pressure values are summarized in Table 4-4.

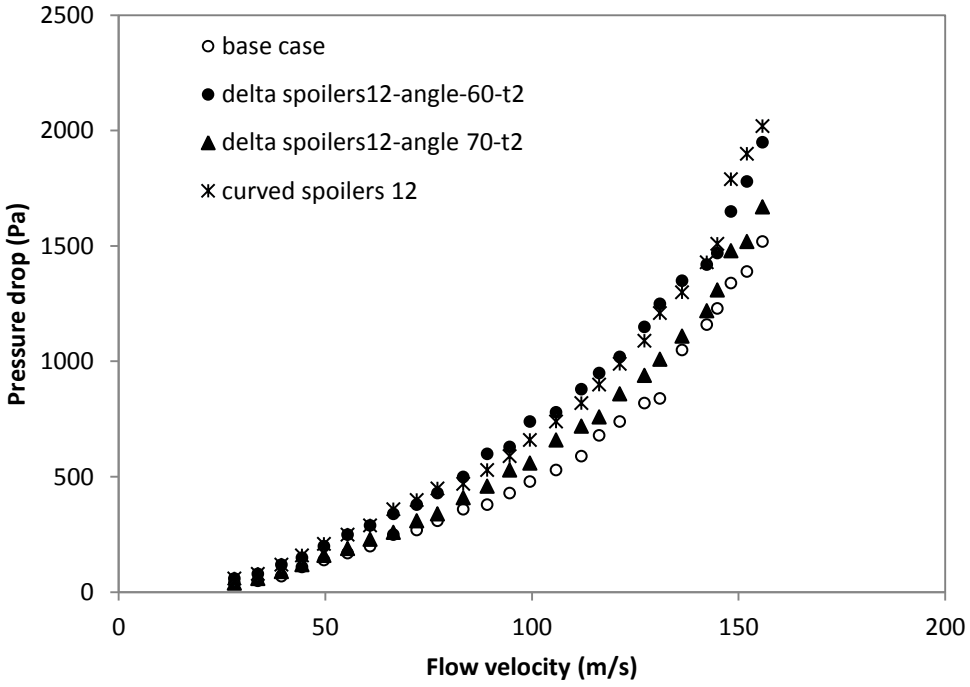

Figure 4-46: comparison of pressure drop for some of the effective spoilers

Table 4-4: dimensionless pressure drop values

Edge geometry	Dimensionless pressure drop
Base case	0.09
Delta spoilers – angle 60°	0.12
Delta spoilers – angle 70°	0.1
Curved spoilers	0.12

4.1.3. Hotwire measurements

In order to understand why some spoilers work better than others, measurements of the velocity fluctuations of the separated shear layer across the cavity were performed before the onset of acoustic resonance. The measurements were taken at a distance of 3 mm from the upstream edge in the x-direction as shown in Figure 4-47, and the velocity profiles in the lateral direction were obtained. The measurements of the velocity profile were taken at different heights (5.08, 10.16 and 25.4 mm) inside and outside of the shear layer which is found to have a thickness of 13 mm, as shown in Figure 4-48, and momentum thickness of 1.2 mm at a mean flow velocity of 28 m/s. Figure 4-49 and Figure 4-51 show the velocity fluctuations along the lateral direction (y) of the cavity for the delta spoilers with angles 60° and 70°. It can be seen that the delta spoilers with both angles are able to introduce velocity fluctuations to the flow. The ability of these spoilers to suppress the acoustic resonance excitation can be attributed to these velocity fluctuations that result in orthogonal vortices formation preventing the development of the main vortices initiated by the boundary layer separation. The existence of the orthogonal vortices in the stream wise direction is also proved by the high velocity perturbations, as shown in Figure 4-50 and Figure 4-52, observed downstream of the spoilers, these high perturbations indicate the wake of vortices and it also gives an indication for the size of the vortices developed. Similar velocity fluctuations are observed with the curved spoilers with a height of 16 mm which is known to have a suppressive effect on the acoustic resonance excitation. The measurements at the height of 25.4 mm indicate that the flow is no longer affected by the spoilers and the velocity is close to the mean flow velocity. However at the height of 10.16 mm which is within the shear layer thickness, the fluctuations are observed to be higher than those at other heights. The same velocity measurements were taken for the straight spoilers with spacing of 4 mm and height of 8.2 mm, which were known to be not effective on suppressing the acoustic resonance excitation. As can be seen in Figure 4-53 and Figure 4-54 the straight spoilers can develop velocity fluctuations across the lateral direction. However, these fluctuations are on small scale compared to the delta spoilers, these

fluctuations result in weak vortices formation that cannot prevent the main vortices formation at the cavity mouth.

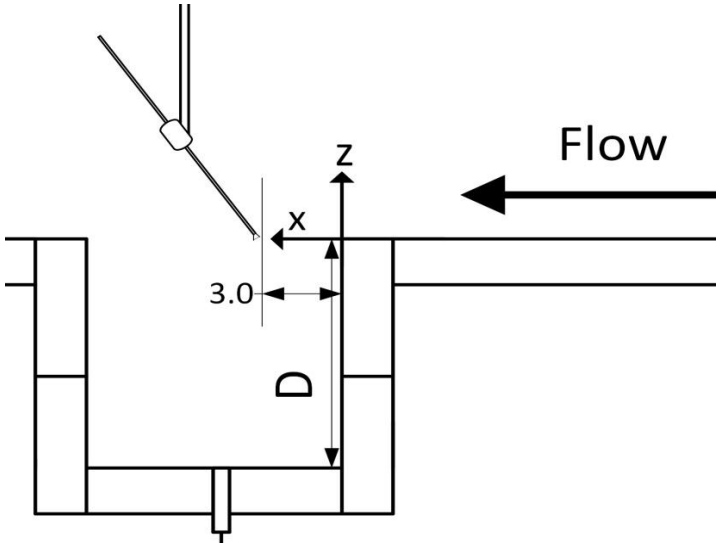

Figure 4-47: schematic drawing for the hotwire measurements along the stream wise direction

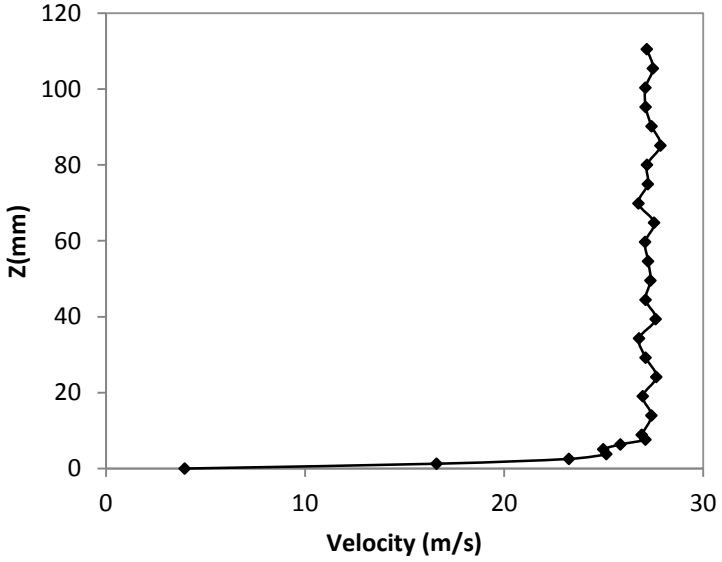

Figure 4-48: shear layer profile at main flow velocity of 28 m/s

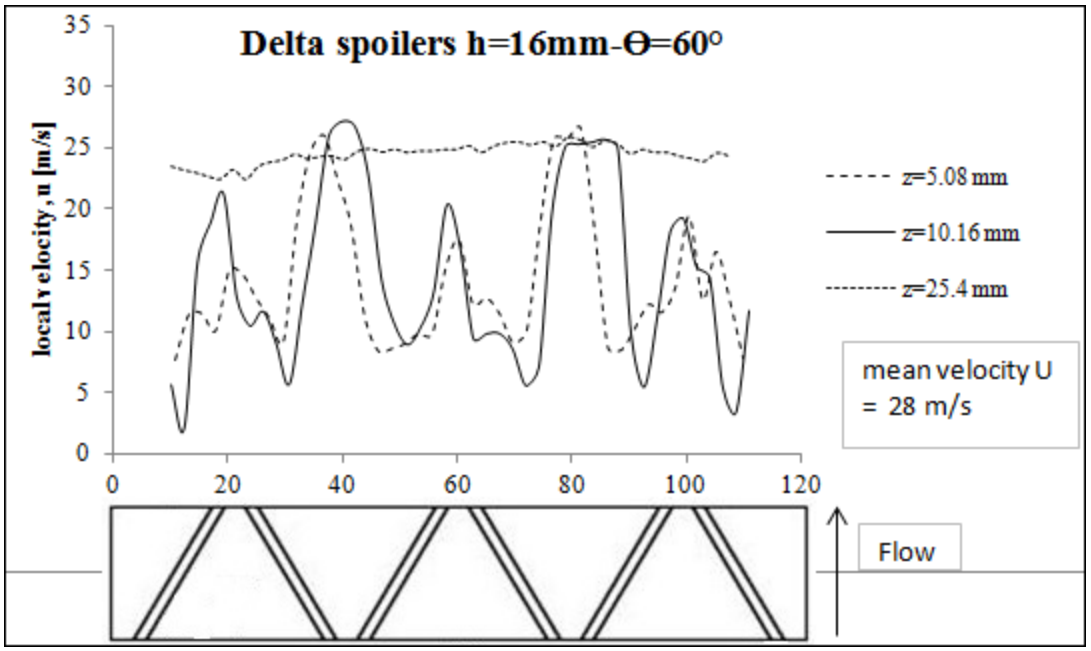

Figure 4-49: velocity perturbations introduced by delta spoilers (angle=60°) across lateral direction at different heights from the edge.

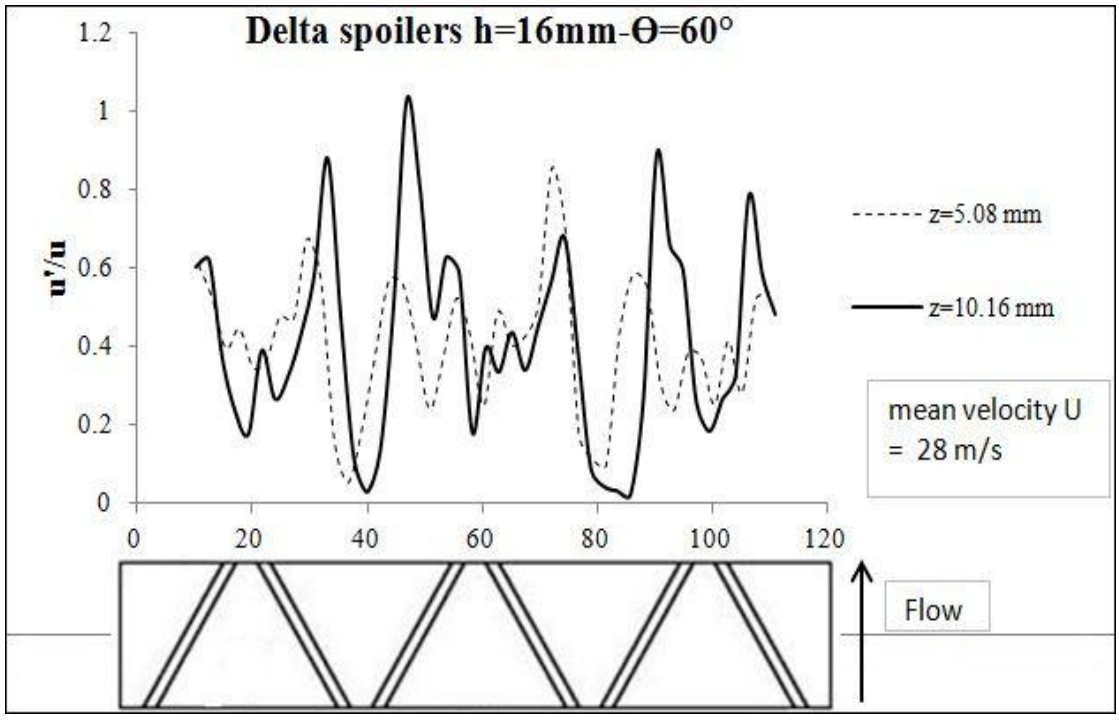

Figure 4-50: velocity fluctuations introduced by delta spoilers (angle=60°) across lateral direction at different heights from the edge.

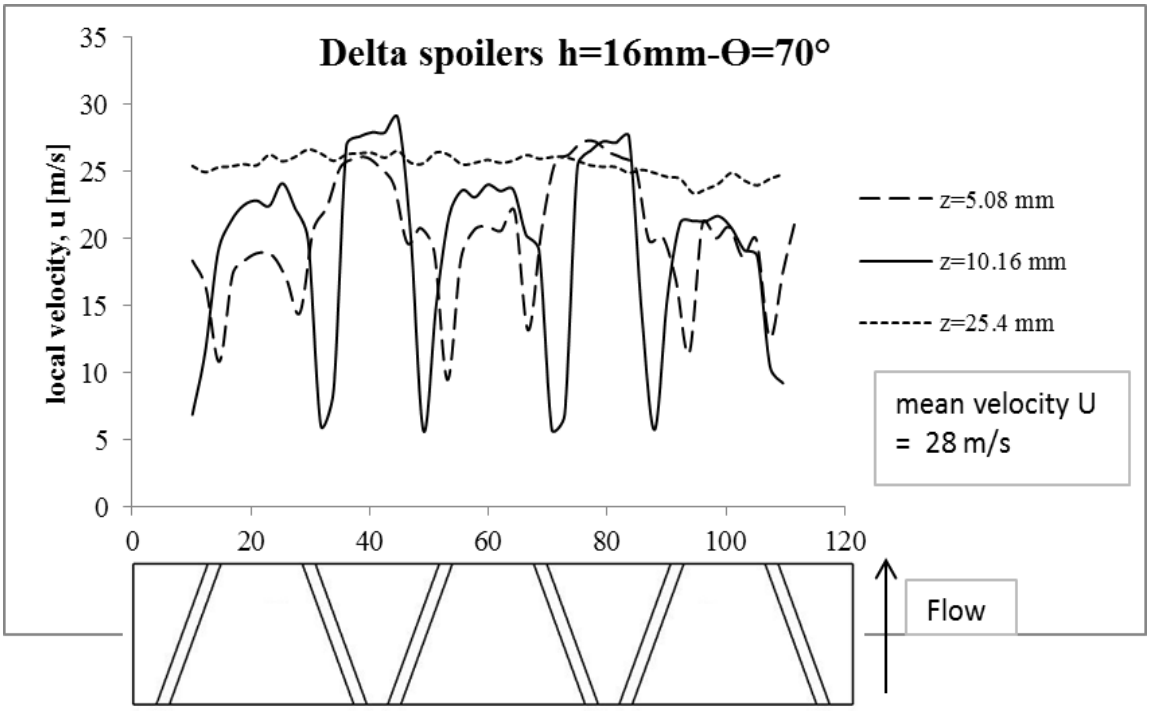

Figure 4-51: velocity fluctuations introduced by delta spoilers (angle=70°) across lateral direction at different heights from the edge.

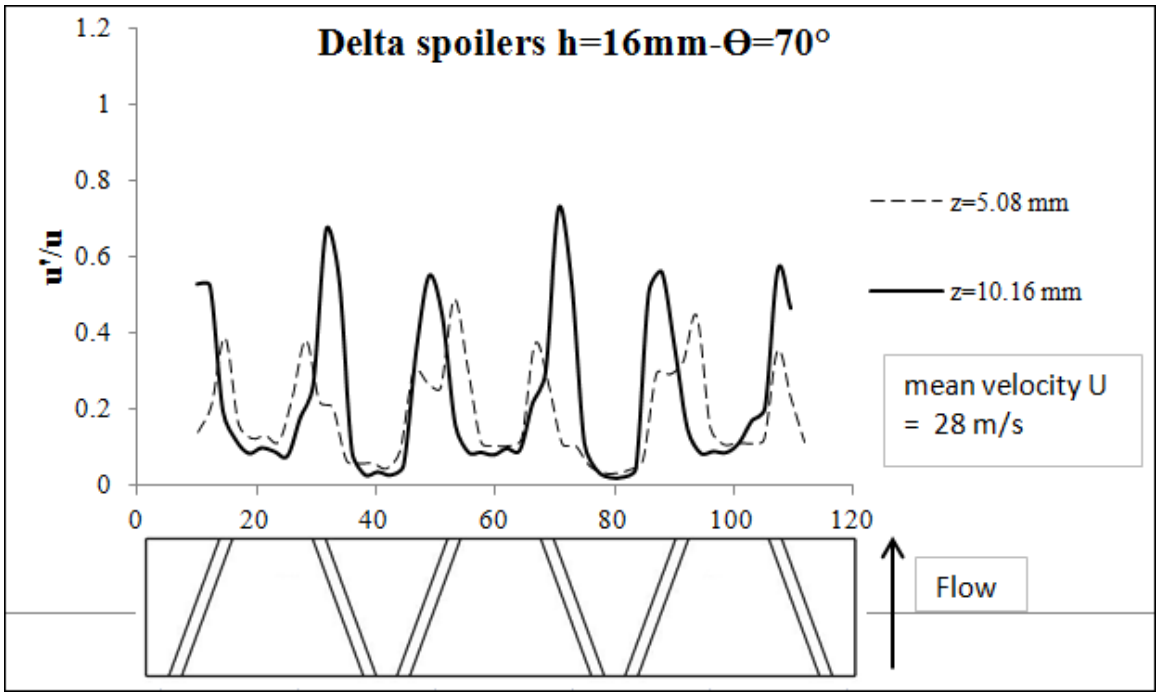

Figure 4-52: velocity perturbations introduced by delta spoilers (angle=70°) across lateral direction at different heights from the edge.

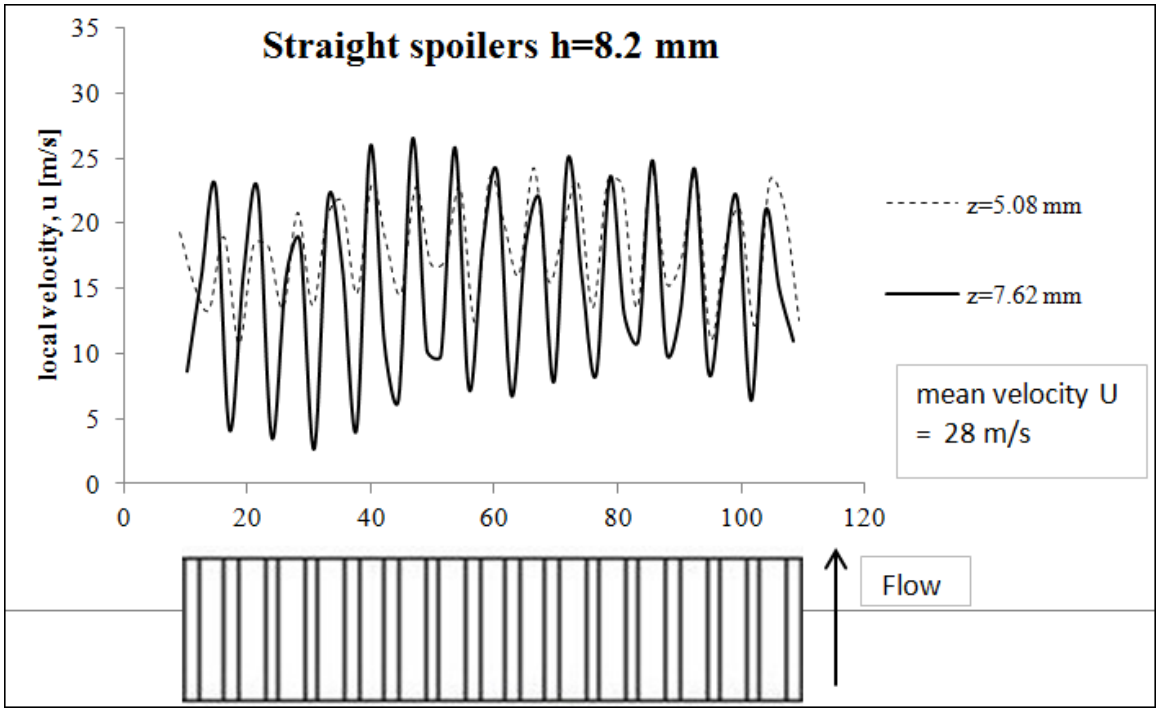

Figure 4-53: velocity fluctuations introduced by straight spoilers across lateral direction at different heights from the edge.

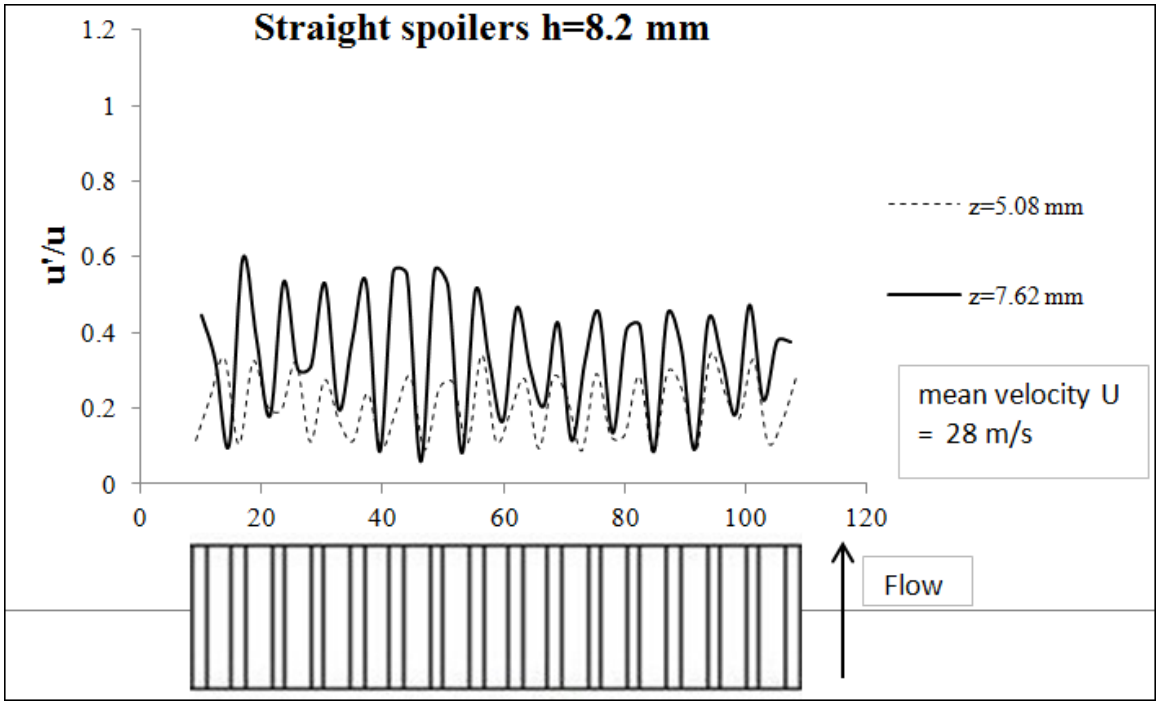

Figure 4-54: velocity perturbations introduced by straight spoilers across lateral direction at different heights from the edge.

4.2. High frequency vortex generator

In this section the results of the cylinder effect on the acoustic resonance excitation are presented. Each cylinder location and diameter is assessed upon the acoustic pressure values recorded and compared to the base case where no cylinder installed. The experiments were conducted in the two cavities with aspect ratios of 1.0 and 1.67.

4.2.1. Results of cavity with aspect ratio of 1.0

Figure 4-55 shows the 2D waterfall plots for the base case without a cylinder installed, and with a cylinder with diameter of 4.57 installed at location (0.0,25.4), the figure shows the three shear layer modes developed at the cavity; N1, N2, and N3. Moreover a vortex shedding mode is also developed by the cylinder. The modes have been identified according to the Strouhal number values obtained. The values of Strouhal number are summarized in Table 4-5.

Table 4-5: Strouhal number values obtained when the cylinder is located at (0.0,25.4) (d=4.57mm)

Shear layer mode	Strouhal number
N1	0.46
N2	0.98
N3	1.55
Nc	0.18

From Figure 4-55 (B) it can be seen that the first acoustic mode is excited by the three shear layer modes of the cavity as in the base case. Moreover, the cylinder vortex shedding mode is also excited. However, the cylinder vortex shedding has no significant amplitudes and no acoustic resonance is excited by the cylinder.

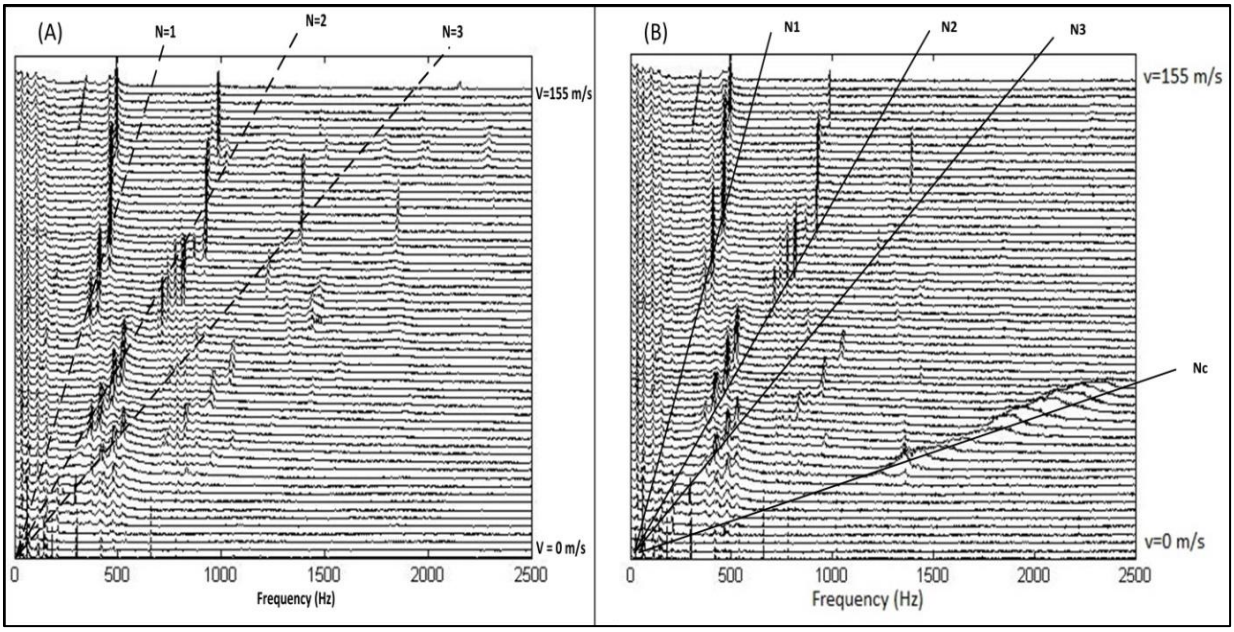

Figure 4-55: 2D waterfall plots (A) base case (B) cylider at location (-25.4,25.4) (d=4.57mm)

To investigate the effect of the cylinder locations in suppressing the acoustic resonance excitation, the first acoustic mode excited when the cylinder is installed at each location is compared to the base case which is the bare cavity without any cylinder installed.

Figure 4-56 shows a comparison between the five locations located at a height of 12.7 mm from the bottom wall, and the base case. Locations (-25.4, 12.7), (0.0, 12.7), and (25.4, 12.7) are able to suppress the acoustic resonance and keep the acoustic pressure at around 1000 Pa. Moreover a shift in the onset of the acoustic resonance is observed with the four locations. It is also observed that locating the cylinder at 50.8 mm upstream the cavity results in less suppression effect.

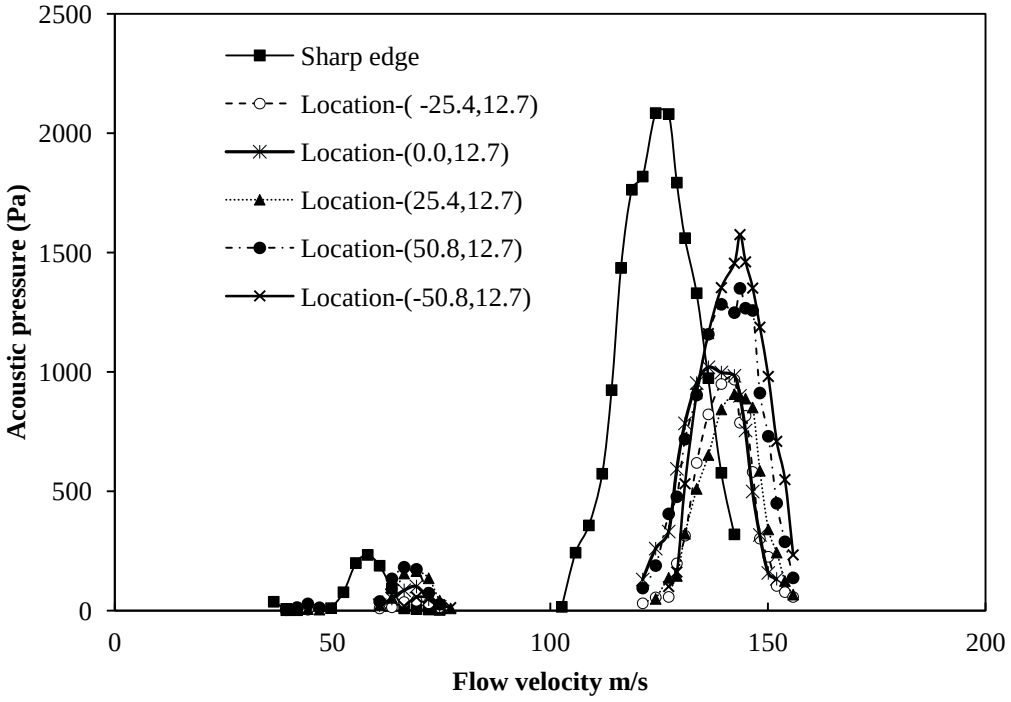

Figure 4-56: comparison between base case and cylinder (d=4.57 mm) at locations of height 12.7 mm

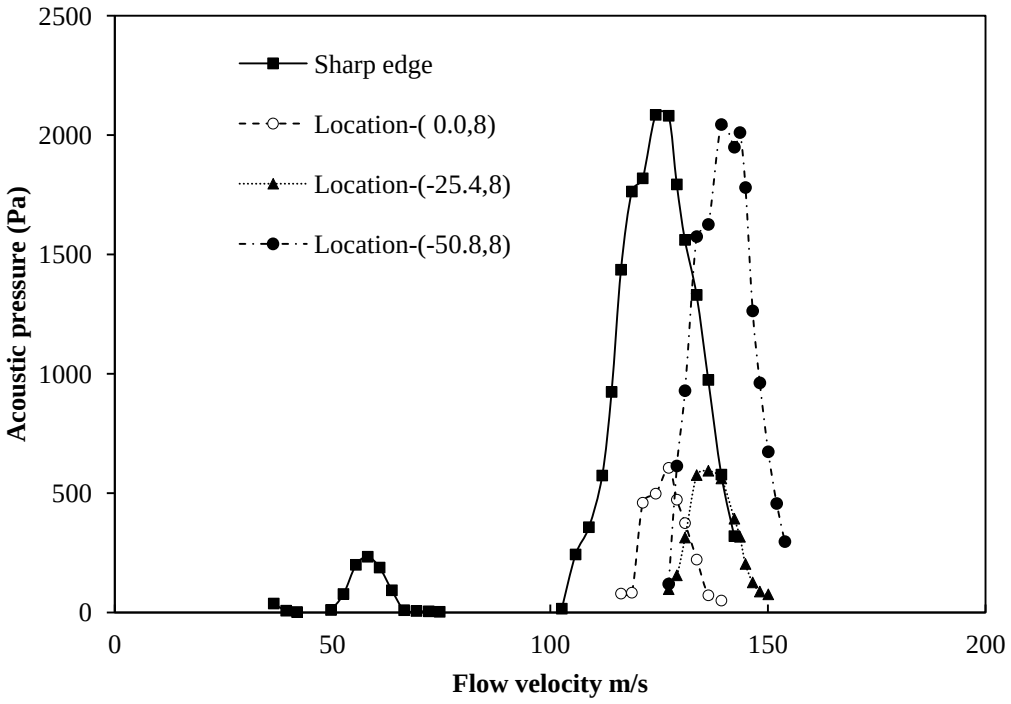

Figure 4-57: comparison between base case and cylinder (d=4.57 mm) at locations of height 8 mm

At height of 8 mm from the test section bottom wall, the suppression effect of the cylinder increases significantly and the acoustic pressure can be reduced to around 500 Pa. The shift in the acoustic resonance excitation observed at the height of 12.7 mm is also observed at height of 8 mm. Moreover, the excitation of the first acoustic mode by the second and third shear layer modes is completely suppressed, this is achieved by locating the cylinder at x= 0 and -25.4 mm. However, locating the cylinder at 50.8 mm upstream the cavity, results in shifting the resonance excitation to higher velocities without any suppression effect. When the cylinder is located at locations with a height of 25.4 mm from the bottom wall it is observed that the cylinder introduce less effect on the acoustic resonance excitation when compared to the locations at the height of 12.7 mm, this is illustrated in Figure 4-58. Increasing the height to 50.8 mm from the bottom wall results in eliminating the effect of the cylinder in suppressing the acoustic resonance excitation, as shown in Figure 4-59, locations (-25.4,50.8) and (0.0,50.8) have no effect on the acoustic pressure amplitudes. Nevertheless locating the cylinder at the mouth of the cavity ((25.4, 0.0) and (50.8, 0.0)) has no significant effect on the acoustic pressure, this is demonstrated in Figure 4-60. To compare the effect of the locations on the acoustic resonance excitation, (Figure 4-61) is constructed from the maximum acoustic pressure recorded with each case. The figure shows that the cylinder can have better effect on suppressing the acoustic resonance when it is located closer to the bottom wall of the test section.

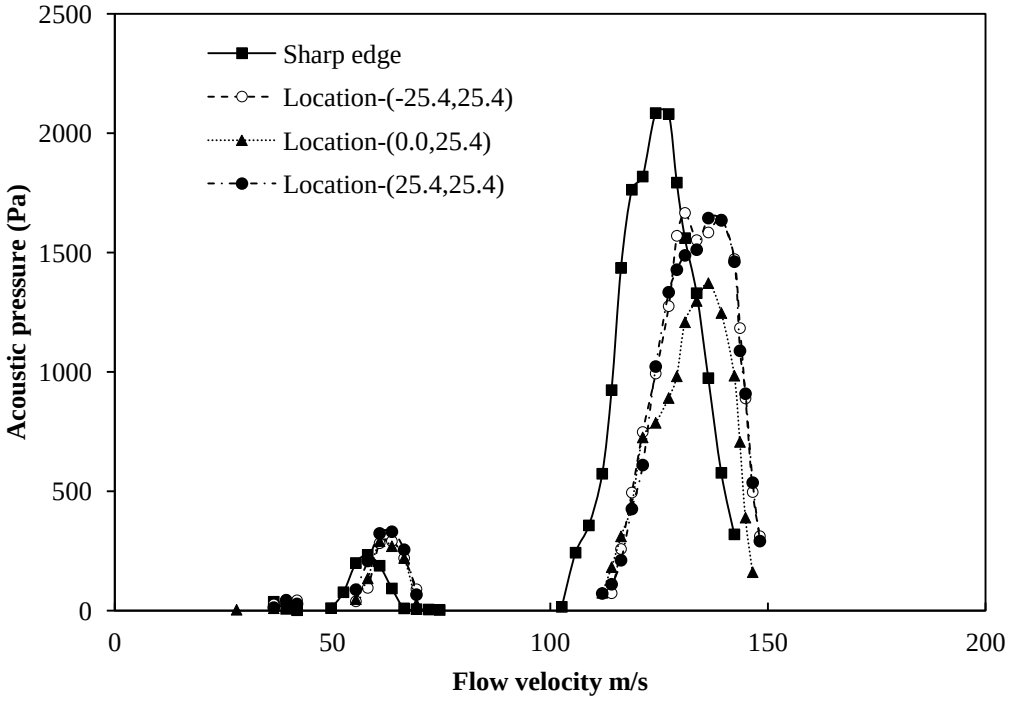

Figure 4-58: comparison between base case and cylinder (d=4.57 mm) at locations of height 25.4 mm

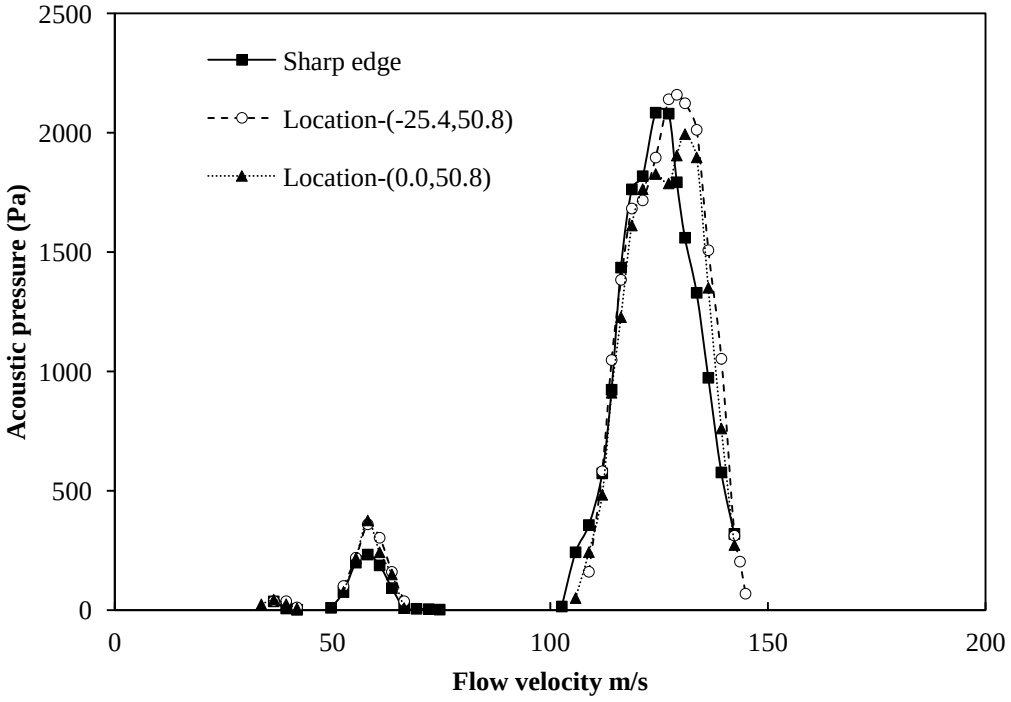

Figure 4-59: comparison between base case and cylinder (d=4.57 mm) at locations of height 50.8 mm

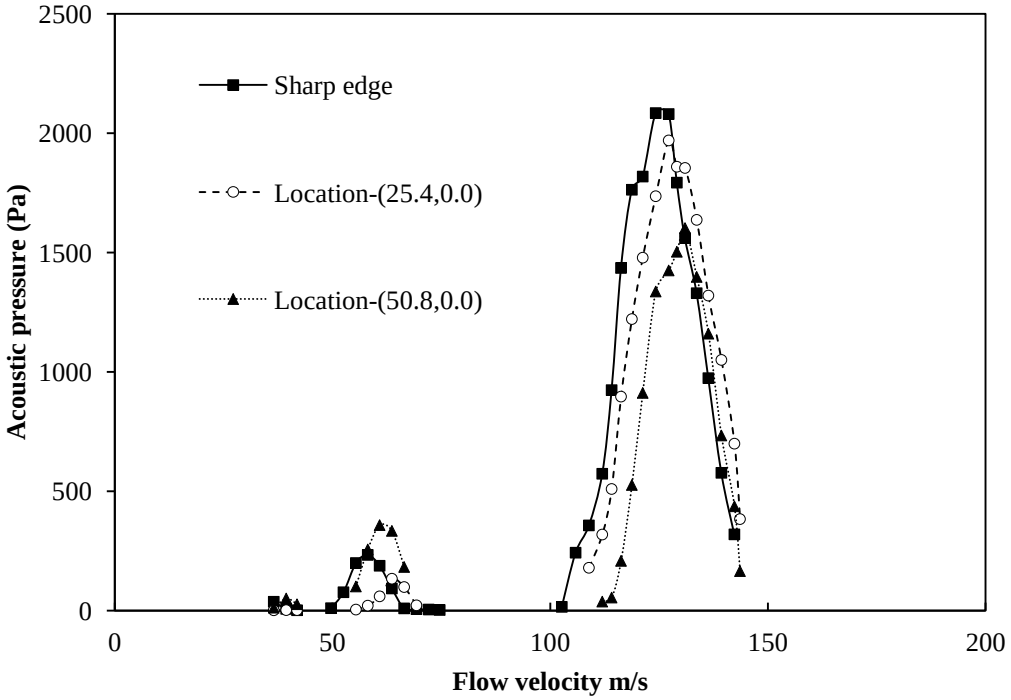

Figure 4-60: comparison between base case and cylinder (d=4.57 mm) at locations at the cavity mouth

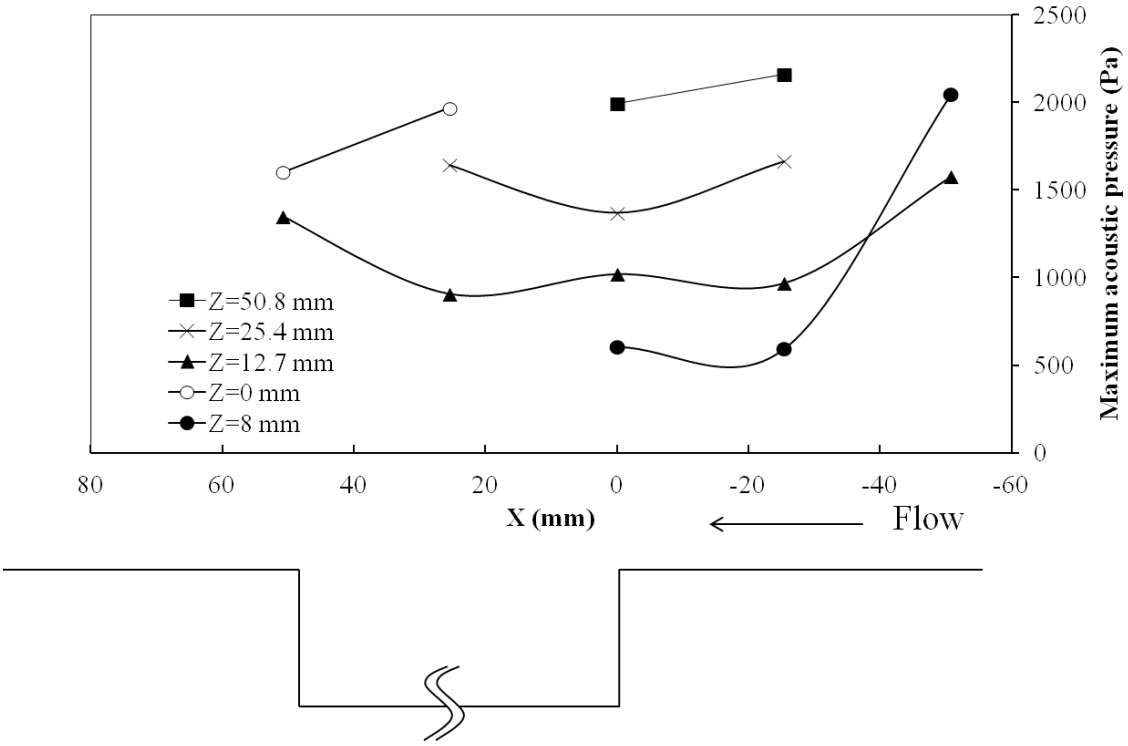

Figure 4-61: maximum acoustic pressure recorded for different locations

4.2.2. Control cylinder diameter effect

To study the effect of the diameter of the cylinder, two other cylinders with diameters of 3.81 and 6.35 mm were tested at the locations; (-25.4,12.7) , (0.0,12.7) , (25.4,12.7), and (0.0, 25.4) which are shown to have good effect on suppressing the acoustic resonance excitation as seen in Figure 4-61. Figure 4-62 shows the effect of the diameter at location (-25.4,12.7). It can be seen that increasing the diameter enhances the performance of suppressing the acoustic resonance excitation, and it is able to keep the acoustic pressure below 140 Pa by using a cylinder with a diameter of 6.35 mm.

The effect of the cylinder diameter at location (0.0,12.7) is illustrated in Figure 4-63, increasing the diameter of the cylinder enhances the performance of suppressing the acoustic resonance excitation and the acoustic pressure is maintained below 450 Pa with a diameter of 6.35 mm. Similar behaviour is observed with location (25.4,12.7) and it is illustrated in Figure 4-64. However location (0.0, 25.4), as shown in Figure 4-65, is observed to have least effectiveness compared to the other locations. This indicates that the vertical distance from the bottom wall is a major factor and it has a significant role in suppressing the acoustic resonance excitation.

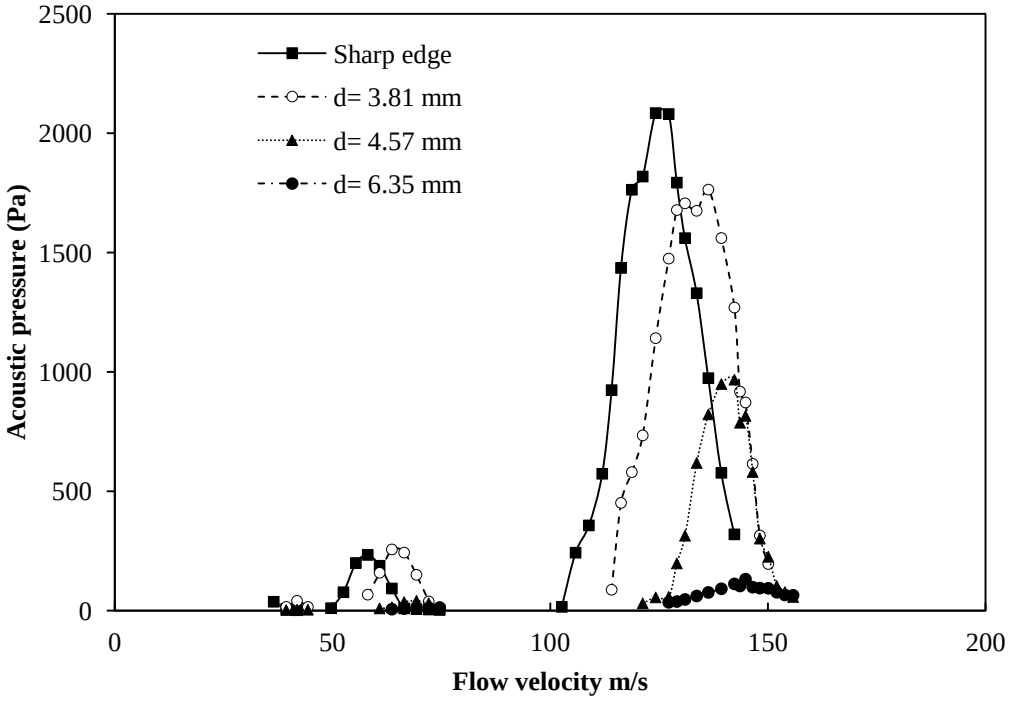

Figure 4-62: effect of cylinder diameter on suppressing the acoustic resonance excitation at location (-25.4, 12.7)

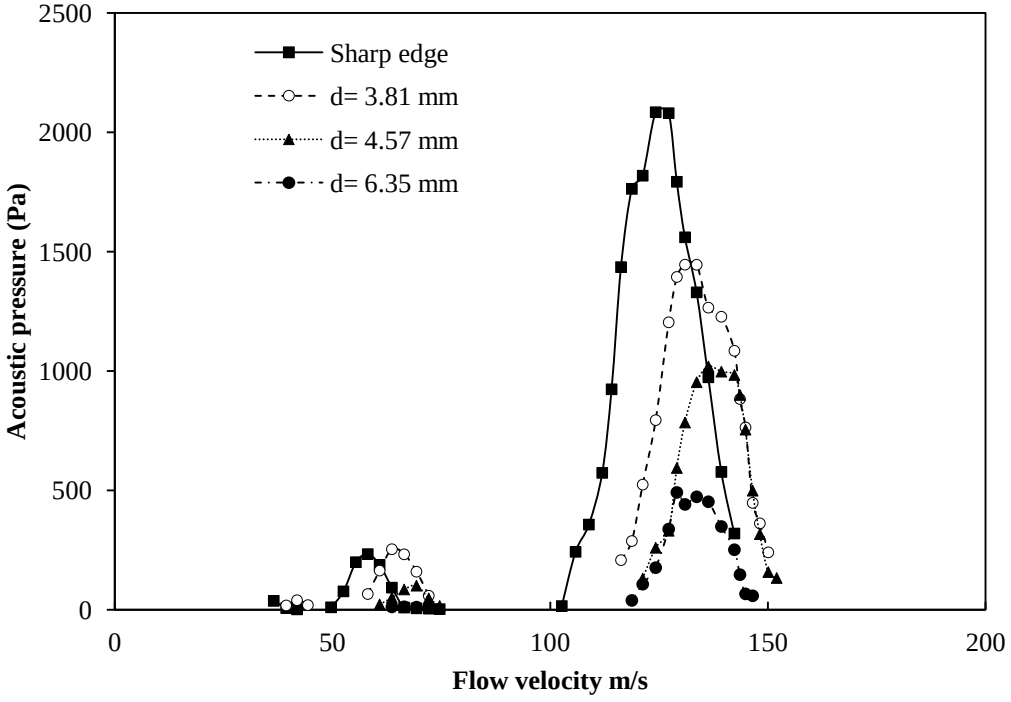

Figure 4-63: effect of cylinder diameter on suppressing the acoustic resonance excitation at location (0.0, 12.7)

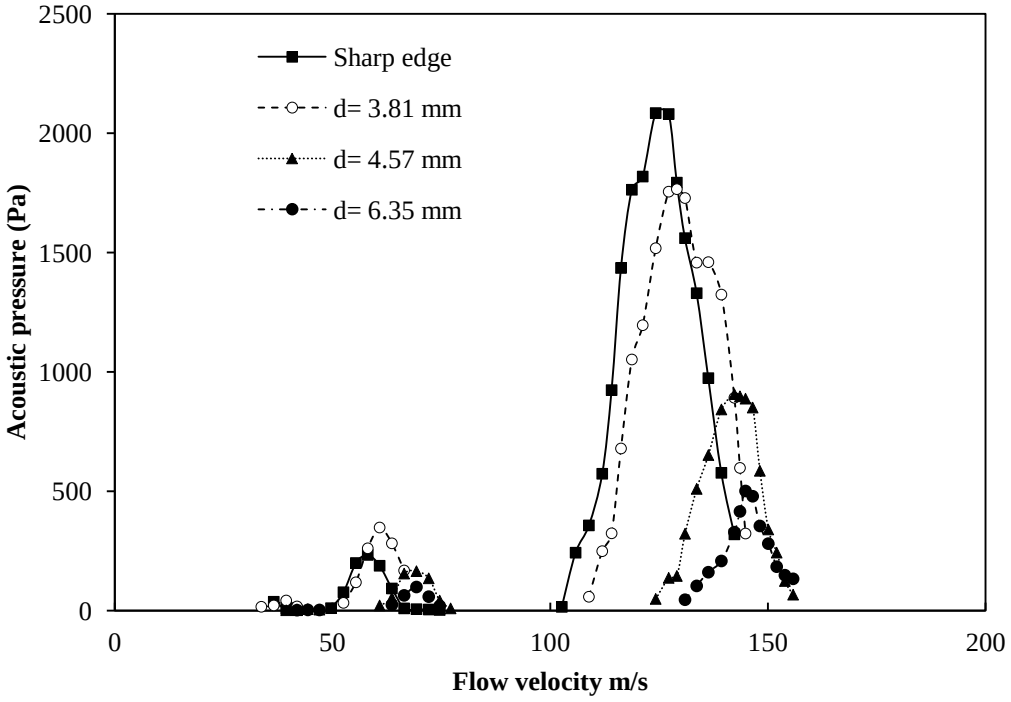

Figure 4-64: effect of cylinder diameter on suppressing the acoustic resonance excitation at location (25.4, 12.7)

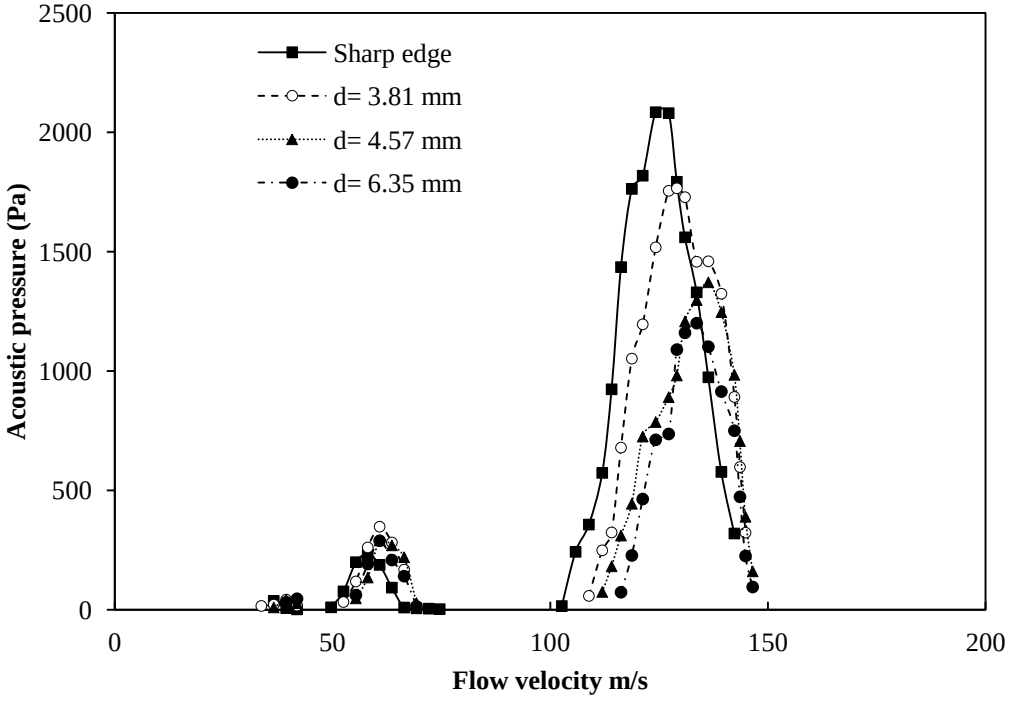

Figure 4-65: effect of cylinder diameter on suppressing the acoustic resonance excitation at location (-25.4, 25.4)

4.2.3. Results of cavity with aspect ratio of 1.67

Different locations were investigated in the cavity with the aspect ratio of 1.67. The locations investigated were at heights of 8 and 12.7 mm. The shift of the acoustic resonance excitation observed with the cavity with aspect ratio of 1.0 is also observed in this cavity, this resulted in shifting the resonance excitation almost out of the range of the experiments in some cases. Figure 4-66 shows a comparison between three different locations at a height of 12.7 mm. The least effective location is found to be the location exactly at the edge (0.0, 12.7) which is consistent with the results of the cavity with aspect ratio of 1.0. The resonance is excited at velocities higher than 140 m/s, and for the two locations (-25.4, 12.7) and (-50.8, 12.7) the resonance is excited at the end of the range and the acoustic pressure is less than 330 Pa for the location (-50.8, 12.7), and 230 Pa for the location (-25.4, 12.7). Comparing the effect of the cylinder at height of 8 mm on the acoustic resonance excitation is illustrated in Figure 4-67, the figure shows that the acoustic resonance excitation is shifted almost out of the range for the locations: (-25.4,8) and (-50.8,0). The location (0.0, 8) has no significant shift on the acoustic resonance excitation, interestingly, this was also observed with the cavity with aspect ratio of 1.0. As the resonance excited earlier compared to other locations, higher peaks are observed with values exceeding 2000 Pa.

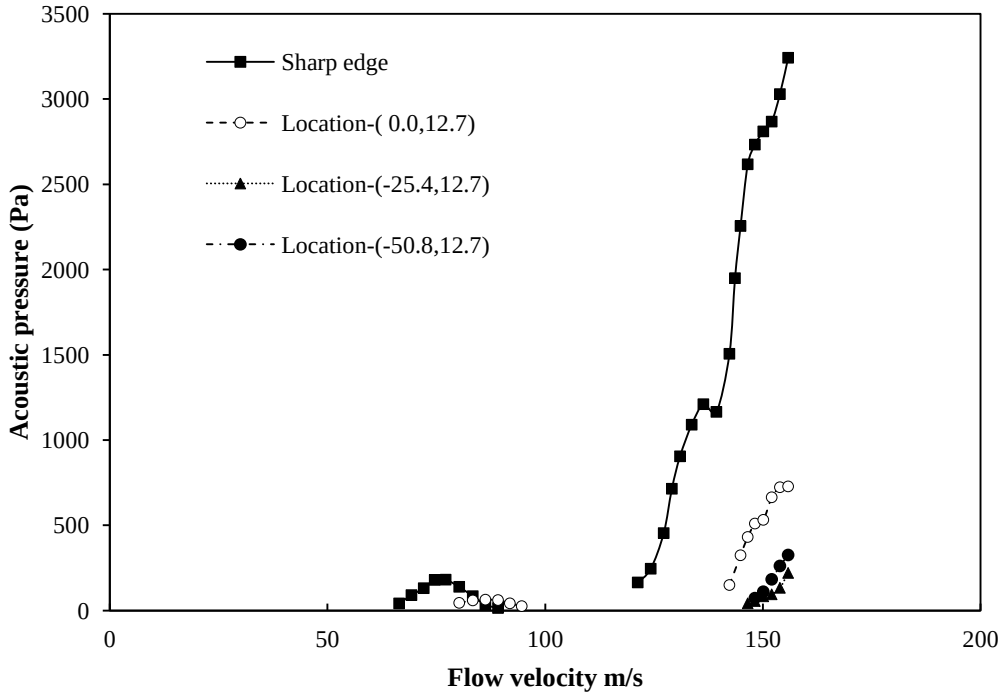

Figure 4-66: comparison between base case and cylinder (d=4.57 mm) at locations of height 12.7 mm

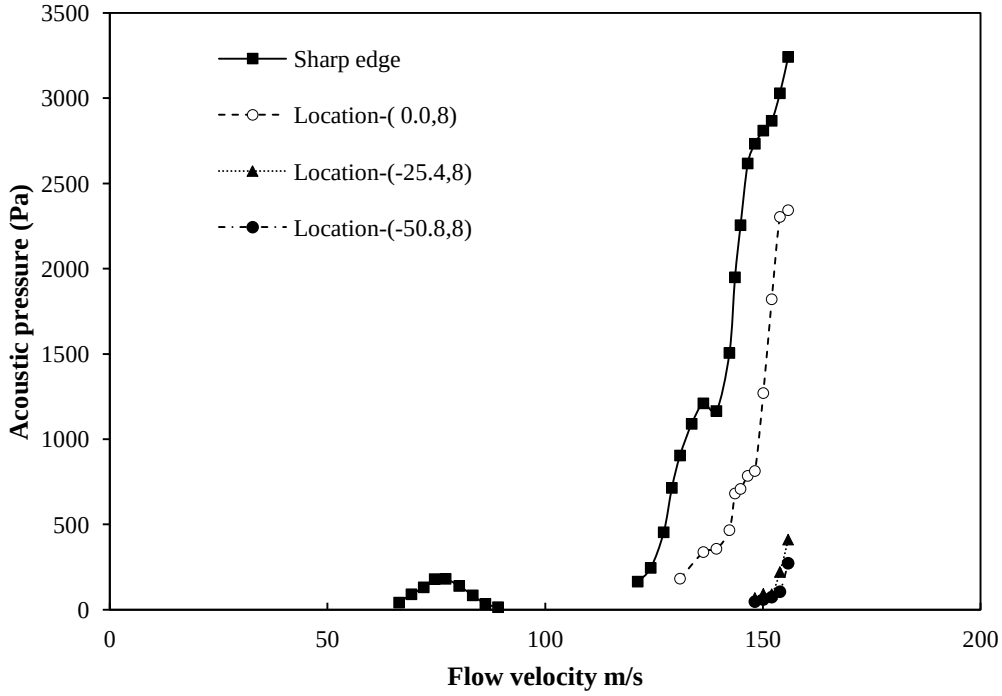

Figure 4-67: comparison between base case and cylinder (d=4.57 mm) at locations of height 8 mm

From these results it can be concluded that attaching a cylinder near the upstream edge of the cavity can be an effective method in suppressing the acoustic resonance excitation. The location of the cylinder has major influence in the effectiveness of the method, specifically the location height from the bottom wall of the duct can significantly enhance the performance of the method. Increasing the diameter of the cylinder generally results in improving the performance of the method, however, this should be tuned carefully to avoid exciting other modes by the cylinder. In most of the cases the acoustic resonance excitation is observed to be delayed to higher velocities, this shift is observed to be dependent on the location of the cylinder.

The pressure drop introduced by the cylinder is also investigated. The pressure drop is measured when the cylinder with a diameter of 6.35 mm is placed at location (-25.4,12.7) this cylinder at this location is found to be able to suppress the resonance excitation significantly with maximum acoustic pressure less than 140 Pa. A comparison between the pressure drop introduced by the cylinder and the other spoilers with height of 16 mm is illustrated in Figure 4-68. It is also noteworthy that the dimensionless pressure when the cylinder is installed is found to be 0.095.

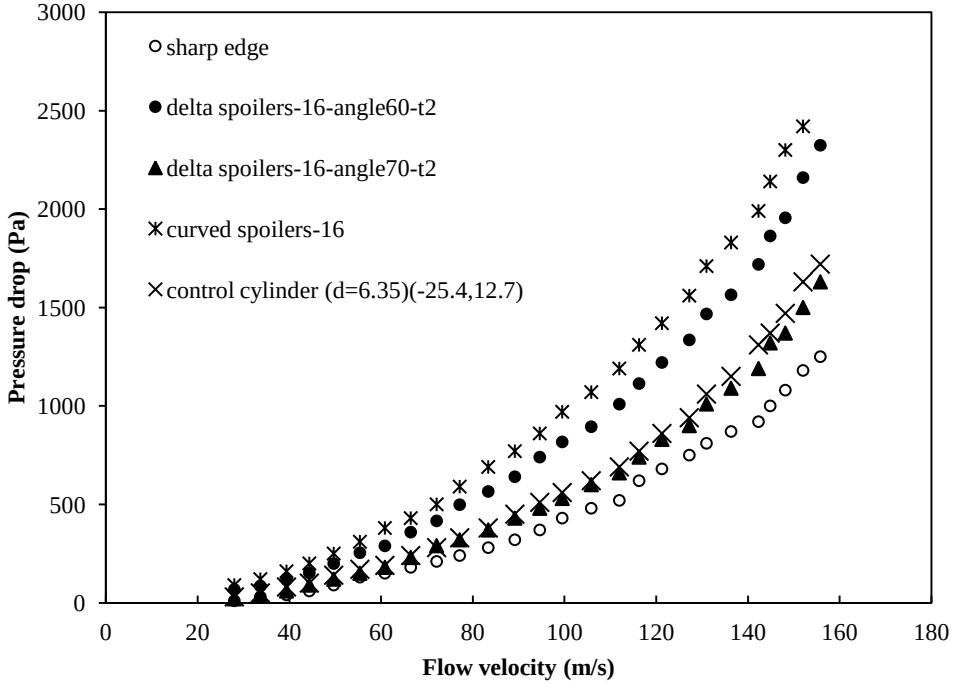

Figure 4-68: comparison of pressure drop for some spoilers and control cylinder (L/D=1)

5. Numerical Simulation

In this section, the numerical simulation conducted is described. The numerical simulation was performed to enrich the understanding of the cylinder effect on the shear layer development at the cavity. Several cases with/without cylinder were simulated to study the effect of the location of the control cylinder on the shear layer characteristics.

5.1. Computational setup

As mentioned in chapter two, the Spallart Almaras DES method is proven to provide very satisfactory results for flow over cavities. Hence, this method is employed for the unsteady simulation. The simulation has been performed using ANSYS Package, where the mesh was generated on ANSYS mesh generator and the computational part was done by ANSYS FLUENT 14. The simulation was done in two parts, firstly, a steady state flow using K-epsilon turbulence model to obtain the average main parameters values in the domain, secondly, unsteady state flow using Spallart Almaras DES method to catch the vorticity fields and the fluctuations with respect to time. The flow at the inlet is set for air with density of 1.225 kg/m^3 with flow velocity of 4.08 m/s which yields Reynolds number of 43974. This flow velocity was chosen for validation purposes and to be compared with hot-wire measurements done at the same flow velocity. The outlet of the domain is set to pressure outlet. The mesh used consisted of approximately 169,000 quadrilateral cell for the cavity with aspect ratio of 1.0, this is illustrated in Figure 5-1. The cavity dimensions were 127 mm in depth and height, and the inlet was set upstream at a distance of 3 times the cavity length, while the outlet was set at 5 times the cavity length downstream. At height of 127 mm from the bottom wall a symmetry line was set as the field beyond that height does not affect the flow in the cavity. The turbulence intensity in the simulation was set to 1% which is the value obtained experimentally using the hot-wire probe. For the unsteady flow case the time step was set to $1e^{-5}$ seconds, this time step value with respect to the flow velocity of 4.08 m/s at the inlet maintain a Courant number less than 0.072 for all the cells in the domain. The solver scheme used in the simulation is the pressure base coupled solver which solve for the pressure and momentum simultaneously, and it is known for the very good predictions in

case of single phase flows. The gradient in the spatial discretization of the cells is set to least square cell based which does not require high computational power and can provide high accuracy in the predictions. A bounded central differencing scheme is used for the momentum equations, this scheme can improve the performance of the DES model and provide better results.

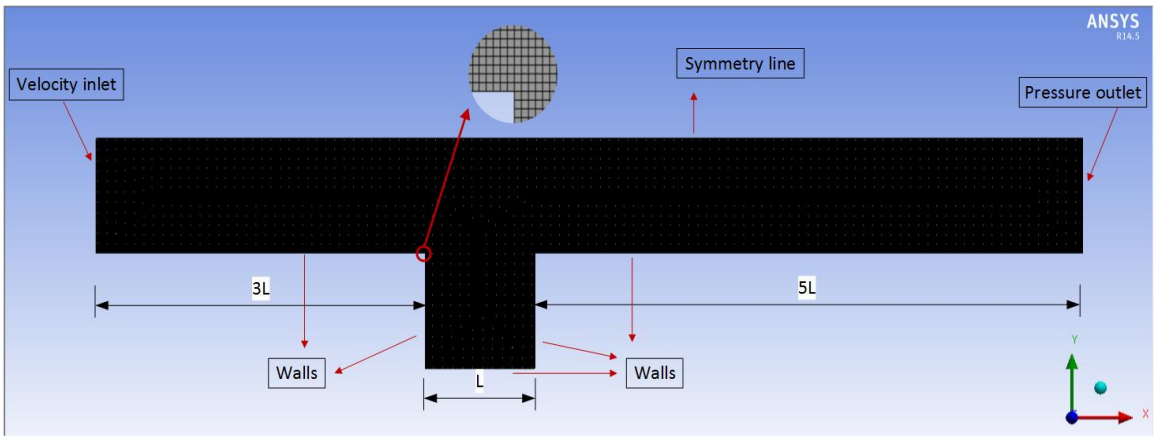

Figure 5-1: base case mesh

5.2. Validation

To validate the simulation results, some of the velocity profiles are compared with experimental results. The velocity profile obtained experimentally was done by using hot wire probe at flow velocity of 4.08 m/s. The measurements were taken at the mid of the cavity, and the profile was obtained along the (Z) vertical direction. Figure 5-2 shows the comparison between the experimental and numerical velocity profiles, it can be seen that the profiles are following the same trend and the shear layer thickness is almost the same (experimental = 22.8 mm, numerical = 19.9 mm).

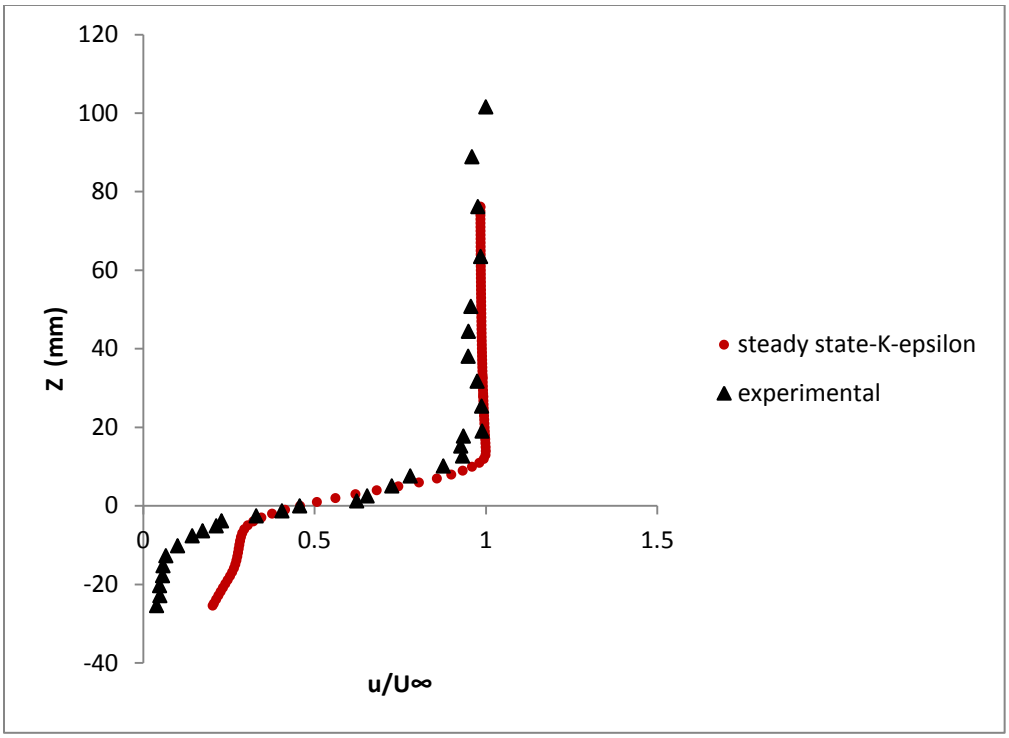

Figure 5-2: comparison between velocity profiles obtained numerically and experimentally

5.3. Results

In this section the results obtained from the numerical simulation are presented and discussed. Several cases have been done with the cylinder located at different locations, to understand the suppression mechanism behind the control cylinder method. For each case the velocity profiles obtained from the steady simulation at different distances along the cavity are compared. Also, the vorticity fields are compared to spot the development of the vortices at the cavity mouth. The oscillations at the cavity was monitored during the unsteady case simulation to obtain Strouhal number value, this was done by measuring the pressure in a point at the mid of the cavity length, also the lift force acting at the cylinder was monitored to obtain the Strouhal number of the vortex shedding developed by the cylinder. The Strouhal number of the cavity is found to be around 2.1, which indicates the fourth shear layer mode, while the Strouhal number for the cylinder vortex shedding is found to be around 0.25. The main concept of the comparison is to address the effect of the location, hence, the comparison is done for different locations in

terms of horizontal and vertical coordinates. Comparing the three locations at the same horizontal distance, 25.4 mm upstream of the edge, and at three different heights: 8, 12.7, and 25.4 mm can be seen in Figure 5-3, the figure represents the velocity profile taken at different vertical lines along the cavity: *x/L*= 0, 0.2, 0.4, 0.6, and 0.8 where *x* is the distance from the upstream edge. The figure is obtained from the steady case run done using K-epsilon model. From the figure it can be seen that the shear layer represented by the velocity gradient at the cavity mouth, when the cylinder is located at the height of 25.4 mm it is clearly seen that the cylinder has no effect on the shear layer at the cavity compared to the base case which is represented by the red line. In general, when the cylinder is located at a height of 25.4 mm, the wake of the cylinder does not interact with the cavity shear layer. It is noteworthy that this location experimentally was less effective in suppressing the acoustic resonance excitation. Moving the cylinder lower, to a height of 12.7 mm, at the same horizontal distance, 25.4 mm, is slightly changing the profile of the shear layer as shown in Figure 5-3-(b). The location at height of 8 mm which was found to be very effective experimentally is clearly influence the shear layer at the cavity mouth, this can be seen in Figure 5-3-(a). The wake of the cylinder interacts with the shear layer at the cavity mouth, introducing different profile for the shear layer. the velocity profiles for the horizontal locations at the same height of 12.7 mm is illustrated in Figure 5-4, in this figure no clear difference is noticed between the two locations, however, the difference can be noticed in the vorticity field as will be discussed later. The stability of the shear layer can be compared in terms of the shear layer momentum thickness, which is defined as:

$$\theta = \int_{-\infty}^{+\infty} \frac{u}{U}\left(1 - \frac{u}{U}\right) dy \qquad (6)$$

where *u* is the local velocity and *U* is the mean flow velocity. From the velocity gradient profile of the shear layer developed with the cylinder located at height of 8 mm, it can be concluded that the shear layer has higher momentum thickness (3.2 mm) compared to the base case (2.1 mm). This high momentum thickness enhances the stability of the shear layer and mitigate its susceptibility to the resonance excitation as discussed by Bruggeman et al. (1991). The shear layer momentum thickness for each case is provided in Table 5-1.

Table 5-1: momentum thickness values for different cylinder locations

Location	Shear layer momentum thickness (mm)
Base case	2.1
(-50.8,12.7)	2.3
(0.0,12.7)	2.3
(-25.4,25.4)	2.1
(-25.4,12.7)	2.4
(-25.4,8.0)	3.2

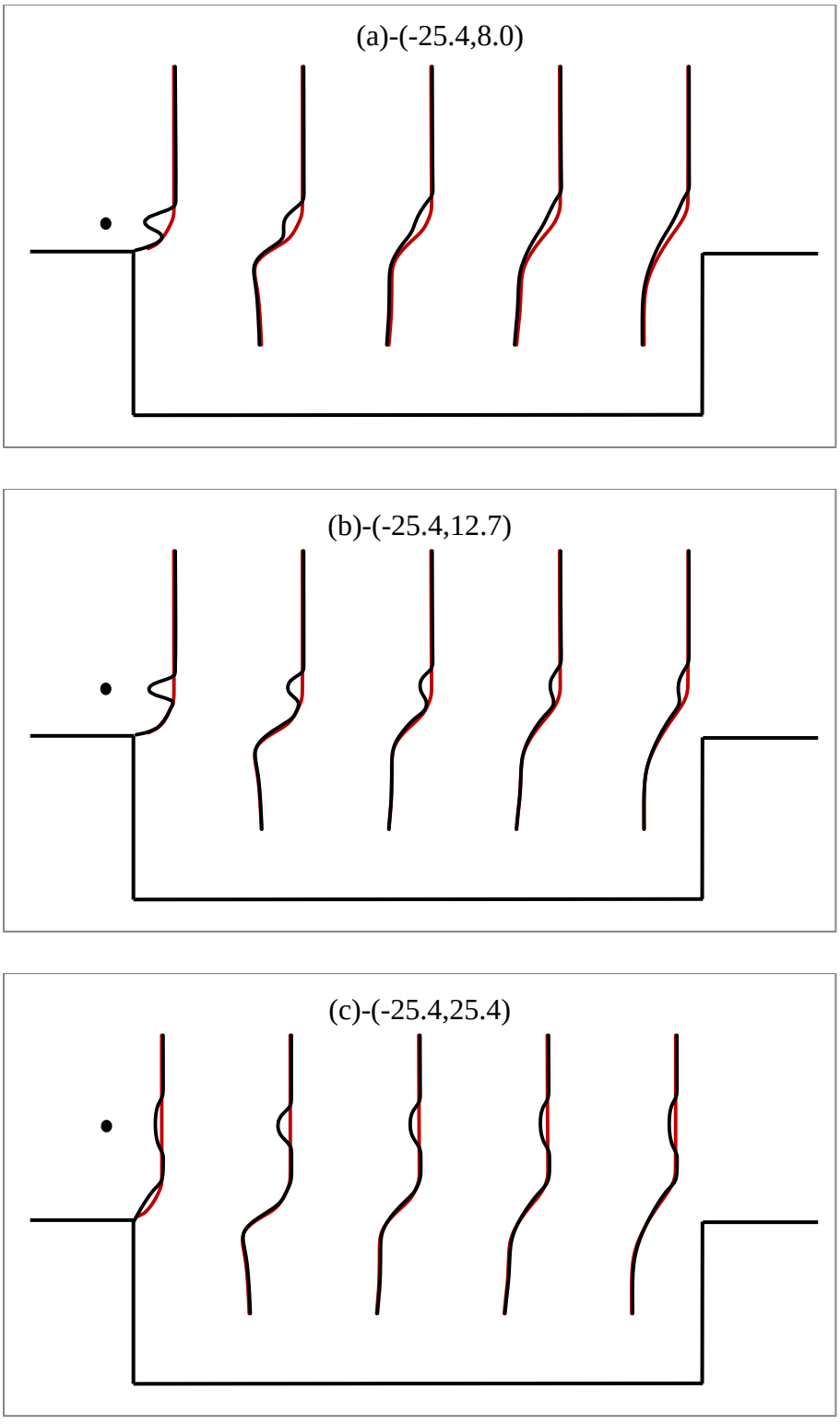

Figure 5-3: velocity profiles at different locations x/L =0, 0. 2, 0.4, 0.6, and 0.8 when the cylinder is located at :(a) (-25.4, 8.0), (b) (-25.4, 12.7), and (c) (-25.4, 25.4) – the red line represent the base case

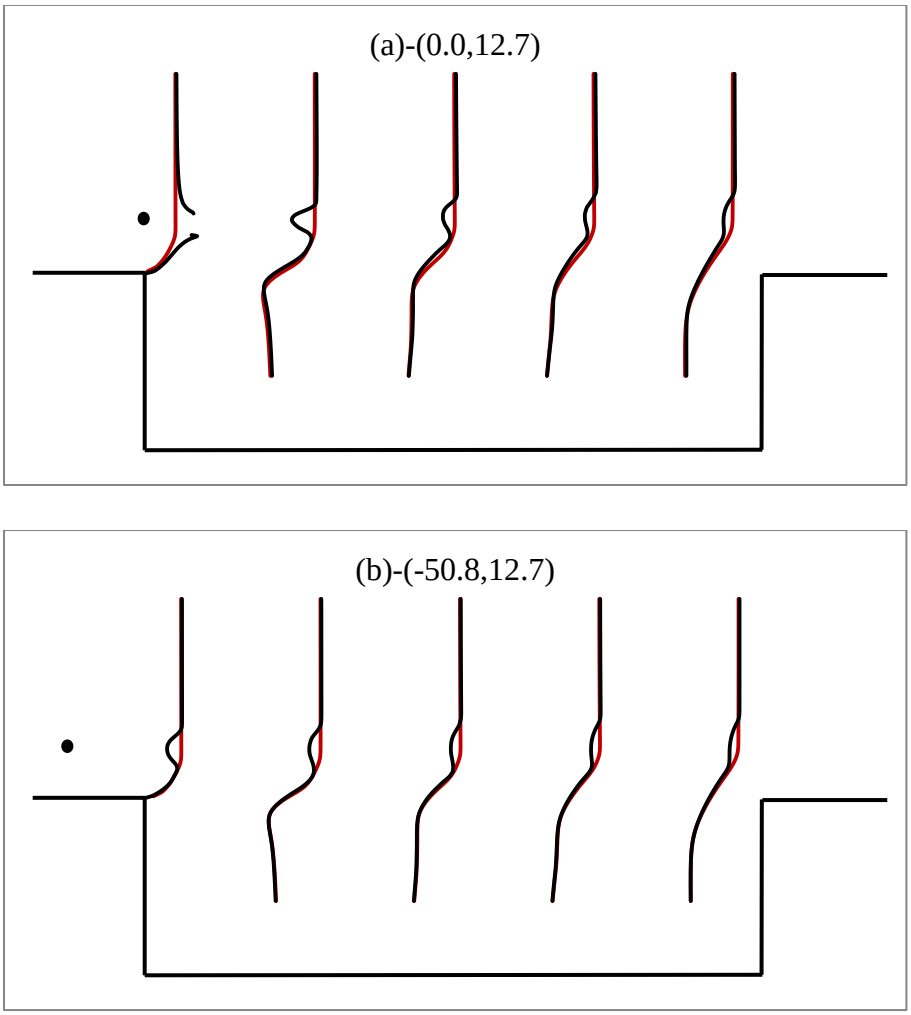

Figure 5-4: velocity profiles at different locations x/L =0, 0. 2, 0.4, 0.6, and 0.8 when the cylinder is located at (a) (0.0, 12.7) and (b) (-50.8, 12.7) – the red line represent the base case

The effect of the horizontal location of the cylinder on the shear layer cannot be easily noticed from the velocity profiles along the cavity. However, the vorticity fields of each case can show the progress of the vortex shedding and the interaction with the cavity shear layer. Figure 5-5 shows the vorticity fields for the base case at four different times, t= 0.04, 0.06, 0.08, and 0.1 sec. The vortices development at the cavity mouth can be clearly seen and they impinge to the downstream edge. The development of the vortices as will be illustrated in the following figures is highly affected by the cylinder vortex shedding in some of the cases that were found to be effective in terms of experimental results. Figure 5-6 and Figure 5-7 show the effect of the cylinder when it's located at the same height of 12.7, and at two different locations in the horizontal direction. Comparing

these two locations it can be seen that when the cylinder is located at 25.4 mm upstream from the edge, as shown in Figure 5-7, a better performance in disturbing the main vortices is observed. The cylinder at this location sends the main vortices into the cavity distracting the downstream impingement which results in interrupting the normal feedback cycle. When the cylinder is located exactly at the upstream edge and at a height of 12.7 as shown in Figure 5-6, the interaction effect is relatively less than the 25.4 mm upstream location and the vortical structures at the cavity shear layer is more evident. Moving the cylinder more upstream to 50.8 mm with the same height of 12.7 results in less effectiveness when compared to the 25.4 mm upstream location and more obvious vortical structures are observed, this can be attributed to the weakness of the pressure oscillations introduced by the cylinder vortex shedding due to the relatively long distance between the cylinder and the shear layer at the cavity mouth. The effect of the vertical distance is illustrated in Figure 5-9 and Figure 5-10. In these two figures it is clearly seen that locating the cylinder at height of 25.4 mm has no effect on the shear layer at the cavity and the vortex shedding does not interact with it, also, the vortical structures in the shear layer is clearly evident. However the cylinder at height of 8 mm results in moving the vortices in the shear layer into the cavity and changing the downstream impingement. As mentioned earlier locating the cylinder at a height of 25.4 mm from the bottom wall and 25.4 mm upstream of the edge, was experimentally found to be slightly affecting the acoustic resonance excitation.

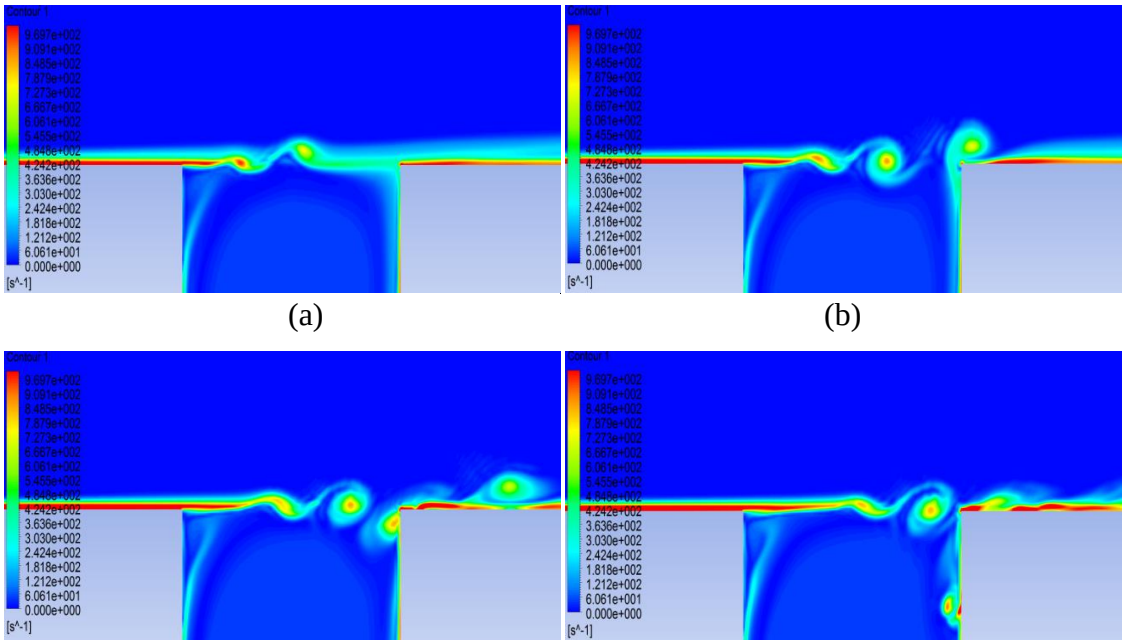

(a) (b)

(c) (d)

Figure 5-5: vorticity field for the base case (a) t=0.04 sec (b) t= 0.06 sec (c) t= 0.08 sec (d) t= 0.1 sec

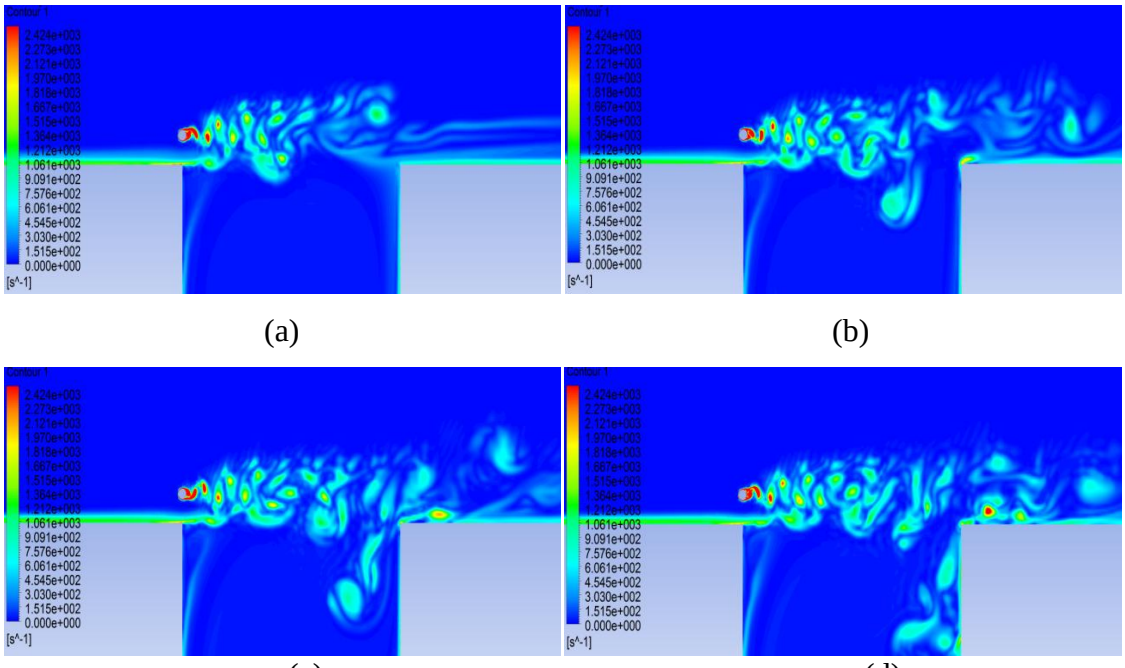

(a) (b)

(c) (d)

Figure 5-6: vorticity field with control cylinder located at (0.0,12.7) (a) t=0.04 sec (b) t= 0.06 sec (c) t= 0.08 sec (d) t= 0.1 sec

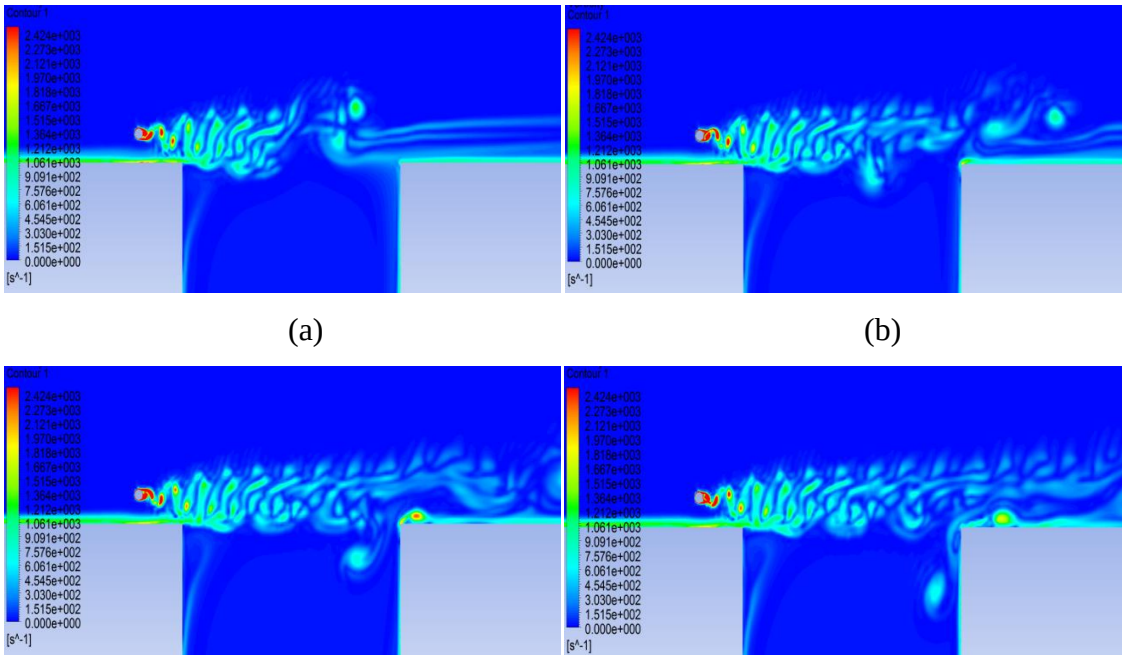

(a) (b)

(c) (d)

Figure 5-7: vorticity field with control cylinder located at (-25.4,12.7) (a) t=0.04 sec (b) t= 0.06 sec (c) t= 0.08 sec (d) t= 0.1 sec

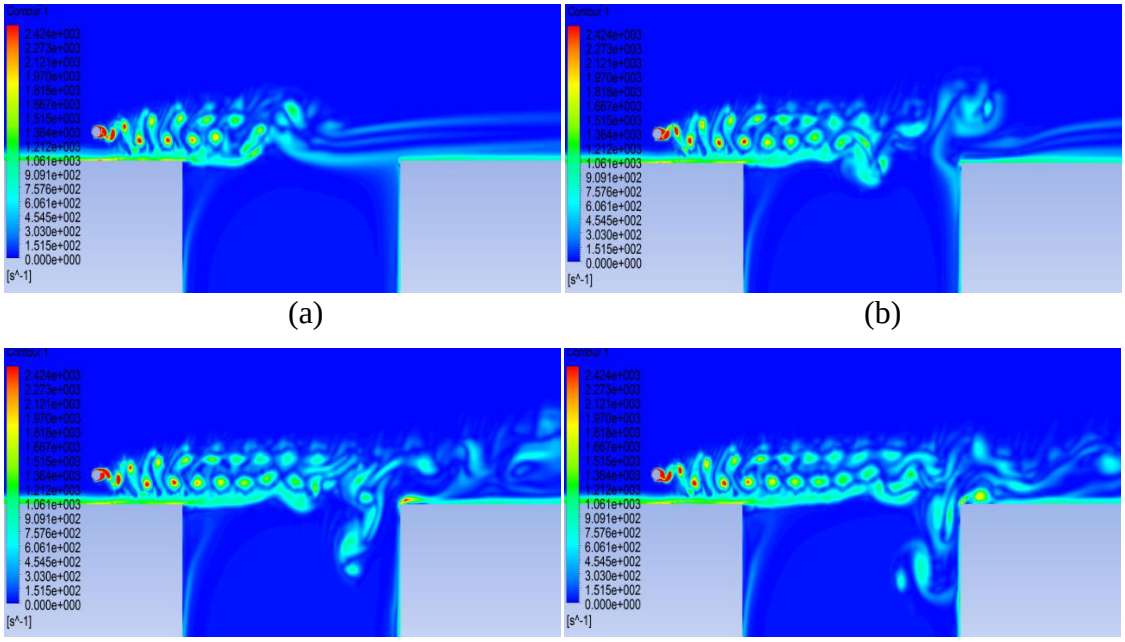

(a) (b)

(c) (d)

Figure 5-8: vorticity field with control cylinder located at (-50.8,12.7) (a) t=0.04 sec (b) t= 0.06 sec (c) t= 0.08 sec (d) t= 0.1 sec

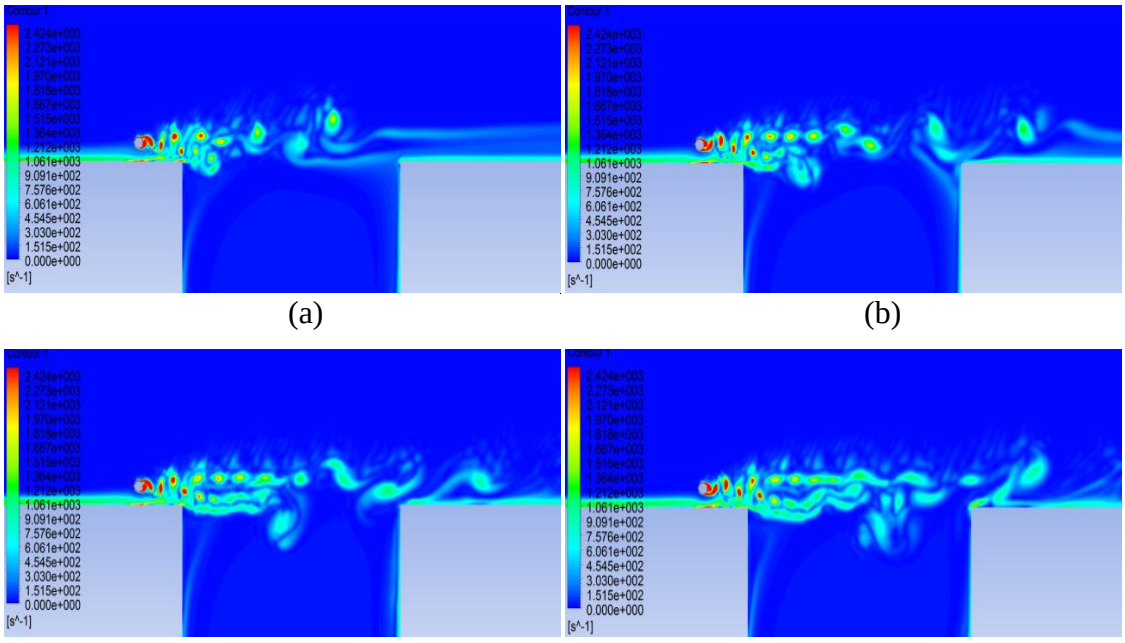

(a) (b)

(c) (d)

Figure 5-9: vorticity field with control cylinder located at (-25.4, 8) (a) t=0.04 sec (b) t= 0.06 sec (c) t= 0.08 sec (d) t= 0.1 sec

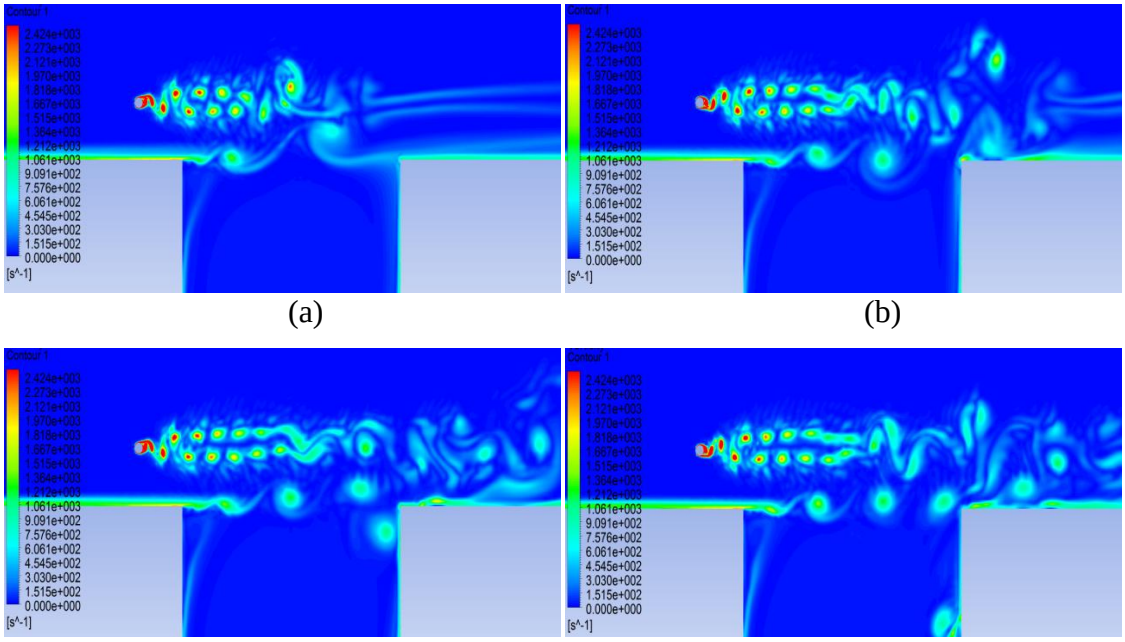

(a) (b)

(c) (d)

Figure 5-10: vorticity field with control cylinder located at (-25.4, 25.4) (a) t=0.04 sec (b) t= 0.06 sec (c) t= 0.08 sec (d) t= 0.1 sec

6. Conclusions

The effect of the upstream edge geometry and high frequency vortex generator on attenuating the flow-excited acoustic resonance in shallow rectangular cavities has been investigated. For the upstream edge geometry, it is observed that the increase in the characteristic length when round and chamfered edges are tested results in delaying the onset of the flow-excited acoustic resonance phenomenon to higher flow velocities. By investigating the round edge in the downstream it is proved that only the upstream edge geometry can shift the acoustic resonance excitation and magnify the acoustic pressure, while the downstream edge can mitigate the resonance excitation considerably without shifting the excitation to higher velocities. The magnitude of the amplification and the delay in the onset of acoustic resonance are affected by the radius in the case of the round edges and by the angle in the case of the chamfered edges. The delay of the onset of acoustic resonance can be useful in many industrial applications as a method of shifting the resonance out of the operating range as observed with the round edge with radius of 25.4 mm and the chamfered edge with angle of 107° in the cavity with aspect ratio of 1.67. However, this should be applied carefully since the acoustic pressure produced with the other round edges and chamfered edges when resonance is materialized is much higher than the original cavity with sharp edges. The curved and delta spoilers are found to be suppressive and they are able to attenuate the acoustic pressure significantly. The increase of the height of the spoilers in the cavity with aspect ratio of 1.0 has no significant effect on the acoustic resonance excitation till the height of 16 mm, while in the cavity with aspect ratio of 1.67 the height of the spoilers is observed to result in a significant change on the acoustic resonance excitation. This indicates that the optimum height of the spoilers required to suppress the acoustic resonance excitation seems to be related to the depth of the cavity. Increasing the angle of the delta spoilers to 65° and 70° are found to have a suppressive effect in the acoustic resonance excitation as the spoilers are still able to introduce velocity fluctuations to the flow, this can be utilized in designing a spoiler with the least amount of pressure drop. In the cavity with aspect ratio of 1.0, it is found that using delta spoilers with an angle of 70° can decrease the pressure drop by about 35%. Moreover, increasing the thickness of the spoilers can improve the

performance on suppressing the acoustic resonance excitation. The straight spoilers with different dimensions are found to have minor effects on the acoustic resonance excitation compared to the other spoilers. From these results, it is concluded that the configuration of the spoilers and their approach of directing and generating velocity fluctuations in the flow is the major factor that affects the performance of the edge in attenuating the acoustic resonance. The hotwire measurements contributed significantly to the understanding of the suppression mechanism. The effectiveness of the delta (angle 60°, 65°, and 70°) and the curved spoilers can be attributed to the size of the orthogonal vortices that prevent the development of the main vortices at the cavity mouth. For the straight spoilers case, the size of the orthogonal vortices is relatively small which has a weak effect and not able to damp the main vortices at the cavity.

For the effect of the high frequency vortex generator on the acoustic resonance excitation, placing a cylinder near to the upstream edge of a cavity can be an effective method in suppressing the acoustic resonance excitation in shallow rectangular cavities and a cylinder with a diameter of 6.35mm at location (-25.4,12.7) is able to keep the acoustic pressure below 140 Pa. However, the most effective locations and the diameter of the cylinder should be determined carefully to avoid exciting other acoustic modes by the cylinder. Moreover, the locations closer to the bottom wall of the test section are found to be more effective on suppressing the acoustic resonance excitation compared to other locations. Placing the cylinder at the mouth of the cavity is found to have no major effect on the acoustic resonance excitation. It is also observed that adding the cylinder results in shifting the acoustic resonance excitation to higher velocities. The 2D simulation shows how the wake of the cylinder interacts with the cavity shear layer. It is found that vertical position of the cylinder can influence the momentum thickness of the shear layer at the cavity. In the case of a cylinder located at height of 8 mm from the bottom wall, it is found that the cylinder increases the momentum thickness of the shear layer, which results in more stable shear layer that is less susceptible to acoustic resonance excitation. In the horizontal direction it is also observed that locating the cylinder 50.8 mm upstream can decrease the effectiveness of the control cylinder on suppressing the acoustic resonance excitation as the vortex shedding effect become weak and not significantly affecting the shear layer at the cavity.

6.1. Recommendations

Flows over cavities are considered very complex type of flows. Several suppression methods are found to have good performance, and the cavity oscillations can be significantly mitigated by these methods. This study addressed the effect of different configurations on the acoustic resonance excitation, this can contribute significantly to the design of passive methods in the future, also further analysis using hotwire measurements and numerical simulation contributed to the understanding of the physics behind the suppression mechanism. However, for future research, it is recommended to consider the following issues:

- Investigate the effect of the number of spoilers, which control the number of orthogonal vortices generated, on the suppression mechanism.
- Perform flow visualization to enrich the knowledge about the spoilers effect on the flow structure.
- The effect of the control cylinder can further be investigated by testing other cross section geometries such as rectangular and triangular.
- Expanding the numerical simulation to 3D can address the three dimensionality introduced at the side walls and enrich the understanding of the interaction between the cylinder vortex shedding and the cavity shear layer.

References

Baldwin, R., Simmons, H., 1986. Flow-induced vibration in safety relief valves. J. Press. Vessel Technol. 108.

Blevins, D., 2001. Flow Induced Vibration. Krieger publishing company, USA.

Bolduc, M., Elsayed, M., Ziada, S., 2013. Effect of upstream geometry on the trapped mode resonance of ducted cavities. ASME PVP2013-97149, pp. 1–8.

Bruggeman, J.C., Hirschberg, A., van Dongen, M.E.H., Wijnands, A.P.J., Gorter, J., 1991. Self-sustained aero-acoustic pulsations in gas transport systems: Experimental study of the influence of closed side branches. J. Sound Vib. 150, 371–393.

Cattafesta, L., Williams, D., 2003. Review of Active Control of Flow-Induced Cavity Resonance 33 rd AIAA Fluid Dynamics Conference 0–20.

Cattafesta, L.N., Garg, S., Kegerise, M.A., Jones, G.S., 1998. Experiments on compressible flow-induced cavity oscillations. AIAA 98–2912.

Chen, Y.J., Shao, C.P., 2013. Suppression of vortex shedding from a rectangular cylinder at low Reynolds numbers. J. Fluids Struct. 43, 15–27.

Comte, P., Daude, F., Mary, I., 2008. Simulation of the reduction of unsteadiness in a passively controlled transonic cavity flow. J. Fluids Struct. 24, 1252–1261.

Dix, R.E., Bauer, R.C., 2000. Experimental and Theoretical Study of Cavity Acoustics.

Ethembabaoglu, S., 1973. on the fluctuating flow characteristics in the vicinity of gate slots.

Franke, M., Carr, D., 1975. Effect of geometry on open cavity flow-induced pressure oscillations. Am. Inst. Aeronaut. Astronaut.

Gloerfelt, X., 2009. Cavity noise. Chap. 0. Von Karman Institute.

Heller, H., Bliss, D., 1975. Flow-induced pressure fluctuations in cavities and concepts for their suppression. AIAA.

Illy, H., Geffroy, P., Jacquin, L., 2008. Observations on the Passive Control of Flow Oscillations Over a Cavity in a Transonic Regime by Means of a Spanwise Cylinder 1–17.

Illy, H., Geffroy, P., Jacquin, L., n.d. -1- Control of cavity flow by means of a spanwise cylinder Hervé Illy, Philippe Geffroy & Laurent Jacquin I 4–5.

Karadogan, H., Rockwell, D., 1983. Toward Attenuation of Self-Sustained Oscillations of a Turbulent Jet Through a Cavity. J. Fluids Eng. 105, 335.

Kegerise, M.A., 1999. An experimental investigation of flow-induced cavity oscillations. Syracuse university.

Keirsbulck, L., Hassan, M. El, Lippert, M., Labraga, L., 2008. Control of cavity tones using a spanwise cylinder. Can. J. Phys. 86, 1355–1365.

Kinsler, L.E., Frey, A.R., Coppens, A.B., Sanders, J. V., 2000. Fundamentals of Acoustics, 4th Edition. John Wiley and Sons, Inc.

Knotts, B.D., Selamet, a., 2003. Suppression of flow–acoustic coupling in sidebranch ducts by interface modification. J. Sound Vib. 265, 1025–1045.

Krishnamurty, K., 1955. Acoustic radiation from two-dimensional rectangular cutouts in aerodynamic surfaces.

Lacombe, R., Lafon, P., Edf, R., Edf-cea-cnrs, L.U.M.R., 2013. Numerical and experimental analysis of flow-acoustic interactions in an industrial gate valve, in: 19th AIAA/CEAS Aeroacoustics Conference. Berlin, pp. 1–11.

Larchevêque, L., Sagaut, P., Lê, T.-H., Comte, P., 2004. Large-eddy simulation of a compressible flow in a three-dimensional open cavity at high Reynolds number. J. Fluid Mech. 516, 265–301.

Lawson, S.J., Barakos, G.N., 2011. Review of numerical simulations for high-speed, turbulent cavity flows. Prog. Aerosp. Sci. 47, 186–216.

Martinez, M. a., Di Cicca, G.M., Iovieno, M., Onorato, M., 2012. Control of Cavity Flow Oscillations by High Frequency Forcing. J. Fluids Eng. 134, 051201.

McGarth, S., Shaw, L., 1996. active control of shallow cavity acoustic resonance, in: AIAA Fluid Dynamics Conference. New Orleans.

Mittal, S., Raghuvanshi, A., 2001. Control of vortex shedding behind circular cylinder for flows at low Reynolds numbers. Int. J. Numer. methods fluid 421–447.

Mohany, A., Ziada, S., 2005. Flow-excited acoustic resonance of two tandem cylinders in cross-flow. J. Fluids Struct. 21, 103–119.

Nakiboğlu, G., Manders, H.B.M., Hirschberg, a., 2012. Aeroacoustic power generated by a compact axisymmetric cavity: prediction of self-sustained oscillation and influence of the depth. J. Fluid Mech. 703, 163–191.

Naudascher, E., 1967. from flow stability to flow-induced excitation. ASCE.,J. Hydrulics Div. 93, 15–40.

Peng, S., Leicher, S., 2008. DES and Hybrid RANS-LES Modelling of Unsteady Pressure Oscillations and Flow Features in a Rectangular cavity 132–141.

Rockwell, D., Knisely, C., 1979. The organized nature of flow impingement upon a corner. J. Fluid Mech. 93, 413.

Rockwell, D., Lin, J.-C., Oshkai, P., Reiss, M., Pollack, M., 2003. Shallow cavity flow tone experiments: onset of locked-on states, Journal of Fluids and Structures.

Rockwell, D., Naudascher, E., 1978. Review — Self-Sustaining Oscillations of Flow Past Cav ities. J. Fluids Eng. 100.

Rockwell, D., Naudascher, E., 1979. Self-Sustained Oscillations of Impinging Free Shear Layers. Annu. Rev. Fluid Mech. 11, 67–94.

Roshko, B.A., 1955. National advisory committee for aeronautics technical note 3488.

Rossiter, J.E., 1964. wind-tunnel experiments on the flow over rectangular cavities at subsonic and transonic speeds.

Rossiter, J.E., Kurn, A.G., 1965. wind Tunnel Measurements of the Unsteady Pressures in and behind a Bomb Bay (Canberra).

Rowley, C.W., Williams, D.R., 2006. Dynamics and Control of High-Reynolds-Number Flow Over Open Cavities. Annu. Rev. Fluid Mech. 38, 251–276.

Sarno, R.L., Franke, M.E., 1994. suppression of flow-induced pressure oscillations in cavities. J. Aircr.

Sarohia, V., 1977. Experimental Investigation of Oscillations in Flows Over Shallow Cavities. AIAA J. 15, 984–991.

Schmit, R.F., Schwartz, D.R., Ganesh, R., Kibens, V., Ross, J., 2005. High and Low Frequency Actuation Comparison for a Weapons Bay Cavity. 43rd AIAA Aerospace Sciences Meeting and Exhibit, Reno, Nevada, pp. 10–13.

Shaw, L.L., 1979. suppression of aerodynamically induced cavity pressure oscillations.

Spalart, P.R., 2009. Detached-Eddy Simulation. Annu. Rev. Fluid Mech. 41, 181–202.

Spalart, P.R., Jou, W.-H., Strelets, M., Allmaras, S.R., 1997. comments on the feasibility of LES for wings, and on hybrid RANS/LES approach. AFOSR international conference on DNS/LES, Columbus, OH.

Stanek, M.J., Raman Ganesh, Kibens Valdis, Ross, Odedra, James, Peto, 2000. Control of cavity resonance through very high frequency forcing. AIAA Aeroacoustic conference.

Strykowski, P.J., Sreenivasan, K.R., 1989. On the formation and suppression of vortex "shedding" at low Reynolds numbers. J. Fluid Mech. 218, 71–107.

Ukeiley, L.S., Ponton, M.K., Seiner, J.M., Jansen, B., 2004. Suppression of Pressure Loads in Cavity Flows. AIAA J. 42.

Ziada, S., Lafon, P., 2013. Flow-Excited Acoustic Resonance Excitation Mechanism, Design Guidelines, and Counter Measures. Appl. Mech. Rev. 66, 011002.

Ziada, S., Ng, H., Blake, C.E., 2003. Flow excited resonance of a confined shallow cavity in low Mach number flow and its control. J. Fluids Struct. 18, 79–92.

Ziada, S., Rockwell, D., 1982. Oscillations of an unstable mixing layer impinging upon an edge. J. Fluid Mech. 124, 307.